

ENDOSCOPIC TISSUE LIQUIDISATION OF THE PROSTATE, BLADDER AND KIDNEY.

M. J. COPTCOAT, M.B., F.R.C.S. (Ed).

Submitted for a Ch.M. degree at Liverpool University in 1990.

Based on work carried out as a research fellow and Resident Surgical Officer at the Institute of Urology, London, between 1985 and 1988, as a Senior Registrar at St. Mary's Hospital, Portsmouth, between 1988 and 1989, and as a visiting fellow at the Klinikum Mannheim, W. Germany, in 1990.

ProQuest Number: 10609765

All rights reserved

INFORMATION TO ALL USERS

The quality of this reproduction is dependent upon the quality of the copy submitted.

In the unlikely event that the author did not send a complete manuscript and there are missing pages, these will be noted. Also, if material had to be removed, a note will indicate the deletion.



ProQuest 10609765

Published by ProQuest LLC (2017). Copyright of the Dissertation is held by the Author.

All rights reserved.

This work is protected against unauthorized copying under Title 17, United States Code
Microform Edition © ProQuest LLC.

ProQuest LLC.
789 East Eisenhower Parkway
P.O. Box 1346
Ann Arbor, MI 48106 – 1346

ACKNOWLEDGEMENTS

This study was inspired and supervised by Mr J E A Wickham. Mr K Parsons has been my patient advisor. I am indebted to my colleague Dr K T Ison without whom I could not have produced this work. Other collaborators are shown below. This project would not have been possible without the financial support of the Smith's charity and the St Peter's Trust. Lastly but most importantly must come the acknowledgement that without my wife's support and encouragement this thesis would never have been completed.

DECLARATION

This thesis is the result of my own work. The material contained in the thesis has not been presented, nor is currently being presented, either wholly or in part, for any other degree or other qualification.

The research was carried out in the Institute of Urology, and Imperial College, London, and the Klinikum Mannheim, W. Germany.

The clinical work was carried out in the Institute of Urology, London, and St. Mary's Hospital, Portsmouth.

Specific technical procedures not carried out solely by myself were:

1. Flow cytometry:

a). Prostate: collaboration with Mr C Charig.

b). Bladder tumours: collaboration with Mr D Rew.

2. Robotic prostatectomy: collaboration with Drs Hibbard and Davies.

3. Tensile strength of stone: collaboration with Mr Saunders.

ABSTRACT

ENDOSCOPIC TISSUE LIQUIDISATION OF THE PROSTATE, BLADDER, AND KIDNEY.

Endoscopic techniques have revolutionised the practice of all specialities of surgery. Endoscopic access has been either via a natural route, such as the urethra, or percutaneously, as in percutaneous intrarenal stone surgery. Potential endoscopic procedures for bulk tissue removal have been limited by the need to reduce that tissue to a size smaller than the endoscopic channel used. An attempt has been made to create a device that will liquidise and aspirate tissue through an endoscope. This instrument has been called the Endoscopic Liquidiser and Surgical Aspirator (ELSA). This report details the design and development of the ELSA which has led to its clinical application.

The device is 5 mm in diameter and is used through a specially made endoscope of 8.5 mm outer diameter (approximately 27 French). It consists of a high speed rotating blade mounted in a housing that provides irrigation for efficient liquidisation and a channel for aspiration of the tissue. Laboratory evaluation was measured by the removal rates of different tissues. The optimum parameters of blade speed, irrigation flow and aspiration were established after a series of controlled experiments. Blade shape was also found to be important and a study of the material strengths of different tissues was required to establish that blade design should vary for each tissue used. Under optimum laboratory conditions

fresh human prostate could be removed at 2.4 g/min and renal cortex at 14.6 g/min.

The resultant aspirate contained particles ranging from 10 microns to 3 mm, but the majority were less than 200 microns. Flow cytometry was required as the only reasonable method of rapid pathological diagnosis.

The action of the ELSA did not confer any inherent haemostatic benefit and a diathermy plate was added to the tip of the instrument.

The ELSA was successfully used to remove benign prostatic tissue from 7 patients with bladder outflow obstruction. However the procedures were slow and visualisation was poor once the liquidisation began. The mean operating time was 85 minutes (range 50 - 120). 1 patient suffered a fatal capsular perforation, but otherwise morbidity was not dissimilar from a control group undergoing a standard transurethral diathermy resection. 6/7 patients regained an improved stream with good control.

The ELSA was used in the same transurethral method for the removal of superficial bladder tumours in 10 patients. The same problem of impaired vision was found, but the removal was very rapid as one would expect with a soft non-fibrous material. The postoperative morbidity was greater than in a control group using a diathermy resectoscope due to bladder perforation with the ELSA in 1 case.

A percutaneous endoscopic nephrectomy has been achieved in 2 dogs. Each kidney was embolised with "Ethibloc" (a material that completely occupies

all arterial capillary beds). An intrarenal approach was compared with an extrarenal, retroperitoneal one; the latter using carbon dioxide insufflation. Both procedures were successful. Haemostasis was not a problem. These may be suitable clinical techniques for the minimally invasive removal of infected kidneys prior to transplantation. The presence of stones would not be a problem because of the ability of the ELSA to fragment and aspirate stone particles as efficiently as any ultrasound device. This was confirmed in a series of laboratory tests on various stone types and in 5 patients with urinary stones.

An extension of the concept of minimally invasive bulk tissue aspiration is the integration of robotics into this form of surgery. The ELSA has been attached to an industrial robot. The mechanism of a transurethral prostatectomy has been studied in order to program the robot. A robotic prostatectomy in a simulation model has been performed. Each procedure can be preprogrammed according to the dimensions of the gland. The in vitro study confirmed that the robot was consistent and therefore safe; and rapid (mean removal time 5 mins) because visualisation was not required for orientation.

In conclusion, the ELSA has proved to be an efficient instrument for endoscopic tissue removal but its clinical superiority is only for less fibrous tissues and improved visualisation will be required. It still requires ancillary methods for haemostasis and the use of a capillary embolisation technique in the kidney may have applications elsewhere. The robotic study was not just an academic exercise. Robotics will be a feature of future surgery.

ENDOSCOPIC TISSUE LIQUIDISATION OF THE PROSTATE, BLADDER AND KIDNEY.

CONTENTS

ACKNOWLEDGEMENTS

DECLARATION

ABSTRACT

CONTENTS

PAGE NUMBER

INTRODUCTION.....1

CHAPTER 1

HISTORICAL REVIEW OF THE TECHNIQUES OF ENDOSCOPIC PROSTATE REMOVAL.....5

Median bar incisors.....5

Diathermy.....6

The Cold Punch.....7

The role of lasers for the endoscopic removal of living tissue.....12

Ultrasonic aspiration of tissue (CUSA).....15

A simple motorised aspirator.....17

CHAPTER 2

DEVELOPMENT OF THE PROTOTYPE ELSA.....	19
Concept.....	19
Performance of the first prototype.....	21
Design of the clinical liquidiser.....	24
A bench assessment of the 5 mm clinical prototype.....	25
Tissue characteristics and blade design.....	29
Results of Load/Strain experiments.....	32
A laboratory comparison between the 5 mm ELSA, CUSA and a Nd:YAG laser for tissue removal.....	36
Particle analysis.....	38

CHAPTER 3

THE INTEGRATION OF FLOW CYTOMETRY AND TISSUE LIQUIDISATION TECHNIQUES..	41
Construction of the Cytolyser.....	44
Particulate size and DNA histograms. Can the Cytolyser help?.....	45

CHAPTER 4

HAEMOSTASIS DURING PROSTATE REMOVAL.....	47
Arterial supply of the human prostate.....	47
Macrovascular casts of the prostate.....	53
Embolisation of the prostate.....	54
The ELSA and Nd:YAG laser in tandem.....	54
The Nd:YAG laser for haemostasis.....	56

CHAPTER 5

CLINICAL USE OF THE ELSA FOR PROSTATE REMOVAL.....	59
--	----

CHAPTER 6

REMOVAL OF OTHER TISSUES USING THE ELSA.....	64
Testicular tissue.....	64
Ovarian tissue.....	65
Bladder tumours.....	65
Renal tissue.....	68
Percutaneous canine nephrectomy.....	69
Appendix: Embolisation of the prostate.....	73

CHAPTER 7

A ROBOTIC PROSTATECTOMY: A LABORATORY ASSESSMENT.....	75
The robot.....	76
The prostate model.....	77
Appendix: A training model for the TURP.....	83

CHAPTER 8

THE ELSA FOR URINARY STONE FRAGMENTATION.....	84
Mechanism of stone fragmentation.....	84
Experiments on stone strength.....	85
A laboratory comparison between EHL, USL, and the ELSA for stone fragmentation.....	89
A clinical comparison between EHL, USL, and the ELSA for stone fragmentation.....	93

CONCLUSION.....97

LEGENDS FOR FIGURES.....99

REFERENCES.....102

INTRODUCTION

Endoscopic techniques have revolutionised the practice of all specialities of surgery. Endoscopic access has been either via a natural anatomical route such as the urethra to the prostate, or percutaneously as in percutaneous intrarenal stone surgery. These minimally invasive routes reduce the postoperative morbidity for that procedure. This in turn results in a faster return to normal activities for the patient. The disadvantage is generally that the operative procedure takes longer, demands greater expertise, and often involves expensive equipment. The subject of this thesis concerns a project to create an instrument that will extend the scope of minimally invasive surgery in general but with particular emphasis on prostate removal.

Endoscopic surgery has taken 3 evolutionary steps. First, instrumentation became available for accurate internal diagnosis. This was followed by the facility to carry out manipulative procedures through the endoscope, such as a biopsy. The third step has been the removal of tissue larger than the sheath diameter of the instrument. These steps are seen in the evolution of percutaneous intrarenal stone surgery where large stones can now be fragmented and removed (Payne 1989). Applications of these principles to other tissues has been difficult with the exception of transurethral diathermy resection of the prostate and bladder tumours. For the further expansion of the field of endoscopic or "minimally invasive surgery" (i.e. where the trauma of the surgical access is reduced) a device is required which will enable the safe and rapid removal of large quantities of tissue

through the endoscope. Conventional endoscopic tissue removal involves removing the tissue in "chunks" (electroresection, cold-punch). Further reduction of the tissue to a liquified form would allow easy removal by aspiration. This thesis describes the work carried out to design, develop, refine and clinically utilise such a technique (endoscopic tissue liquidisation and aspiration).

The ideal instrument would:

- a) reduce all types of tissue to a liquid state,
- b) remove large volumes of tissue rapidly and cleanly,
- c) allow a good endoscopic view to be maintained during tissue extraction,
- d) leave no dead tissue at the margin of the removal,
- e) be able to operate in a liquid or gaseous medium,
- f) have an haemostatic effect,
- g) be easily controlled by an inexperienced operator,
- h) be safe for the patient,
- i) be inexpensive to construct and to maintain.

The concept of endoscopic tissue liquidisation was introduced by J.E.A. Wickham almost 15 years ago. Unfortunately, little progress was made. The Cavitron Ultrasonic Surgical Aspirator (CUSA) was a potential solution but had severe limitations when used endoscopically. The potential of laser ablation has not been borne out when attempting to remove large volumes of tissue as would be required in the prostate. This is disappointing because of the associated haemostatic effect it would offer. A review of these modalities appears in Chapter 1.

Substantial progress has been made in this thesis work because the initial design, construction and experimentation was undertaken by enthusiastic amateurs in a home work shop. The working prototype was then enough to convince an instrument manufacturer that this was a project worth investing in. The resultant refined instruments have now been used clinically.

The main aim of this work was to undertake an endoscopic transurethral liquidisation and aspiration of the human prostate. The following chapters will begin with an historical background to endoscopic transurethral prostate removal and then progress chronologically through the early design work, a clinical evaluation of the new instrument, and finally a possible future robotic application. The potential of this technique has also been applied to bladder tumours, calculi and the endoscopic removal of renal tissue. The animal and clinical studies of these associated areas are also reported in this thesis.

The effect of any instrument or energy on a particular target tissue depends on the characteristics of that tissue. Materials science is a large discipline only outside of medicine. The material characteristics of the prostate and other tissues required investigation before the ideal cutting instrument could be designed. These experiments were in themselves breaking new ground in surgical and materials science research.

The instrument has been called the Endoscopic Liquidiser and Surgical Aspirator (ELSA). The ELSA produces a suspension of particles suitable for analysis by flow cytometry. This indirectly lead to a modified ELSA being used for the preparation of other tissue samples for flow cytometry. This

second instrument has been called the CYTOLYSER. The ELSA and Cytolyser have both been patented (8822273.1&2).

CHAPTER 1

HISTORICAL REVIEW OF THE TECHNIQUES OF ENDOSCOPIC PROSTATE REMOVAL.

This review will concentrate on those methods which have been described for the transurethral removal of human prostatic tissue under direct vision.

Transurethral techniques for the relief of bladder neck (outflow) obstruction were initially mechanical and not under endoscopic vision. Ambroise Pare' (1840) had a catheter made with a sharp cutting cup at its tip with which pieces of the bladder neck could be torn away. James Guthrie (1836) introduced a urethral sound with a concealed knife which could be projected to cut the bladder neck. Guthrie also considered that the underlying obstruction may not just be a bar or stricture at the bladder neck. It is clear that he thought his knife would relieve cases with prostatic "middle lobe" enlargement by cutting the ring of bladder neck tissue which imprisons and traps the adenoma. Civiale and Mercier devised very similar devices and claimed great success (Gutierrez 1933). These techniques had three major drawbacks - they were blind, they were bloody, and they were suitable only for true bladder neck strictures rather than prostatic hyperplasia.

The next major step was in a sense ahead of its time in that the new application by Bottini in 1874 of galvanocautery lacked visual control but was still a significant advance. Bottini's instrument (1877) was essentially a classic lithotrite, the blades of which were insulated from one another and

powered with galvanic current to produce heat. It was possible to "cook" portions of the prostate, (and anything else that got in the way), and achieve reasonable haemostasis. It was still essentially an incision rather than excision of the prostate. In 1897 Freudenberg attempted to improve upon Bottini's instrument with better insulation and later by the addition of vision with an irrigating cystoscope.

Several developments were occurring parallel to these latter events. Of universal interest was the introduction of the irrigating cystoscope by Brown and Buerger (Wallace 1973) that could be used in conjunction with a working instrument. There had been a rapid evolution from Nitze's early cystoscope which used a heated platinum wire to illuminate the bladder, to Edison's early filament light and to the Brown-Buerger operating cystoscope which is essentially the same instrument in use today, 90 years later.

In contrast to the universal desire to visualise just what damage was being done there was a dichotomy of approach as far as the design of an instrument to remove prostatic tissue. The two different methods which were developed and modified, and subsequently polarised clinical urologists, were diathermy and the mechanical punch.

Surgical diathermy has evolved on an empirical basis (D'Arsonal 1983). At frequencies above 100 KHz, alternating current produces tissue heating by an ohmic effect, without neuromuscular stimulation. The principle of monopolar diathermy relies upon a high current density delivered by an active electrode.

Electrical energy is converted to heat as a result of tissue impedance. The effect of this tissue heating depends on a) waveform of the current, b) method of application of the active electrode, and c) the shape of the active electrode. Empirical observation showed that a continuous sine wave delivered by a fine point or narrow gauge electrode would strike an arc of intense energy capable of vaporizing cells to produce a surgical incision. Similarly the recognition of the most suitable waveform for coagulation was also empirical. The damped sinusoidal output of the original spark gap generator commercialized by W. T. Barre in the late 1920s produced haemostasis by both assisted coaptation of vessel walls and tissue fulguration (Ramsay 1986).

Stern in 1926, in collaboration with the Western Electric Company which had developed the undamped current, constructed a resectoscope through which he could cut out longitudinal, parallel spaghetti-like sections of prostatic tissue under vision. His resectoscope had a window near the distal end and a moveable tungsten loop to resect the tissue engaged in this opening. McCarthy used a loop and an additional coagulating current to modify Stern's instrument. This instrument (McCarthy 1931) was known as the Stern-McCarthy resectoscope and is the close ancestor of contemporary resectoscopes.

Young, on the other hand, brought out his mechanical punch in 1909 (Young 1913). The outstanding disadvantage of this mechanical yet endoscopic procedure was postoperative haemorrhage, and its author recommended that a piston syringe be kept at the patient's bedside for immediate evacuation of

clots postoperatively. This punch will be described in more detail because of the similarity in its evolution compared with the ELSA.

Young's original punch (figure 1:1) had provision for viewing via a small magnifying window through which a light could be directed. The cutting action itself was blind and there was no way to control bleeding. However, with this instrument Young excised variable amounts of obstructing tissue under "adequate" vision and controlled resulting bleeding with a 29 French two-way gum rubber catheter and piston syringe. The first operation was performed under local cocaine anaesthesia "almost without pain, with little subsequent haemorrhage and a splendid functional result" (Young 1913). A piece of tissue 7 mm in diameter and 13 mm long was excised. He reported in 1913 one hundred cases with no deaths. This simple instrument received wide acceptance, and was used through the open bladder as well as transurethrally.

In 1911 Young attempted to reduce the complications and limitations imposed by haemorrhage by incorporating electrocauterisation into his punch. Provision for heating the end of the tubular knife by electricity was made, and the outer sheath was water cooled. But this did not increase its popularity significantly. Young's punch was also modified by others. Geraghty in 1922 used a concave solid knife. Kreutzmann in 1925 suggested a knife with a serrated cutting edge. Also in 1925, Tolson used diathermy to heat a solid nickel-silver electrode the size of the fenestra in Young's punch to control bleeding by "cooking" the entire cut surface. Later he added irrigation and a telescope.

Braasch (1918) went one step nearer to solving the problem of vision. He adapted his direct irrigating cystoscope for excision of tissue, devising a tube with a fenestra for engaging tissue. This was passed through the Braasch cystoscope and a tubular knife excised the tissue. Tissue could be visualised as it was cut but again, the inability to control haemorrhage limited the use of the instrument to excision of median bars.

The next big advance broadening the scope and acceptability of transurethral resection of the prostate, and of the punch, was made by Caulk (1920). He put a one-quarter inch "irrido-platinum cutting edge" on the knife. This was heated with a 150 ampere current to burn through bars and contractures. It was used primarily as an outpatient procedure. One patient was reported to have had fourteen pieces of tissue removed in three sittings.

Modifications to the punch were not only occurring in the USA. Walker in England (1925) modified the cautery punch in several important ways. He was the first to use a bakerlite sheath. He originally heated the terminal metal edge of the fenestra with diathermy current to coagulate the tissue to be excised. This was later replaced with a coagulating needle. Light, telescope and irrigation were all utilised.

These last refinements were thus being made and used in the same period (1925 - 1932) when Stern (1926) and McCarthy (1931) were completing their work on the electrotome and a machine to provide adequate cutting and coagulation

currents that made the loop resectoscope the more widely acceptable instrument for transurethral prostate removal.

The punch continued to be used by a minority of urologists. Further minor improvements were made, notably by Thompson (1934) who reported that 25g could be removed in 10% of procedures. In one memorable case the 16 grams of tissue were photographed next to the very similar mass of a baseball. In 1962 Carlson made a spring activated punch in his hospital machine shop. Foley also produced a powered punch. A punch with a rotating blade was also developed. This latter concept is simply noted by Nation (1976) in a review of the knife-punch resectoscope but apart from the comment that it did not achieve much popularity, no other leads are available. This is obviously unfortunate because of its possible similarity to the ELSA.

One must not lose sight of the unfortunate fact that, despite the availability of what were now safe and efficacious transurethral punch and diathermy loop instruments, the majority of urologists outside of the USA were still arguing over the finer points of open prostate surgery (Blandy 1978). The choice of transurethral resection is now the first choice procedure for nearly all urologists for the treatment of bladder outflow obstruction due to prostatic enlargement (Chisholm 1989).

The only recent modifications to the diathermy loop resectoscope have been the availability of larger loops to increase tissue removal rate and the construction of an extra inner tube to facilitate continuous low pressure.

irrigation (Inglesias 1975). This latter addition has had a great impact in reducing the incidence of the fluid absorption syndrome. The diathermy loop resectoscope has become the reliable clinical instrument that all newcomers must measure up to.

Two new modalities for tissue removal have been put forward in the last decade. These are lasers and ultrasonic tissue aspiration. Attempts have been made to apply both to transurethral prostate removal and these will be described below.

The role of lasers for the endoscopic removal of living tissue.

Lasers produce a narrow beam of monochromatic light of higher intensity than is possible by any other means. The effect of laser light at any point depends upon the intensity at that point, the absorption, refraction and reflection by the tissue concerned, the wavelength used and the biological response to the energy absorbed. The effects of a continuous wave laser can be approximated below.

Energy Density

(joules/sq. cm.)

Biological Effect

4	biostimulation
10	biosuppression
40	non-thermal cytotoxic phototherapy with sensitising agents
400	photo-coagulation)
) Thermal effects
4000	vaporization)

It is the thermal effect of high energy densities that can be utilised for the destruction and to some extent the removal of living tissue endoscopically. The three lasers in common use medically are the carbon dioxide laser (wavelength

10,600 nanometres(n.m.) in the far infrared), the Neodymium-Yttrium Aluminium-Garnet(Nd-YAG) laser (wavelength 1,064 n.m. in the near infrared), and the Argon laser (two main lines at 488 and 514 n.m. in the blue and green regions of the visible spectrum). Both the Argon and the Nd-YAG beams can be transmitted via fully flexible single quartz fibres (diameter 200 - 600 microns) but at present there is no suitable fibre available for the carbon dioxide beam. The latter must be used via a system of pivoted straight light guides, and so has restricted the use of the carbon dioxide laser for endoscopic work in urology.

The infrared beam of the carbon dioxide laser is absorbed mainly by water in living cells, whereas the Nd-YAG and Argon beams are absorbed more by pigmented tissue. With all three lasers if sufficient energy is absorbed at the surface of the tissue, the superficial cells will be destroyed and further application of the beam will create a cavity. When soft tissue absorbs a small amount of energy it merely warms up. As the amount of energy increases the next effect is thermal contraction of the area treated without causing cell death, which is probably due to vaporization of water. Still higher energies kill the cells in situ and the ultimate effect is the vaporization of cellular material in the exposed area. Thermal contraction can seal vessels as in the endoscopic treatment of haemorrhage from peptic ulcers. This is most effective when the volume of tissue heated is large. The Nd-YAG laser can seal vessels of up to 1 mm in diameter in suitable supporting tissue. The Nd-YAG laser has been used palliatively at endoscopy to provide symptomatic relief of malignant obstruction to the main bronchi, oesophagus and stomach by vaporizing nodules of tumour protruding into the lumen. However, deeper penetration produces

tumour damage with cell death, but without vaporization. In these areas late sloughing of dead tissue may occur. The rate at which the energy is put in (the power) is not so critical in this context, although if the power is low some of the energy absorbed may be conducted away from the target areas thermally, reducing the severity of the damage. At local energy levels below those which lead to sloughing, the thermal insult to the tissue stimulates a local inflammatory response which can be followed by the laying down of fibrous tissue (Bown 1980).

The energy density required to vaporize tissue of a particular size by external Nd-YAG irradiation is fairly constant and reports have shown that depth of tissue damage in normal tissue depends closely on the applied energy (Bleehan 1982). The clinical applications of laser tissue ablation have been restricted to fairly small lesions of a maximum of 1 cubic cm because of the charring to the tissue that soon occurs. This carbonisation both prevents further penetration of the laser energy and itself requires a substantial rise in temperature to be removed by vaporization. However, the use of a Nd-YAG laser for tissue vaporization with an haemostatic effect might be enhanced by some form of mechanical tissue removal such as the ELSA (see Chapter 4). Bearing these theoretical and practical considerations in mind, it is not surprising that clinical results in removing prostatic tissue with a Nd-YAG laser have been poor. Bladder neck incision is the only viable manoeuvre possible but haemorrhage has been troublesome because of the poor haemostatic effect of the Nd-YAG laser on prostatic arteries (Shanberg 1986). *Postscript*

Ultrasonic Aspiration of tissue

The ultrasonic surgical aspirator has already been clinically evaluated in neurosurgery and to a limited extent in open renal surgery. The ultrasonic surgical aspirator converts electrical energy to mechanical motion at the tip of a hollow scalpel that vibrates longitudinally along its axis at ultra-high frequencies. The system combines fragmentation, irrigation and aspiration in one instrument and in a controlled manner can selectively fragment tissue with a high water content and yet produce sparing of collagen rich tissues such as blood vessels and the renal collection system. This scalpel is a larger and more powerful version of the Kelman-Phaco aspirator (1973) which was used for the removal of cataracts. Similar appliances are currently being used for the removal of neurogenic tumours (Epstein 1983) and the performance of partial nephrectomies (Chopp 1983) and hepatectomies (Hodgson 1979). More recently Addonizio (1987) has unsuccessfully attempted prostatic resection with the CUSA (Cavitron ultrasonic surgical aspirator).

The CUSA system consists of a surgical hand piece (aspirator/scalpel) connected by a cable to control and power console with an activator switch which requires standard operating room electrical connections. A light-weight pencil grip hand-piece is the actual functioning portion of the system (figure 1:2) and is the only part to be introduced into the operating field. This scalpel employs the principle of an acoustic vibrator for fragmenting tissue and is constructed of a stainless steel water cord jacket inside which is a magnetostrictive transducer. A connection body attaches the transducer to a hollow cone-shaped

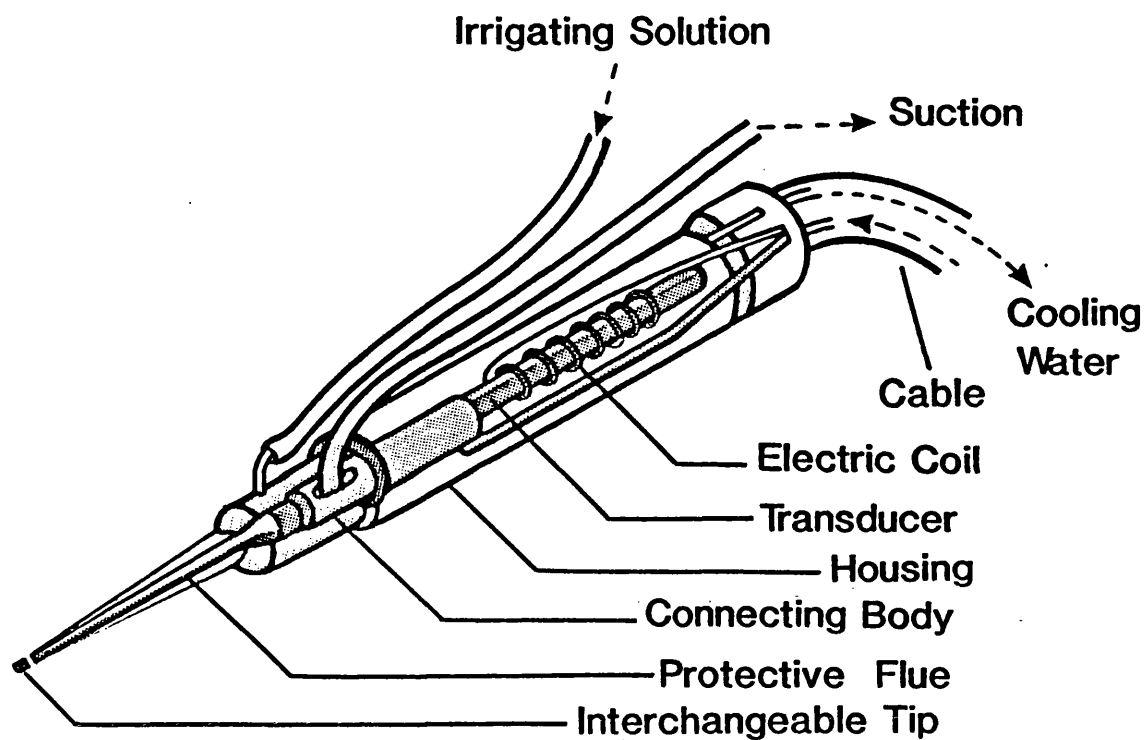


Figure 1:2. CUSA handpiece.

titanium amplifier that is housed in a protective plastic tube except for the distal 4 mm. The console relates the intensity of vibration and variable irrigation and suction requirements of the hand-piece.

The magnetostrictive device contained in the body of the hand-piece converts electrical energy into mechanical motion confined to the tip of the scalpel. This results in acoustic vibrations. The tip of the ultrasonic scalpel has an annular configuration with a diameter of 2 mm. When it contacts the target tissues, cellular fragmentation and disruption to a depth of approximately 150 microns occurs within a radius of 2 mm of the vibrating tip. Tissues such as renal and hepatic parenchyma as well as adipose tissue fragment readily. Blood vessels, collecting systems, and nerves are generally resistant and less likely to be perforated by accident unless subjected to extremely high vibration intensities. The operation field is irrigated by a continuous flow of normal saline at a rate of 3 to 10 ml/m. The saline helps to suspend the fragmented tissue in the form of an emulsion and reduces the heat generated by the rapid excursion of the tip. The heated tip is not able to produce haemostasis.

The mechanism of action of such ultrasonic aspirators is predominantly the result of a rapid vibration of the tip rather than the effect of generating secondary ultrasound waves within the tissue (e.g. cavitation, micro-acoustic streaming, or ultrasonic heating). Amplification is possible by designing the probe as an acoustic horn, but this is not suitable for urological endoscopic use because it is too short. Lengthening the probe produces a dramatic decrease in efficiency.

A Simple Motorised Aspirator

Chan (1984) has shown that a similar effect on soft tissues can be gained from a simple motor driven device. This is shown below (figure 1:3). A high speed DC motor operating up to 24 volts was used. The highest speed of the Chan instrument achieved by the motor was approximately 20,000 rpm. A hollow stainless tube of outer diameter 2.3 mm was coupled with the shaft of the motor by an off-centre cam. The rotational motion of the motor was then converted into the reciprocating motion of the hollow tube which was fixed on the cam housing with a screw. The amplitude of the reciprocating motion was determined by the off-axis distance of the cam. Suction can be applied to the hollow tube. Irrigation of saline was applied through another plastic tube attached to the probe's casing. The frequency of the reciprocating motion could be adjusted by using varying voltages across the DC motor. The vibration amplitude could be adjusted by using different cams with different off-axis distances.

This appliance was compared with the ultrasonic surgical device in the removal of ox liver per unit time in bench experiments. In each experiment, a piece of ox liver was weighed. Then the ultrasonic aspirating tip, operating at full vibration amplitude (300 microns) with maximum suction pressure of about 60 cm of mercury (Hg) and a slow irrigating rate of saline was continuously applied to the ox liver for one minute. This piece of liver was then carefully dried with absorbent paper and re-weighed. The amount of liver removed by the ultrasonic surgical aspirator was 7.9 g + or - 1.6 g (one standard deviation in 10 readings) per minute. The motor-driven probe was used in exactly the same way

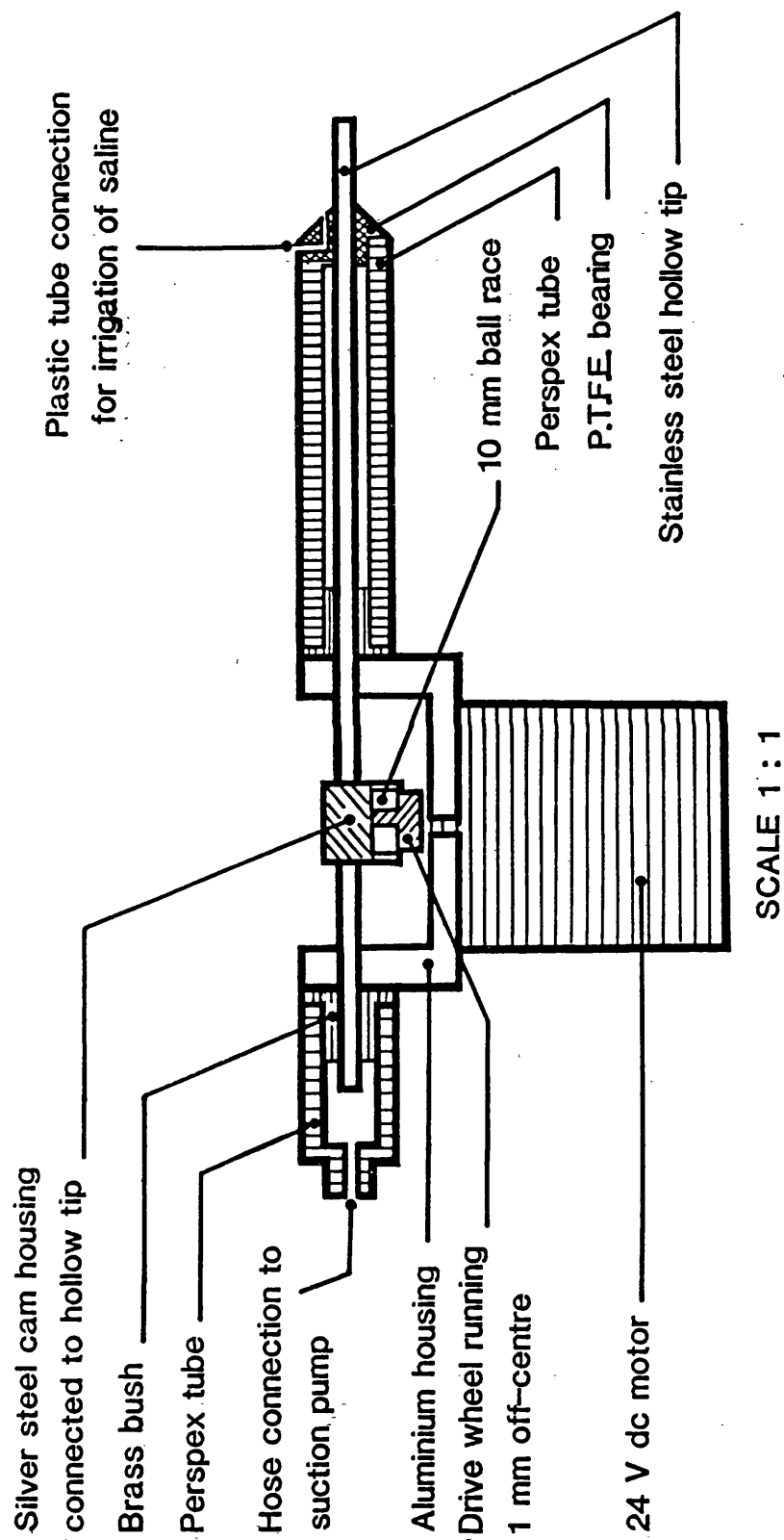


Figure 1:3. Chan's motorised aspirator.

with a frequency of vibration of 250 Hertz and a maximum amplitude of vibration of approximately 1 mm with a maximum suction pressure of 55 cm of Hg (irrigation rate of 20 ml/min). The motor-driven probe could remove liver at 7.0 ± 1.1 g/min (one standard deviation in 10 readings). The simple, inexpensive motor-driven device designed by Chan was therefore shown to be as effective as the much more expensive and quite complicated ultrasonic surgical aspirator.

The ultrasonic device which makes use of ultrasonic vibration is a resonating system, the frequency of which depends on the length of the magnetostrictive transducer. The length of the velocity amplifier is constrained by the ultrasonic wavelength. The drive circuit has to be matched with the exact resonant frequency for efficient ultrasonic vibration, but the motor-driven vibrator/aspirator can be operated over a range of frequencies and with different vibration amplitudes. No restriction is therefore imposed on the length of the vibrating tip of the simple motor-driven device and this can be changed to suit surgical purposes, e.g. an endoscopic application, which has as yet proved very difficult with the ultrasonic aspirator.

These initial experiments comparing Chan's motor-driven device with the expensive ultrasonic aspirator lead us to believe that we could produce our own efficient liquidiser and aspirator that would go further than these devices in that it would be able to remove all forms of tissue, be they soft or fibrous.

CHAPTER 2

DEVELOPMENT OF THE PROTOTYPE E.L.S.A.

(or The Kitchen Blender in Cordon Bleu Urology)

The function of tissue liquidisation is one already performed by commercial food processors and simple kitchen blenders. These rely on extremely high blade speeds and the confinement of the medium being liquidised in order to break up its inherent structure. The typical power requirement of an ordinary kitchen food processor varies from 200 to 400 watts; hand held versions are also available and these use a lower power (100 watts). My first practical step was to purchase a "Braun Multiprac" hand held blender from a local store. This uses a 30 mm blade rotating at approximately 2,000 rpm. It is sufficient to liquidise raw liver in a matter of seconds and portions of steak within a few minutes. An attempt has been made to miniaturise such a kitchen blender to a size that could be used endoscopically. My conceptual idea for this instrument required the following components:

- a) a high speed rotary cutting action,
- b) irrigation for liquifaction,
- c) aspiration of all material,
- d) the ability to carry out this technique in a confined housing with good visualisation of the whole process.

In order to use such an instrument within the working channel of a cystoscope, a maximum outer diameter of approximately 5 mm was required. This was technically an enormous design step from the crude large ^{h.f.} _{so!} commercial kitchen instruments and it was felt that the first prototype should be approximately 10 mm which could be more easily constructed and still answer our hypothetical questions. - It was set up as a bench model (figure 2:1 and 2:2a). This was constructed from a stainless steel tube (outer diameter 12 mm, internal diameter 10.5 mm) attached to a Black and Decker model drill motor (max 10,000 rpm.). The brass bearing carried a steel shaft and also confined the liquification process to the terminal portion of the tube. Into the terminal "active" portion were drilled ports for irrigation and aspiration at points 180° apart. Vibration necessitated fixation to a rigid frame.

Satisfactory liquifaction had occurred with a 30 mm blade at 2,000 rpm (rotational speed = 3.14 m/sec) with the hand-held Braun Multiprac blender. The most important parameter when considering the effectiveness of the cutting blade is the blade speed relative to the object being cut. The speed at the tip of 2 blades of different lengths vary directly as the ratio of their lengths for a constant rotational speed. The first bench prototype had a blade diameter of 10 mm (ratio 1:3) and therefore the prototype's motor would have to be capable of at least 6,000 rpm (3:1), to produce the same rotational speed (*Rotational speed = distance tip of blade travels in 1 revolution ($\pi \times D$) / time for one revolution*).

The blade itself was surrounded by a housing which confined the tissue being cut at the same time as drawing fresh tissue into the blade. The



Figure 2:1. The first experimental bench liquidisor/aspirator.

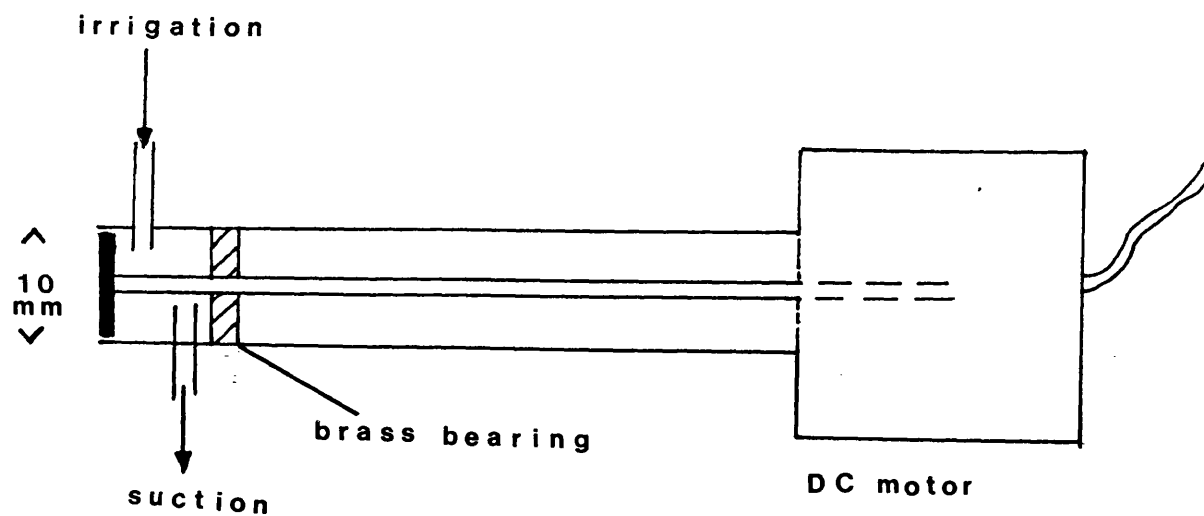


Figure 2:2a. Diagram of the first experimental bench liquidisor/aspirator.

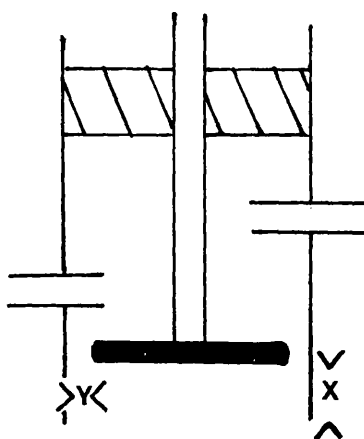


Figure 2:2b. Diagram of housing parameters in bench model.

mechanism of cutting and the flow of fluid and particles into the housing has been demonstrated on the bench model by replacing the stainless steel tube with one made of rigid perspex. This allowed close up video monitoring during liquidisation with freeze-frame analysis. Confining the liquifaction process to the housing not only provides a mechanism for repeated cutting of tissue, but also prevents tissue splashing and one could foresee better visualisation of this process once adopted in an endoscopic form. Interchangeable blades were cut from 2 mm stainless steel plate.

An important part of the device was the provision for irrigation of the cutting blades by water or saline and the removal of this fluid along with the liquidised tissue via a suction tube. These tubes would ultimately run alongside the drive shaft to aid cooling but in our initial model entered from the side.

Performance of the First Prototype Tissue Liquidiser/Aspirator

The most important question was "Would it work?". It did! Important parameters in such a new device were unknown. The parameters considered were:

- a. *Blade profile.*
- b. *Blade position.*
- c. *Housing design.*
- d. *Irrigation.*

e. *Suction.*

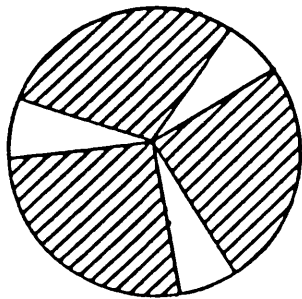
f. *Blade speed.*

The effect of varying each component or parameter was judged by the removal rate of the target tissue whilst keeping all other parameters constant. The liquidiser was lowered onto the target tissue. All specimens were weighed dry with absorbent paper before and after 1 minute of continuous action. Each experiment was repeated ten times. The mean results are given below. Statistical significance for any of these parameters has been evaluated using the "Student t test" (Student 1908) suitable for comparing the means and standard deviations of 2 sets of measurements where the number of observations is less than 30. In accordance with this protocol, the null hypothesis, that there is no difference, has been considered.

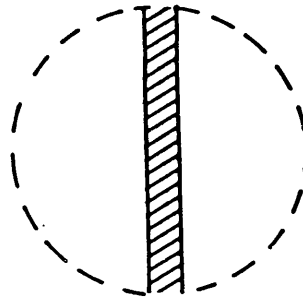
The blade profile, position and housing design were investigated with the bench prototype. Suction pressure was at "maximum" (approximately 30 cm Hg) from a house-hold pump. Irrigation was delivered at a standard rate of approximately 20 ml/min from an intravenous giving set. The motor was run at its maximum of 10,000 rpm. Fresh pig's liver was used as the target tissue.

a. *Blade profile:* 2 different blades were cut from a 2mm stainless steel sheet with contrasting surface areas or profiles (figure 2:3). The bar blade was used in a second run of experiments with its leading edges filed down.

BLADE DESIGN



A



B

Figure 2:3. End on view of blades made for the bench model in figure 2:1.

<u>Blade</u>	<u>Mean removal rate (g/min)</u>
Large surface area	3.4
Small surface area	6.0
Small surface area + sharp edges	6.2

There is a significant statistical difference between the large and small surface area blades ($t = 8.5$, $p < 0.001$), but not between the sharp and blunt bar type blades ($t = 1.12$, $0.5 > p > 0.1$).

b. Blade position: The bar blade was positioned at varying distances from the outer rim of the housing (see figure 2:2b (x)).

<u>Position x</u>	<u>Mean removal rate (g/min)</u>
0 mm	7.2
2 mm	5.8
5 mm	5.0

There is a significant statistical difference between $x = 0\text{mm}$ and $x = 2\text{mm}$ ($t = 13.46$, $p < 0.001$) but not between $x = 2\text{mm}$ and $x = 5\text{mm}$ ($t = 2.7$, $0.02 > p > 0.01$).

c. Housing design: The bar blade was kept flush with the end of the housing ($x = 0\text{mm}$), but it's tips were gradually filed away (see figure 2:2b (y)). Removal rates were measured with clearances of 2/1000, 5/1000 and 15/1000 inch from the tip of the blade to the side of the housing.

Position y

Mean removal rate (g/min)

2/1000 inch	7.0
5/1000	6.5
15/1000	3.2

There is no statistical difference between $y = 2/1000$ and $y = 5/1000$ ($t = 1.16$, $0.5 > p > 0.1$), but there is between $y = 5/1000$ and $y = 15/1000$ ($t = 6.45$, $p < 0.001$).

The housing of the blade is important to allow the tissue to be drawn onto the blade by the negative pressure, facilitate recirculation for repeated cutting and to prevent extrusion which would impair visualisation in future endoscopic forms. Some experimentation with suction, irrigation and blade speed were carried out with the bench prototype but results were inconsistent due to the inability to calibrate these parameters. Empirical observation showed that the main role of the irrigation was for cooling and that the correct rate was that which the suction pressure provided would completely remove without splashing occurring. The accurate analysis of (e) suction and (f) blade speed was achieved with the next prototype.

Design of the Clinical Liquidiser/Aspirator

Sufficient encouraging information had now been gained to design an instrument small enough to be passed through an endoscope. Reduction of the blade diameter to approximately 5 mm would always reduce the efficiency

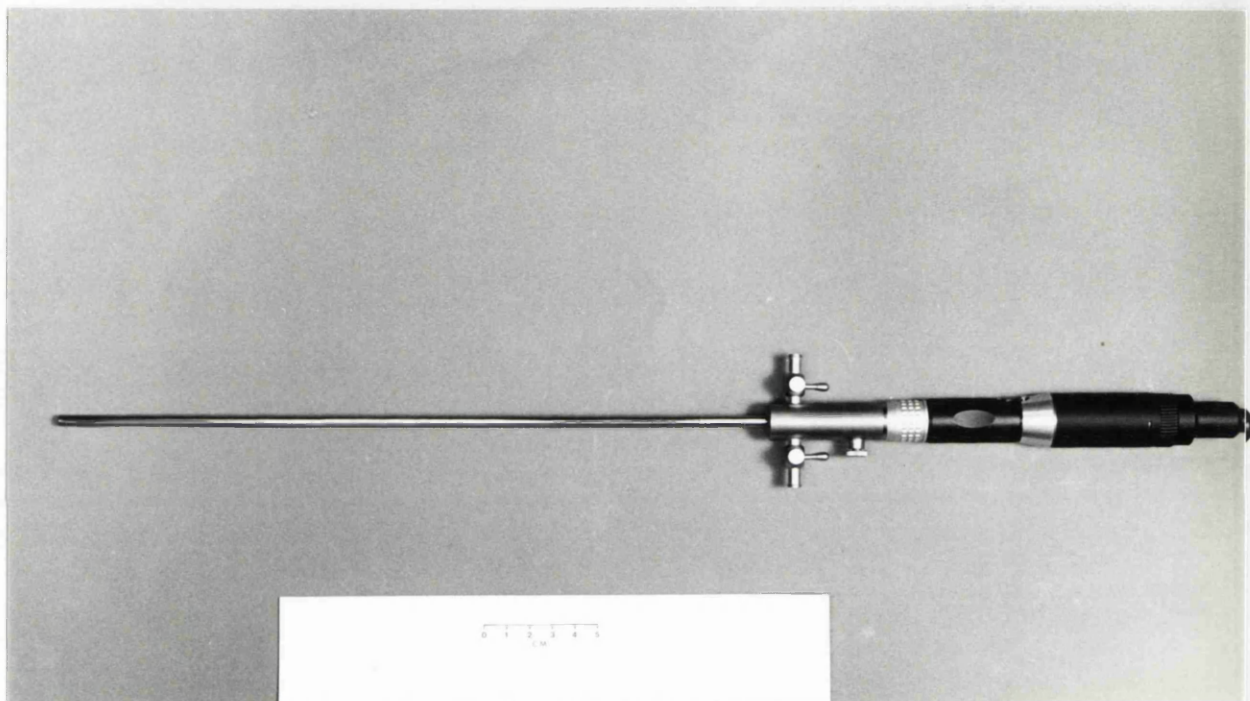


Figure 2:4. Bien Air MC 40 GT DC motor connected to the 5 mm clinical liquidiser.

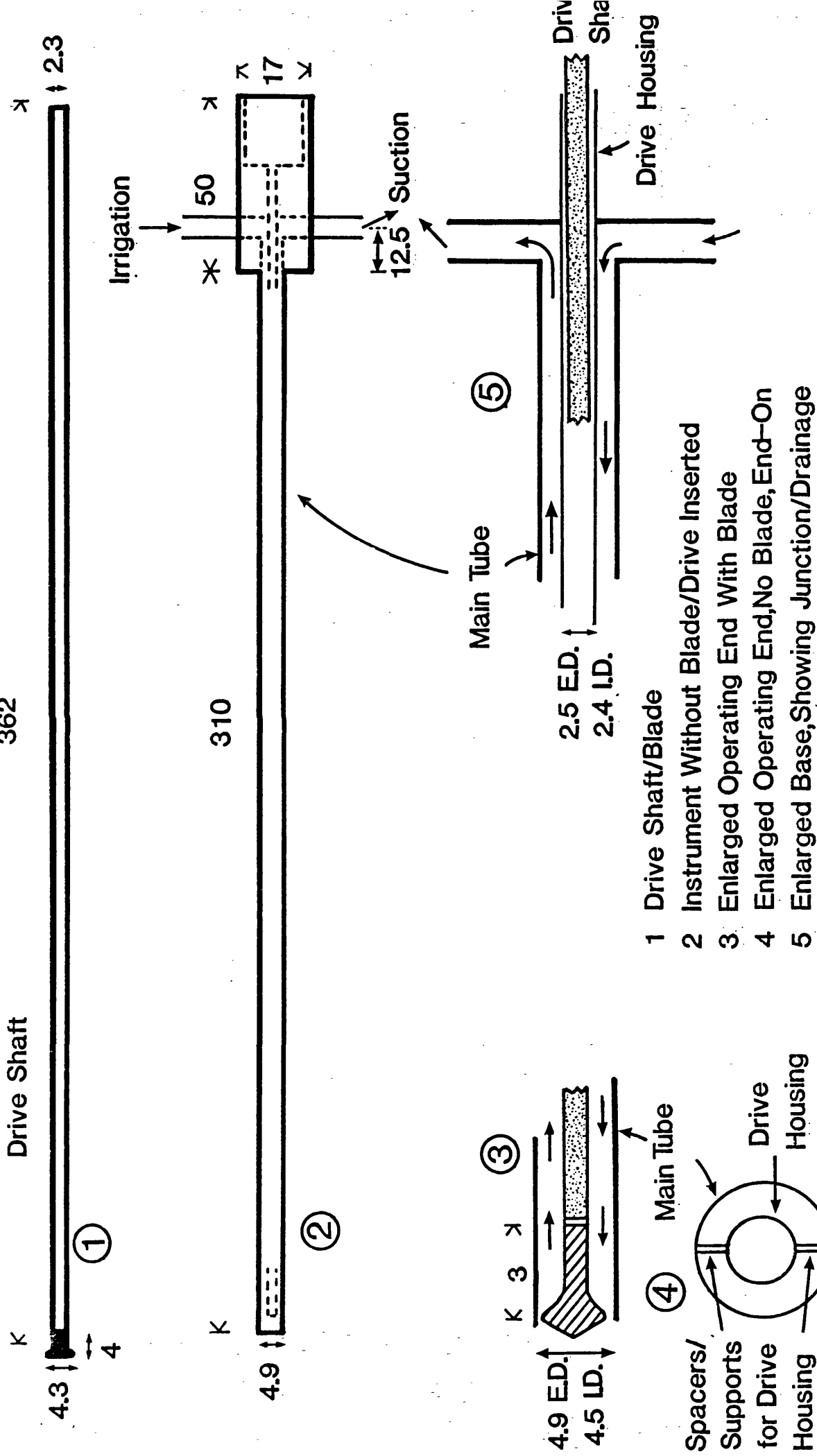


Figure 2:5. Design of the 5 mm liquidiser/aspirator of the ELSA.

of the instrument and so a 10 mm design was also created for use as a hand held instrument at open operation or as a laparoscopic tool operated through a separate sheath to the endoscope. Both instruments were to be driven by an electrical motor weighing only 300 g and capable of speeds up to 40,000 rpm, well in excess, despite the reduction in blade size, of our bench experimental requirements (BIEN AIR MC 40 GT - figure 2:4).

Several motors were compared at the Eastman Dental Hospital. The motor chosen had the advantage of a very high torque. The current through the motor was monitored during the instrument's action on not only soft tissue but also wood, bone, and urinary stones. No detectable change in current occurred indicating the that torque was so high that no significant resistance was met. Such torque is not present in air driven motors. The design of the 5 mm instrument is shown in figure 2:5. The Genito Urinary (GU) manufacturing Company assembled these designs. The design and use was patented in April 1987.

The accepted reduction in blade diameter was more than compensated by the increase in potential rotational speed of the blade from a more powerful motor. The maximum power of the new motor was 40,000 r.p.m. which produced a rotational speed of 9.4 m/sec at the tip of the 4.5 mm blade (cf: 3.14 m/sec for the original Braun commercial blender).

This second prototype was assessed according to tissue removal rate on pigs' liver and human prostate (removed at retropubic prostatectomy) whilst varying the following parameters:

- e. *Suction* (0 - 75 cm Hg); from a "Wolf" peristaltic pump.
- f. *Blade speed* (0 - 40,000 rpm). Blade speeds throughout this study were also confirmed with an optical tachometer.

Previous experiments had shown that: irrigation was essential but its rate immaterial; the blades should be flush with the end of the housing and have minimal side clearance; and the best blade shape was a flat, thin bar. All assessments were for 1 minute using both liver and prostate. Each assessment was repeated ten times.

The following matrix of variables was considered:

	250		10,000	
suction (mm Hg)	500	X	20,000	blade speed (rpm)
	750		40,000	

with the same bar blade, $x = 0$, $y = 2/1000$ inch and 10 mls/min of irrigation for both tissues.

Results

1. Liver (mean of 10 measurements in g/min).

	<u>250</u>	<u>500</u>	<u>750 mm Hg.</u>
<u>10,000 rpm</u>	1.0	3.4	3.2
<u>20,000</u>	2.0	4.0	3.8
<u>40,000</u>	2.20	7.8	14.6

These results are shown graphically in figure 2:6. At 40,000 rpm, the removal rate was statistically significantly greater for 75 cm Hg than for 50 cm Hg ($t = 3.2$, $p < 0.001$) and for 50 cm over 25 cm Hg ($t = 7.8$, $p < 0.001$). At 75 cm Hg, the removal rate was statistically significantly greater for 40,000 rpm than for 20,000 rpm ($t = 10.2$, $p < 0.001$), but not for 20,000 over 10,000 rpm ($t = 2.65$, $0.02 > p > 0.01$). At relatively low suction pressures and blade speeds there are other negative forces coming more into play. This was ultimately found to be due to the relative particle sizes (vide infra).

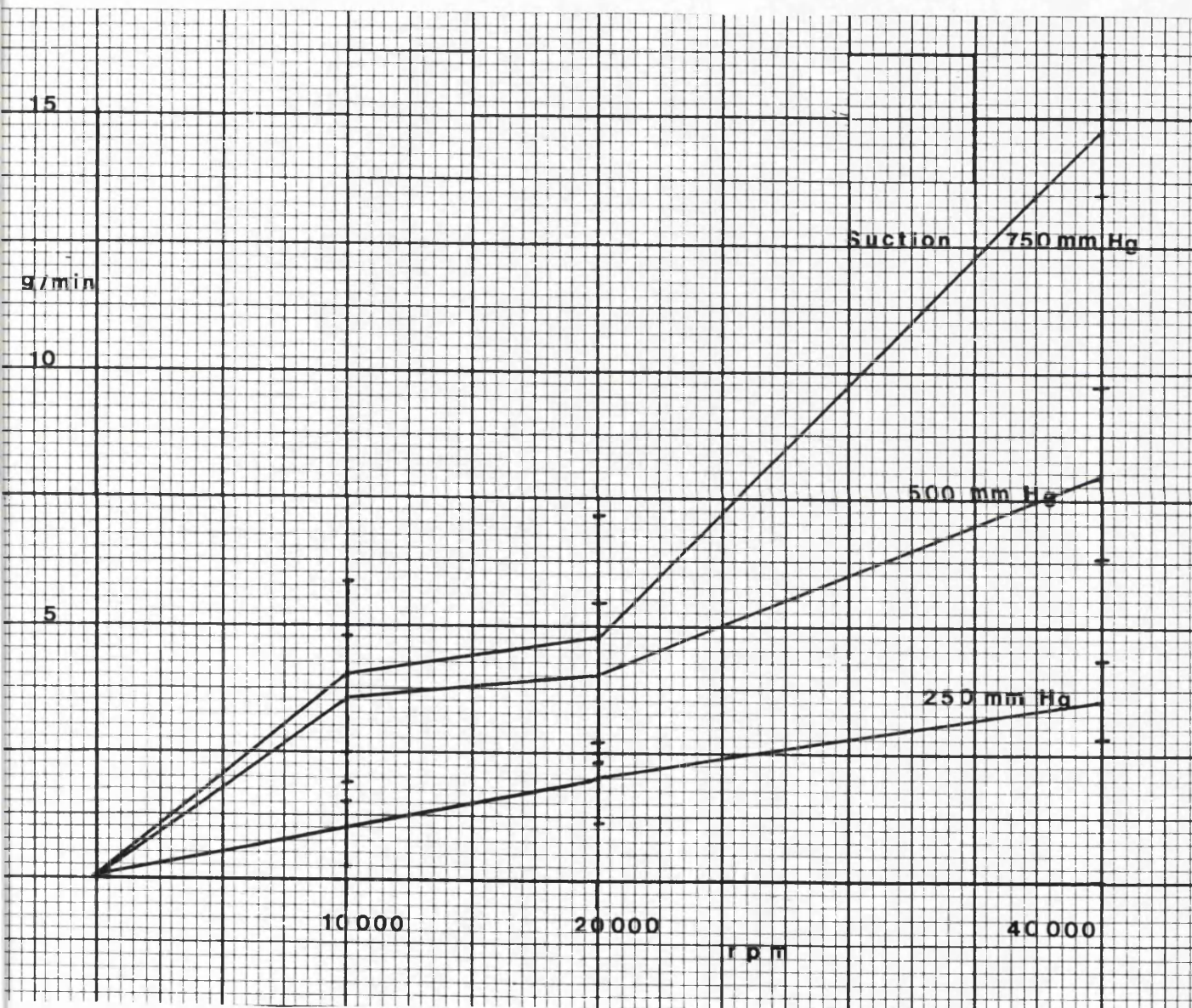


Figure 2:6. Removal rate of liver plotted against blade speed for 3 different suction pressures, using the 5 mm clinical ELSA. Each coordinate is a mean of 10 measurements.

2. Prostate (mean of 10 measurements in g/min).

	<u>250</u>	<u>500</u>	<u>750 mm hg.</u>
<u>10,000 rpm</u>	0.3	0.3	0.4
<u>20,000</u>	0.4	0.5	0.6
<u>40,000</u>	1.2	2.0	2.4

The most efficient rates of tissue removal were at the highest blade speeds and suction for both tissues. Tissue removal is directly proportional to both blade speed and suction pressure. The difference between the action on liver and prostate is large after 1 minute (14.6 cf 2.4 g/min)but is exaggerated further when looking at the accumulative rate of tissue removal measured for each subsequent minute.

Figure 2:7 graphically shows the problem that the ELSA was having with the fibrous prostate. This shows the mean removal rates from both liver and prostate tissue, assessed every 30 seconds, in the standard way for 3 minutes. The accumulative removal rate rapidly decreases after 1 minute at all speeds. Fibrous strands from both tissues, but more so from the prostate, would both wrap around the blade and block the suction channel within the first minute. A "trimmer" principle was suitable for soft tissues, but anything containing a significant fibrous element possibly required a cutting blade. This problem had first appeared to a much lesser degree with the 10 mm bench model but was exaggerated with minaturisation.

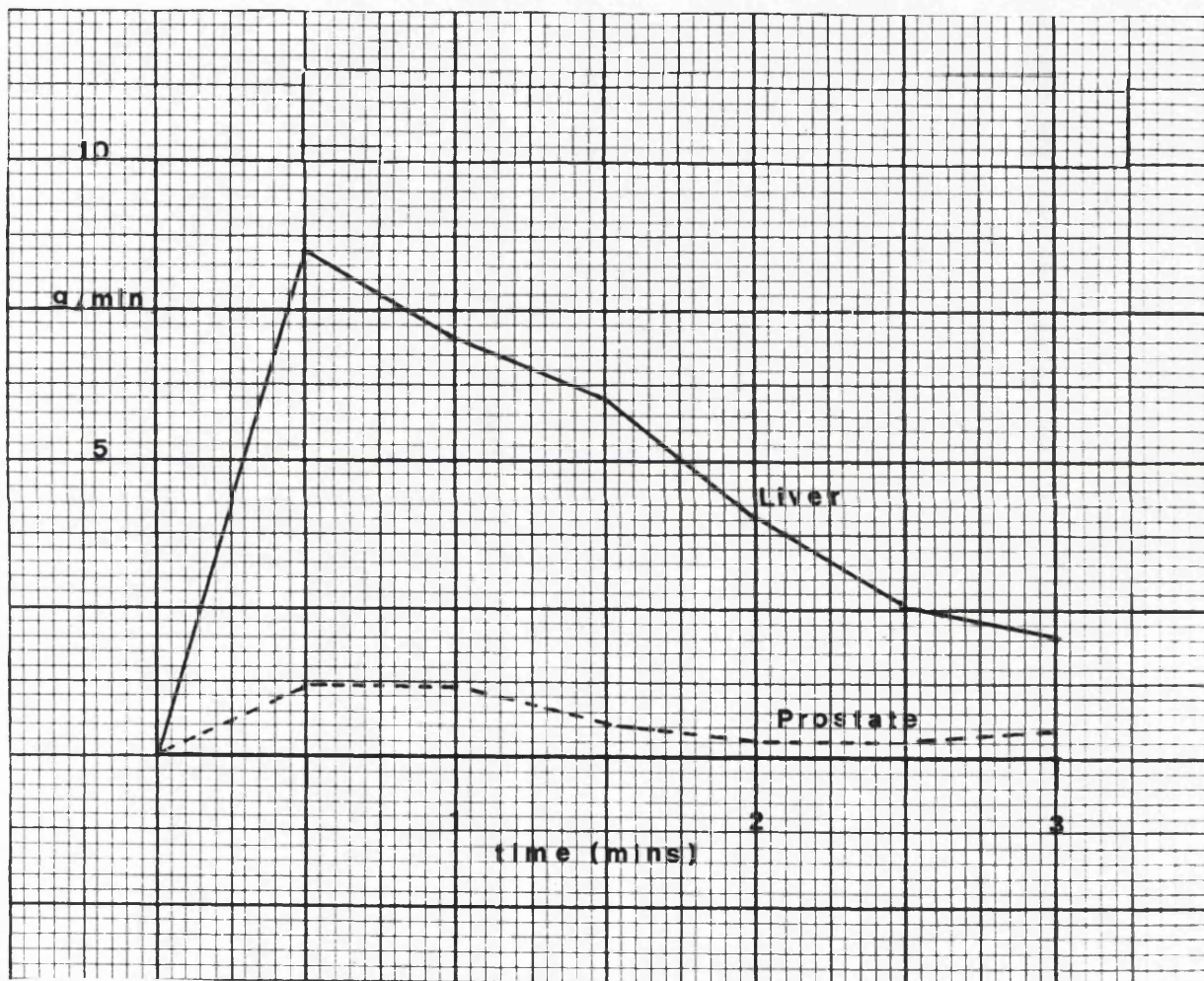


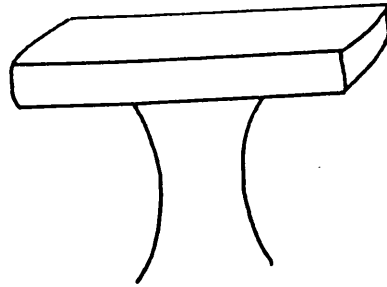
Figure 2:7. Removal rate of liver and prostate tissue plotted against time with the 5 mm clinical ELSA at 40,000 rpm and 75 cm Hg suction. Each coordinate is a mean of 10 measurements.

Despite the encouraging information gained a problem remained with very fibrous tissue. The blade configuration would not penetrate this without great force. This was also found with capsular materials and unfortunately with benign prostatic tissue specimens. The advantage with this limitation is that as it stood the newly designed instrument would have the same selective action as the ultrasonic aspirator. It could therefore be seen as a viable, cheaper, yet more efficient instrument for the removal of soft tissues such as liver, kidney or brain either at open surgery or endoscopically. But to make a liquidising/aspirating instrument that would penetrate and remove fibrous tissue further work was required.

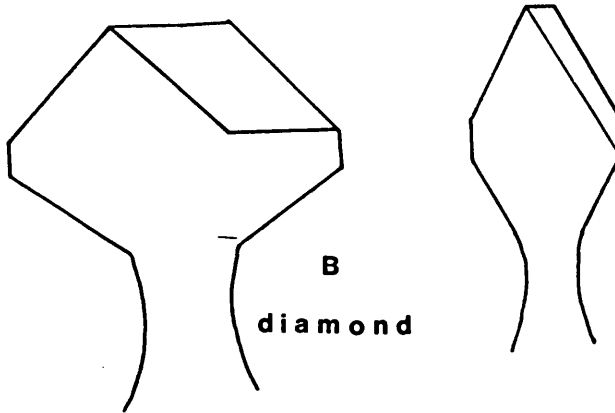
Tissue Characteristics and Blade Design

A system had been found that could efficiently remove soft tissues such as liver or renal cortex but the blade lacked penetration into capsular materials and a significant effect in prostatic tissue. In order to determine the shape of blade that would penetrate such tissues, different shaped blades (figure 2:8) at different speeds and suction were analysed in relationship to the load/displacement characteristics of each tissue used in this study. All the blades were long and narrow when viewed end on (high aspect ratio as in the simple bar blade) in accordance with the optimum design for liquidisation shown above. This brought into consideration the relatively unexplored field of material sciences of organic tissues. Much work has been done concerning the characteristics of tendons, bone, and ligaments in relation to orthopaedic applications, but little reference could be found to work detailing the characteristics

A
flat bar



B
diamond



C
raked "propellor"

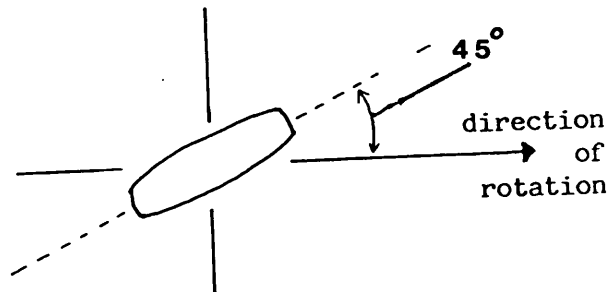
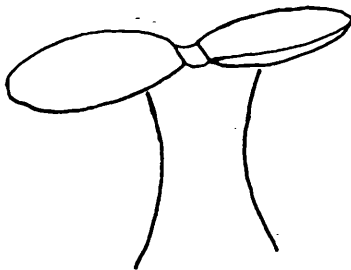


Figure 2:8. Blades made for the clinical ELSA.

of liver, kidney, prostate, muscle, and fibrous capsular material in response to compression and cutting. A blade's action is mainly dependent on the effects of compression and tension in a particular material. The ideal blade to penetrate a fibrous capsule (and the very fibro-elastic prostate) should show a high strain/displacement rate through such tissues with minimum applied stress (load) under standard conditions.

Strain is the amount of stretch under load per unit length. Obviously, different lengths of material stretch or compress different distances under the same load. So:

$$e = \frac{l}{L}$$

where e = strain, l = total amount of stretch and L = original total length. Strain is independent of the size of a specimen and is thus a fraction of the original length and remains as a fraction or a ratio and has no units. For example, if an object 100 cm long stretches 1 cm under load then it is subject to a strain of $1/100$ or 0.01 or 1.0%. So also is an object of 50 cm which stretches 0.5 cm and so on. This behaviour is related to the bonds between the component molecules. The physico-chemical bonds between inorganic and organic materials produce a linear relationship between stress and strain up to strains of a few percentage for inorganic materials, to over 50% for some organic composites (Gordon 1983). Furthermore, for small strains the whole process of extension or compression and recovery is reversible and the behaviour is termed elastic.

If we consider the stresses and strains in a material, inorganic or organic, then;

stress = \underline{s} = constant (E)

strain e

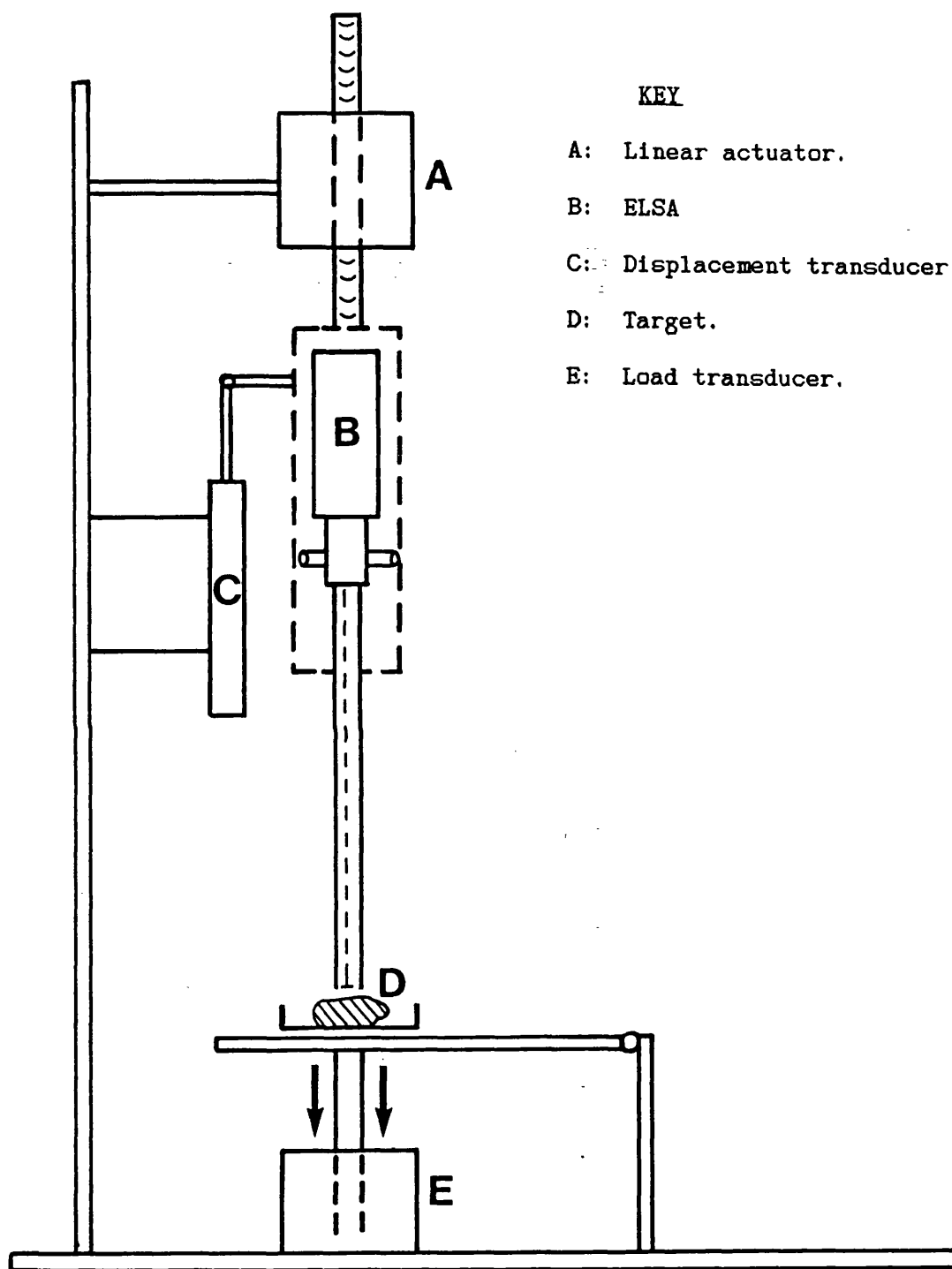
This constant can be said to represent the springiness of a tissue. Its equivalent in the engineering world is Young's Modulus. E is then an estimation of the deflection or displacement in a tissue when it is loaded.

The problem encountered in penetrating and cutting prostatic tissue is that the displacement must be taken past the point of elasticity with the minimum of stress, to the point of fracture or rupture. The relationship of stress (load) and strain (displacement) in different tissues and their characteristic points of dislocation with different blades have been shown in a series of experiments.

The apparatus used is shown in figures 2:9 and 10. The apparatus allows the ELSA to be loaded onto a linear actuator (A). As it is driven into the target, two variables can be measured: the applied load, by means of a load transducer (E); and blade displacement, via a displacement transducer (C). These measurements were recorded directly onto a paper chart recorder. The specimens used were renal parenchyma, beef steak and human prostate tissue. Although liver has always been the standard target tissue (Chang 1986), renal parenchymal tissue was now being used because it had almost identical characteristics and was more relevant to future clinical use of the ELSA. All specimens were fresh.



Figure 2:9. Apparatus assembled for measuring load/stain characteristics of different soft tissues.



KEY

- A: Linear actuator.
- B: ELSA
- C: Displacement transducer.
- D: Target.
- E: Load transducer.

Figure 2:10. Diagram and key to apparatus shown in figure 2:9.

Each measurement was achieved in the following way: the measuring point of the displacement transducer was set to correspond to the cutting tip of the ELSA in line with the base of the target tissue. The ELSA was taken up above the target and brought down onto the target until a load of 1 gram was applied for the specific thickness of the target. The speed of the motor was varied to maintain a strain rate of 0.025 mm/sec. This ensured that thickness did not affect the results. The ELSA was then brought down at this fixed strain rate in 25 micron steps and the displacement recorded on a paper chart as load increased.

The first (M1) experiment was designed to assess the load strain characteristics of the 3 tissues. A constant area applicator was required in each case under different loads and the ELSA with an immobile flat blade was used for this. The experiment was repeated three times for each tissue.

Experiments M2, M3, and M4 were designed to examine the effect of load on strain, measured as displacement of the ELSA through the sample for each individual tissue. The experiments were repeated at varying blade speeds and with either a flat or diamond shaped blade.

Results of load/strain Experiments; see figures 2:11 - 2:14

Experiment M1 (figure 2:11): Both prostate and muscle show a load/strain curve typical of a complex visco-elastic material, whether inorganic or organic in origin. An initial loading produces a significant strain which

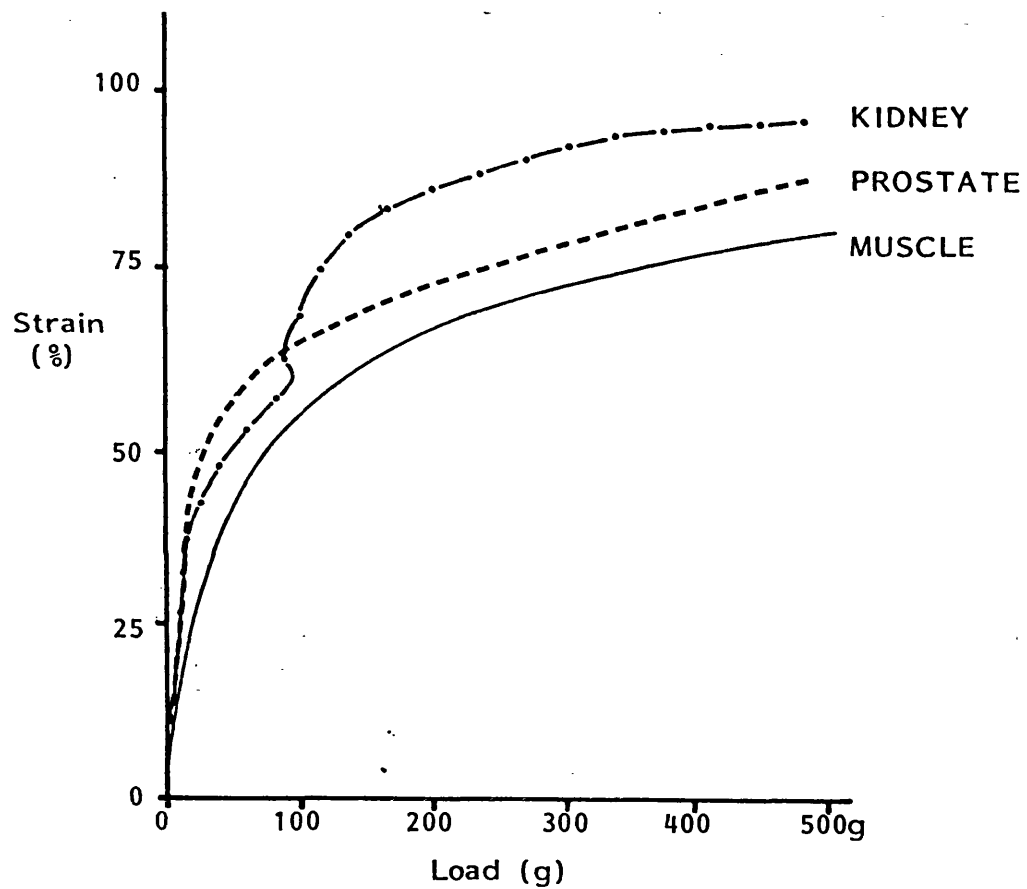


Figure 2:11. Load/strain curves for kidney, prostate and muscle samples.

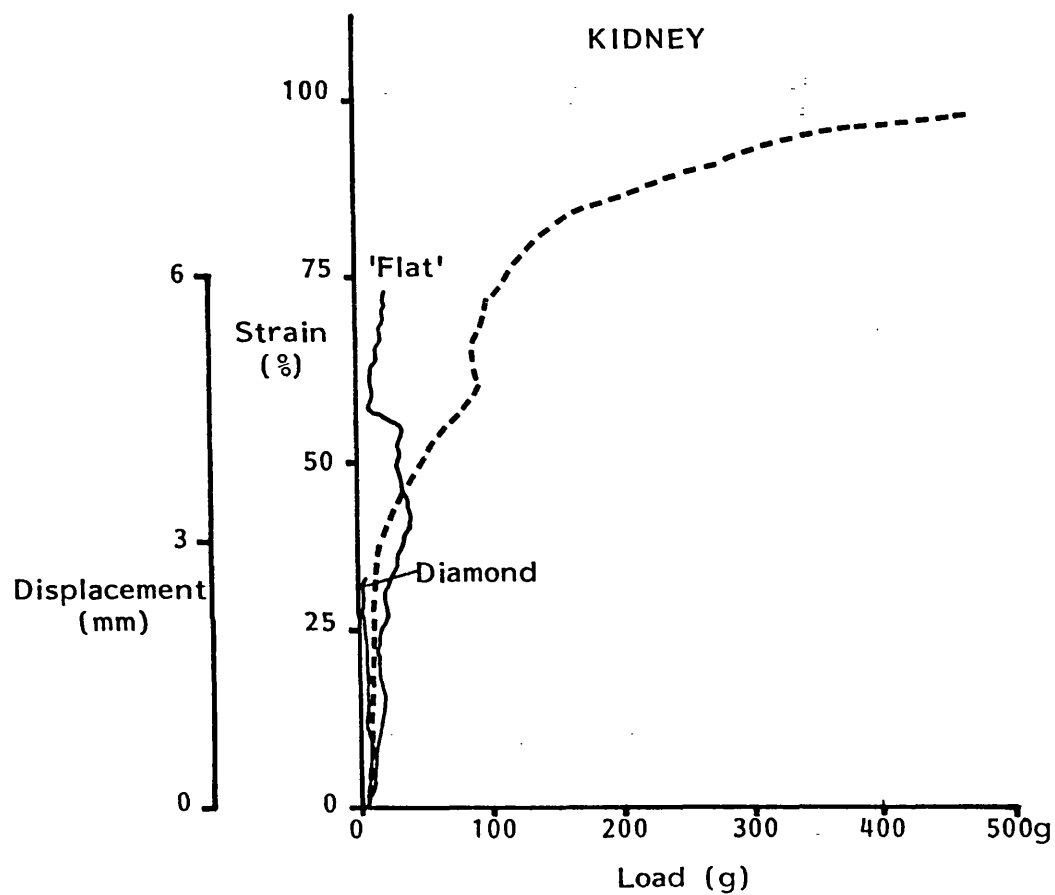


Figure 2:12. Load/strain (displacement) curves in renal cortical tissue showing the effect of the working ELSA with flat and diamond blades.

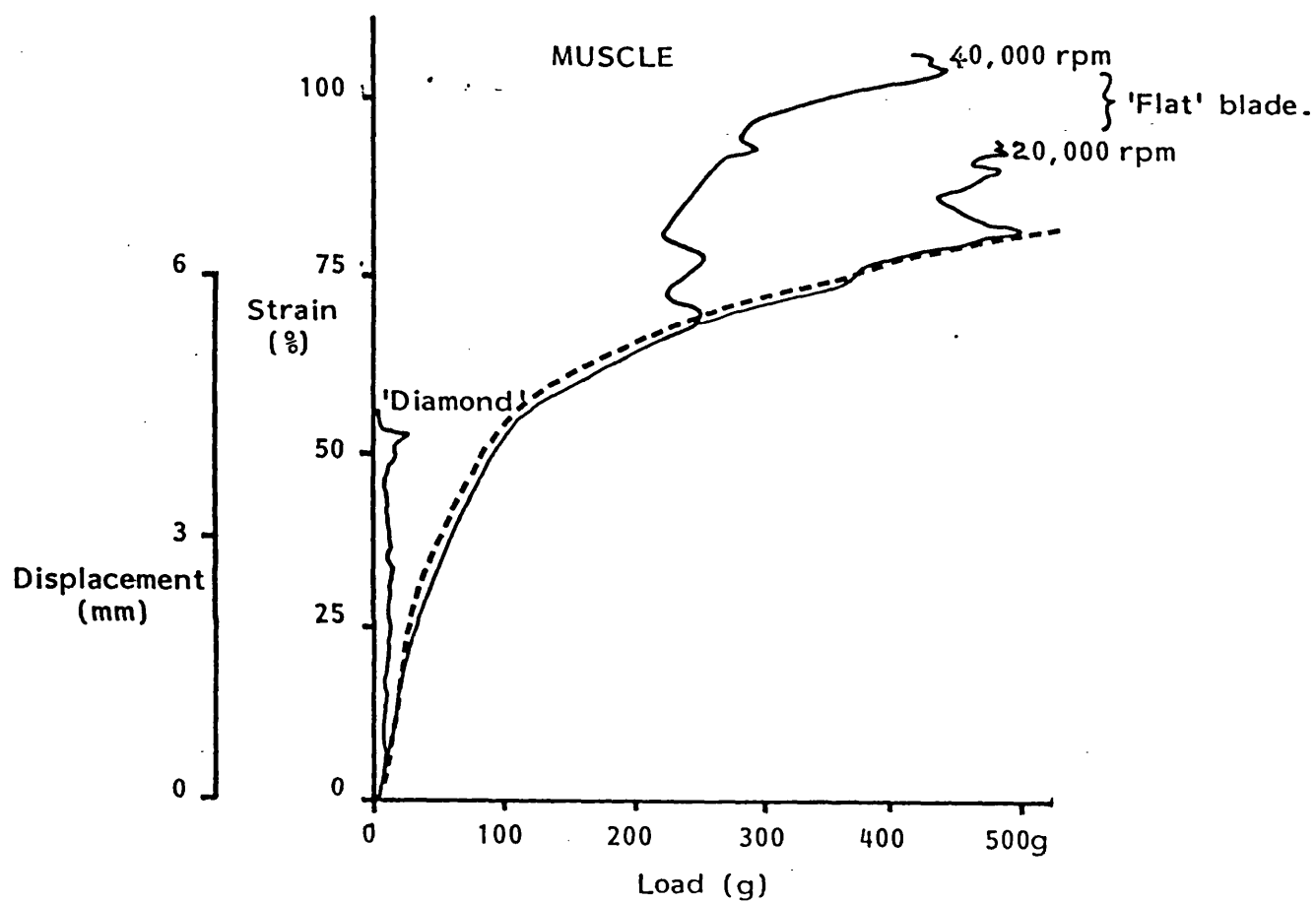


Figure 2:13. Load/strain (displacement) curves in muscle tissue showing the effect of the working ELSA with different blades at varying speeds.

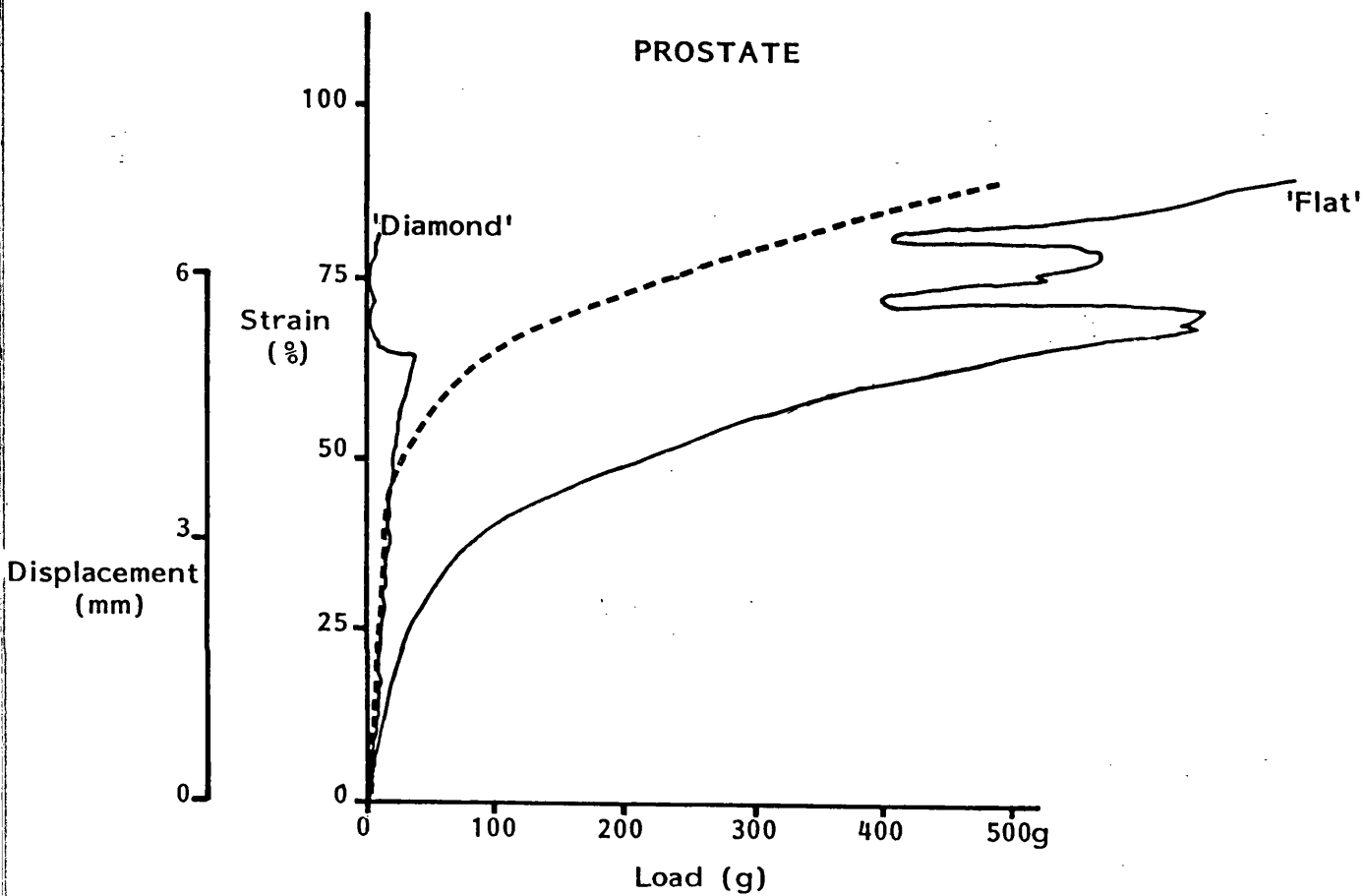


Figure 2:14. Load/strain (displacement) curves in benign prostatic tissue showing the effect of the working ELSA with different blades.

is then resisted and counteracted as the molecules are further compressed. Both muscle and prostate samples slowly returned to their original size when a maximum loading of 500 g was removed. In contrast to this, the renal tissue shows a sudden displacement at 100 g loading. The instrument had forced its way through the sample and a return to its original undamaged state was impossible.

Experiment M2 (figure 2:12): The pure load/strain curve for renal tissue has been superimposed (dotted line). Both the flat and diamond blades were used at 20,000 rpm. The results of using either blade is similar on renal tissue. With minimal loading (10 - 20 g) the instrument rapidly fragments the sample. Penetration by a rotary instrument, whatever the blade design, is easy in renal tissue.

Experiment M3 (fig 2:13): The pure load/strain curve for muscle has been superimposed (dotted line). The curves for the rotating flat blade follow the same curve initially, but a sudden displacement then occurs; this is initiated at 250 g at 40,000 rpm but is delayed until 500 g at 20,000 rpm. However, neither performance matches the high displacement, low loading characteristics of the diamond blade, which was similar at both speeds.

Experiment M4 (fig 2:14): Similar results were seen with the prostate as with the muscle specimens. A rotating flat blade will eventually displace the tissue, but only at high loads. In contrast, the diamond blade rapidly penetrates the tissue at minimum loads.

These experiments have quantified what we were beginning to see empirically. A diamond shaped blade is the ideal configuration for fibrous tissue penetration. A flat blade is protective within a fibrous tissue boundary providing the tip velocity is below 5 m/sec (5 mm blade at 20,000 rpm) under 500 g loading, but efficient at penetrating, displacing, and cutting soft tissues.

Having shown that a diamond shaped blade penetrates fibrous tissue effectively, it then required evaluation with respect to tissue removal rate. At 40,000 rpm and 75 cm Hg suction, the removal rate of prostatic tissue was only 0.4 g/min - less than the flat blunt blade (2.4 g/min). However, a 45° raked blade (figure 2:9"C") provided a compromise in that it had penetrated fibrous tissue almost as well as the diamond blade in the load/displacement experiments, and at optimum settings with this new blade the removal rate of prostatic tissue was 2.0 g/min. (+/- 0.4 after 10 runs of 1 minute each). The two blades that would be used clinically would therefore be a flat blunt bar for selective removal of soft tissue, and the 45° raked blade for penetration and removal of fibrous tissue.

The integrated endoscope

The initial role of the smaller integrated endoscopic instrument was for use transurethrally. With this in mind the GU Company supplied a modified nephroscope of a 27 French (F) outer calibre (fig 2:15).

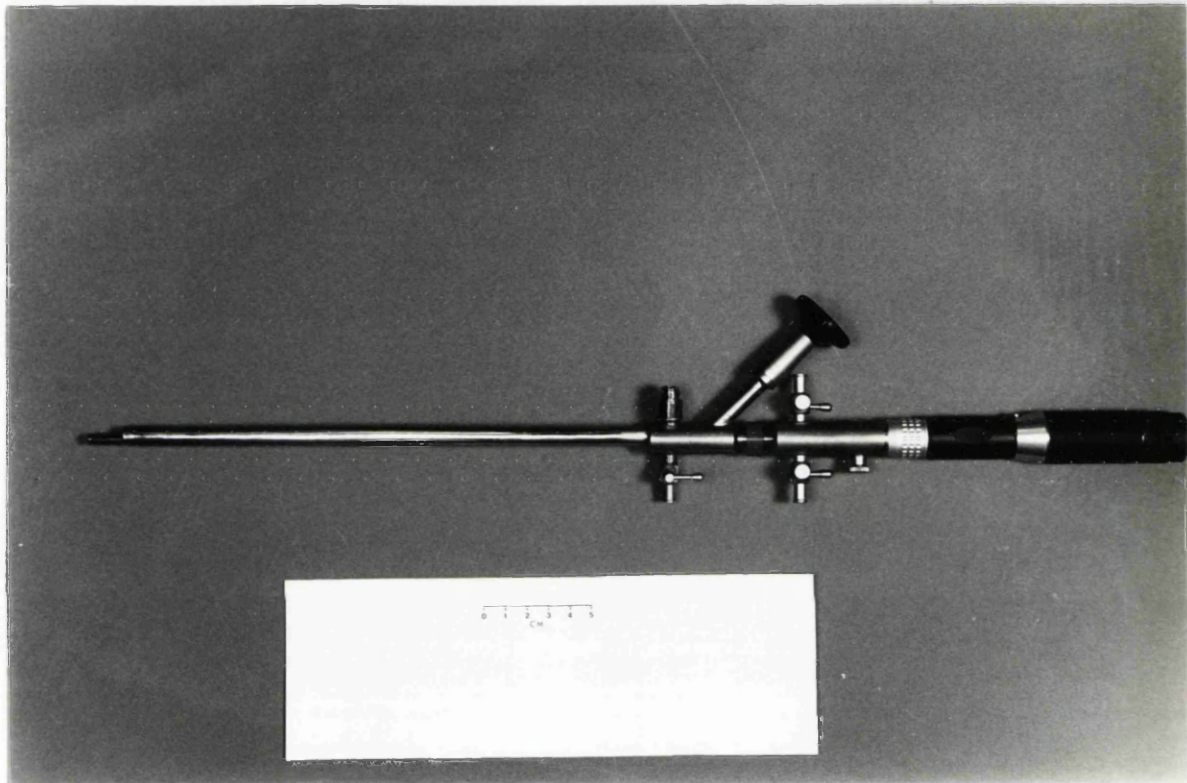


Figure 2:15. The complete 5 mm ELSA showing the liquidiser/aspirator within the modified nephroscope.

This contained a Hopkins rod lens system with an off-set eye piece to allow the introduction of the rigid 5 mm ELSA through the instrument channel. The objective lens has a field of vision of 100° and a focal point 2 cm distant and 10° inferiorly. This therefore became the ideal visual working position of the ELSA (2 cm from the tip of the endoscope), the instrument channel being below the lens.

The outer diameter of the small ELSA is 5 mm. The internal diameter of the instrument channel of its endoscope is 5.8 mm. For transurethral work the subtracted space provides the facility for 110 ml/min of saline irrigation at a back pressure of 60 cm H_2O . This is comparable to the working conditions during routine transurethral diathermy resection (100-180 ml/min at 60 cm H_2O). This is essential for clear visualisation because the infusion into the ELSA itself is only for liquidisation. Adding methylene blue to the ELSA infusion has shown that it is confined to the blade housing before being aspirated. Adding methylene blue to the endoscope irrigation infusion has shown that most is aspirated through the ELSA. This was fortuitous because it later enabled us to utilise the infusion space inside the ELSA for a diathermy cable and yet still achieve satisfactory liquidisation when used with the irrigating endoscope. Both spaces, for infusion and aspiration, are required in the larger, 10 mm, ELSA because it is usually used laparoscopically where visualisation is achieved with gaseous insufflation.

A laboratory comparison between the 5 mm ELSA, CUSA, and a Nd:YAG laser for tissue removal

The C.U.S.A. and Nd:YAG laser have been described in Chapter 1. It now seemed appropriate to compare the 5 mm ELSA with its newer efficient blade. Pigs' liver and human prostate were again the target tissues. Each modality was used at its highest setting.

CUSA: Max suction, level 10 tissue interaction.

Nd:YAG (Pilkington Medilase): 80 Watts, continuous waveform,
non contact 600 micron fibre.

ELSA: 40,000 rpm. and 75 cm Hg suction.

Each tissue sample was targetted under glycine for 5 minutes but brought out, dried with blotting paper, and weighed every minute.

Results

1. Liver (mean of three runs):

CUSA:	7	g/min)
Nd:YAG:	0.5	g/min) after 5 minutes
ELSA:	15	g/min)

2. Prostate (mean of three runs)

CUSA: 0.75 g/min)

Nd:YAG: 0.3 g/min) after 5 minutes

ELSA: 1.8 g/min)

The Nd:YAG laser cannot reach temperatures required for vaporization because of the cooling effect of the glycine. It can only denature the protein and produce charring. This in turn needs an even greater temperature rise to vaporize this carbonised material. Thus the use of such a laser for tissue bulk removal is self-limiting and can be of little clinical value in prostate removal. The clinical value of the Nd:YAG laser lies in tissue destruction but not removal.

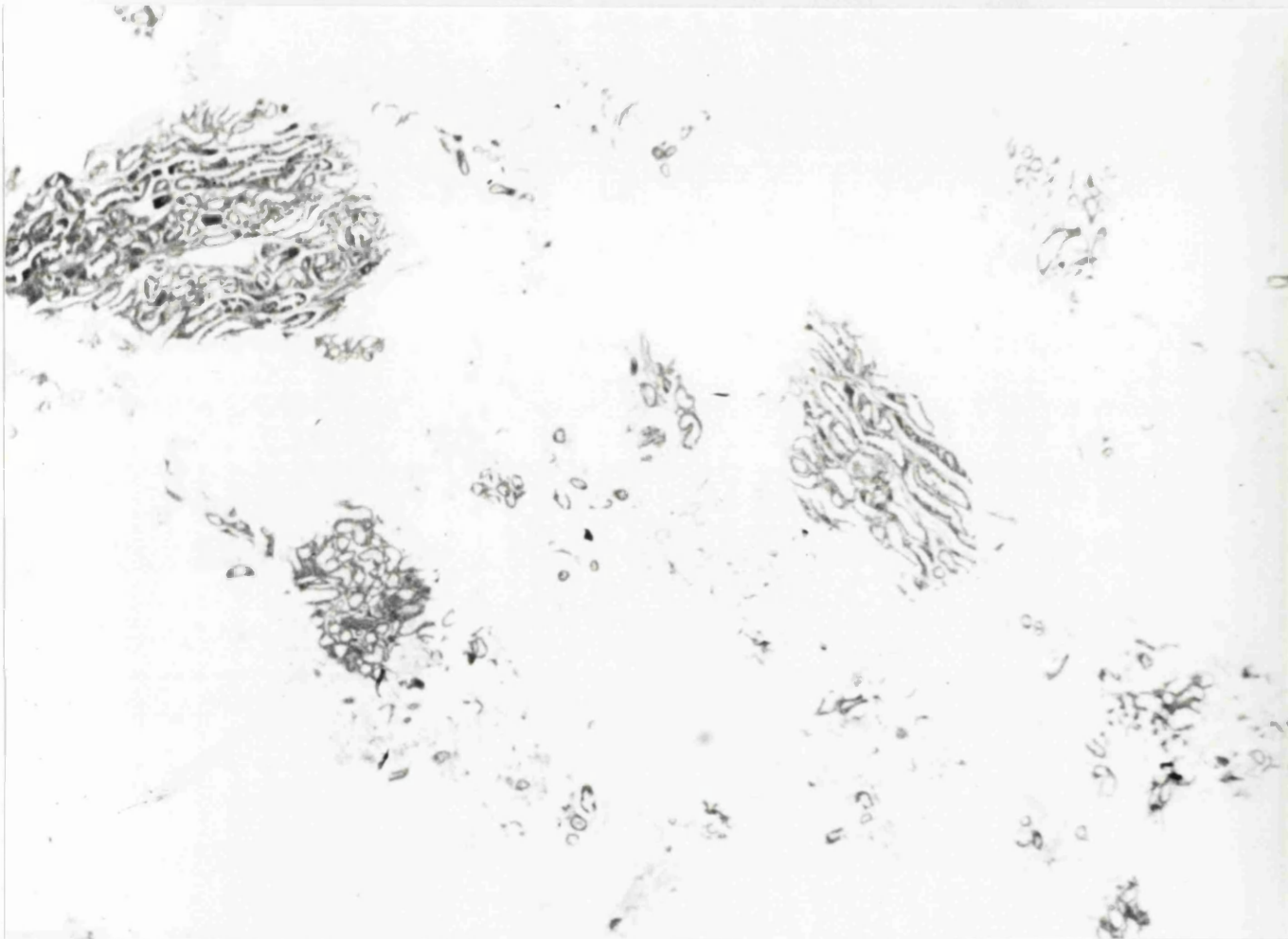
The CUSA acted as predicted. That is, soft tissue was removed with ease, but the same mechanism that allows sparing of collagen rich tissues such as blood vessels in hepatic resections prevents its application on fibrous prostatic tissue.

The 5 mm ELSA was far superior in both liver and prostate samples. However, it was evident that although a relatively rapid removal rate of prostatic tissue was achieved with the new blade (2.7 g/min after 1 minute), wrapping did still gradually occur and the accumulative removal rate decreased over 5 minutes (1.8 g/min). It was now much easier to push the ELSA into prostatic tissue; previously quite strong force was required to engage that tissue.

Particle Analysis

Although tissue removal rate remained the most important criterium for assessment, it was also shown that the distribution of particle size varied with blade speed. At all speeds, and with all tissues, the resultant suspensions contained particles ranging from 10 microns to 3 millimeters, as shown by light microscopy (figures 2:16 and 2:17). The distribution in that range varied with different tissues and more importantly with blade speed. Figures 2:18 & 19 show the comparison of particle distribution of liver and prostate samples liquidised at 2 speeds. The particles were counted with a light microscope using a standard counting frame and a micrometer in the objective lens, and allocated into 1 of 5 size distributions. Light microscopy has shown that this consists of fragmented cells, intact cells, and clumps of fibrous tissue. A striking difference between the liver and prostate particles was that the latter contained a large proportion of rectangular strands of cells. These formed the basis of the material found wrapped around the blade and in the aspiration channel of the 5 mm instrument. The higher the blade speed the greater the proportion of smaller particles for both tissues.

Such a sample cannot be evaluated by standard histological techniques. Cell cytology by both light microscopy and flow cytometry (DNA analysis) provided the necessary diagnostic information to allow the potential use of the ELSA in a clinical setting. This will be described in detail in Chapter 3.



1000 microns

Figure 2:16. Microscopic appearance of renal tissue liquidised by the 5 mm clinical ELSA for 30 seconds at 40,000 rpm.



1000 microns

Figure 2:17. Microscopic appearance of prostatic tissue liquidised by the 5 mm clinical ELSA for 30 seconds at 40,000 rpm.

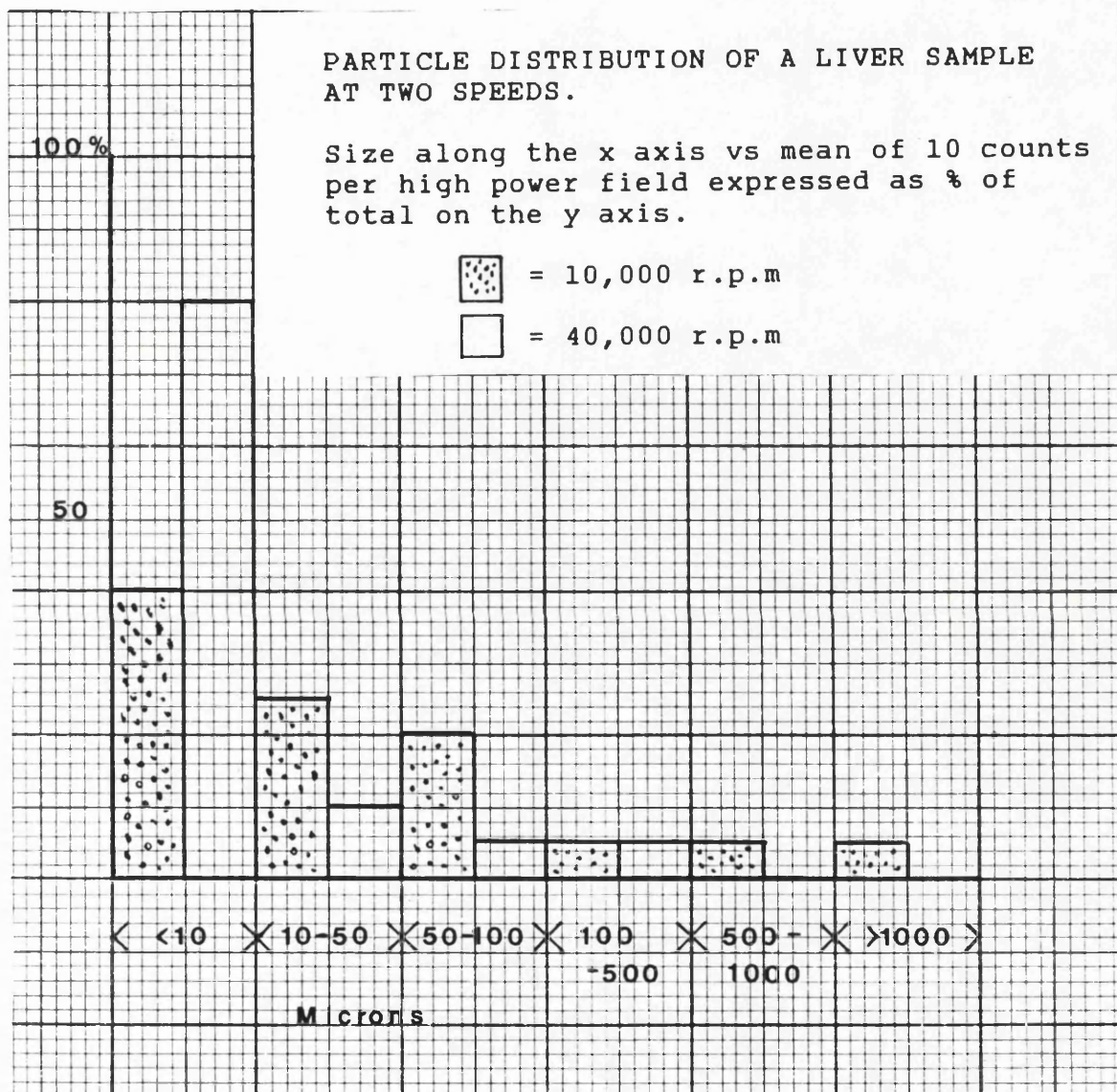


Figure 2:18. Graph showing particle distribution from a liver sample at 2 blade speeds, assessed by light microscopy.

PARTICLE DISTRIBUTION OF A PROSTATE SAMPLE
AT TWO SPEEDS.

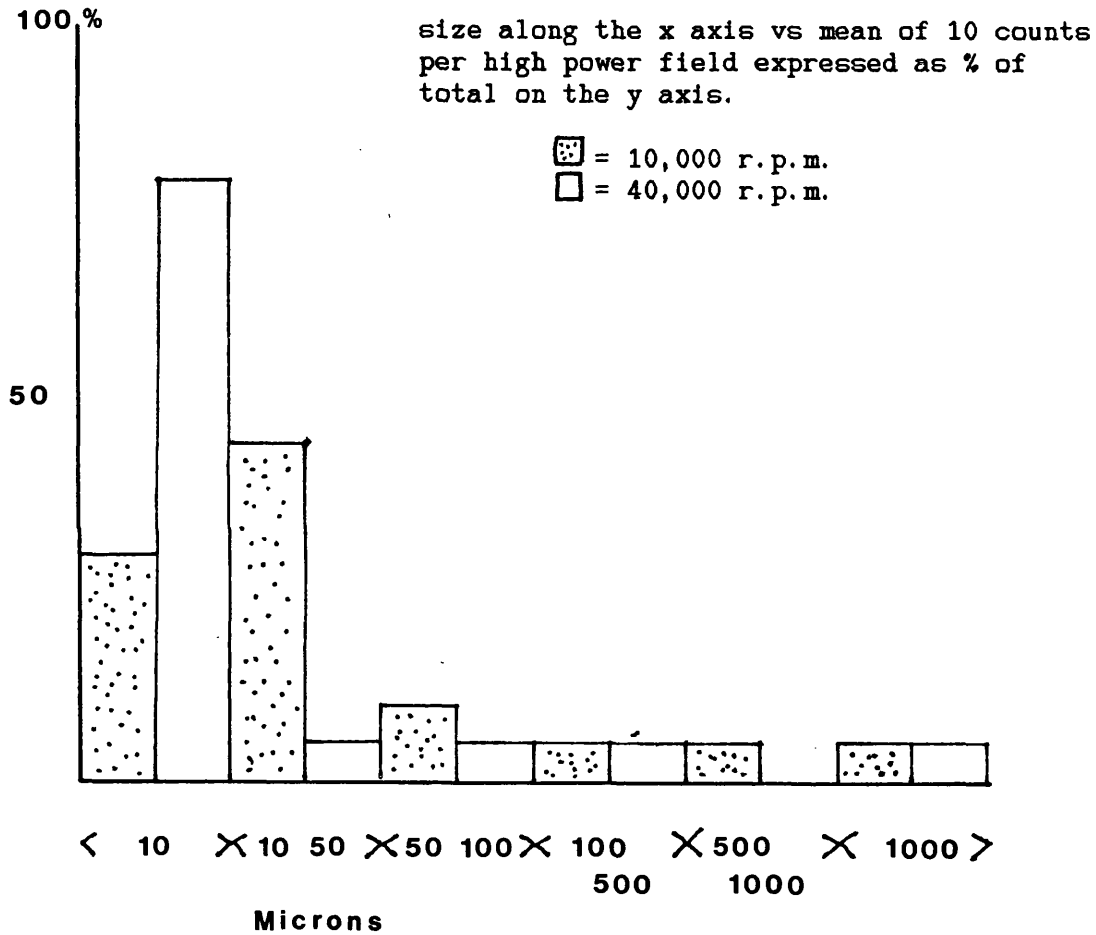


Figure 2:19. Graph showing particle distribution from a prostate sample at 2 blade speeds, assessed by light microscopy.

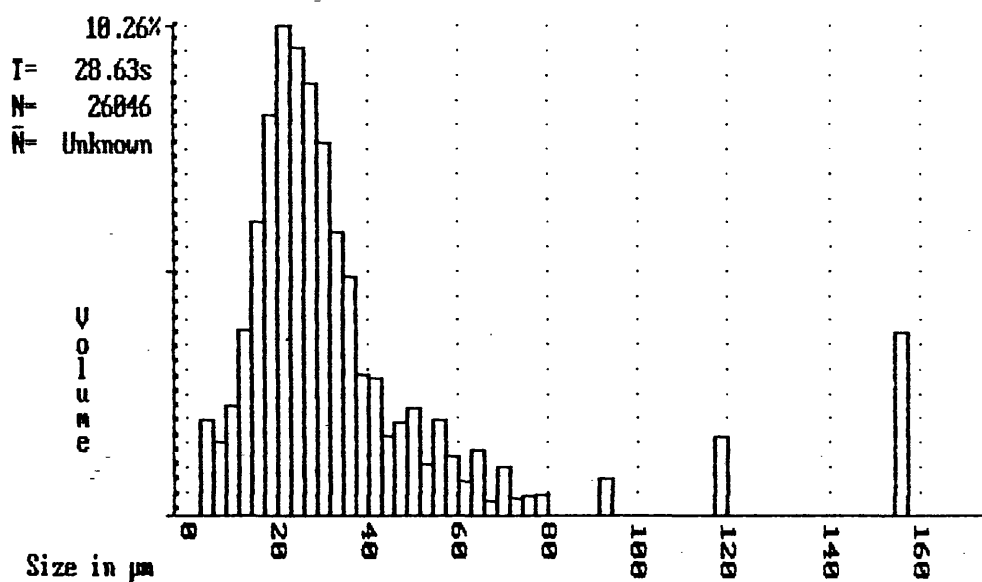
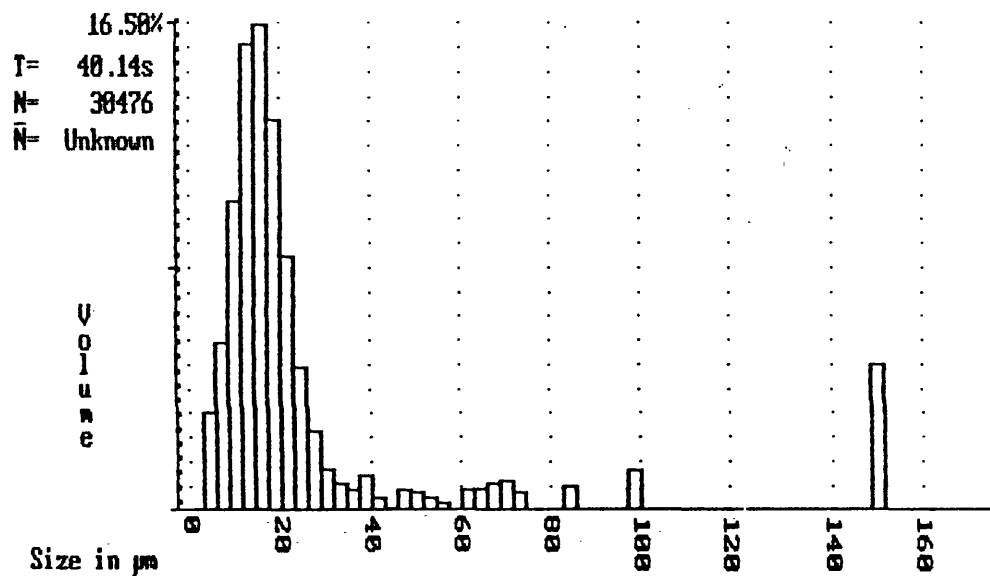
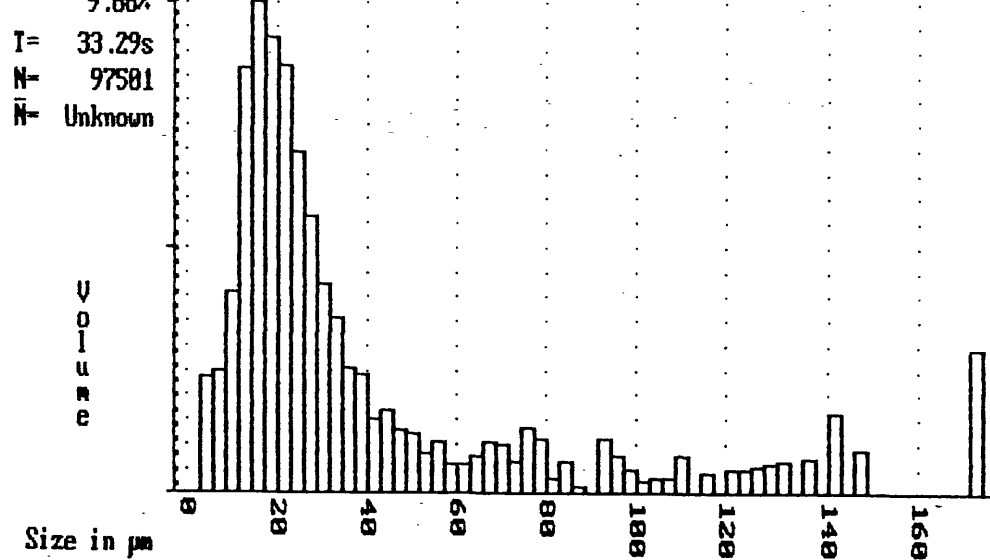


Figure 2:20. Coulter counter analysis (by volume) of a liver sample using the ELSA at 3 speeds (top: 10,000, middle: 20,000, below: 40,000 rpm). Sample size has been gated at 200 microns.

More accurate evaluation of particle size was achieved by passing the suspension of particles through a Coulter Multisizer. This uses the "Coulter" principle to measure particle volume - the most representative and universally accepted expression of particle size.

Samples from both liver and prostate were measured in this way at three separate blade speeds (10, 20 and 40,000 rpm.). It is technically impossible to use a Coulter principle for measuring the entire spectrum of particle sizes anticipated (10 - 3,000 microns). The specimens were filtered through 200 micron pore paper. Two runs were therefore required for each specimen, one using the residue (200 - 3,000 microns) and the other using the filtrate (less than 200 microns). Examples of these results are shown graphically below (figures 2:20-21). Figure 2:20 shows the increasing volume of smaller particles (10-50 microns) which occurred as blade speed was increased in 3 liver samples. Figure 2:23 shows that the particle distribution is similar for the prostate, below 200 microns.

Particles of 1 - 2 microns were also demonstrated by this method. The main conclusion however is that an overall increase in blade speed increased the proportion of smaller particles (notably 10 - 30 microns) for both prostate and liver. This did not however prevent a significant proportion of larger tissue fragments occurring irrespective of speed. However, just one large fragment is significant if it obstructs the aspiration channel.

Two interesting findings were made on microscopic assessment of the particles selectively gated by the multisizer. Particles 10 - 30 microns

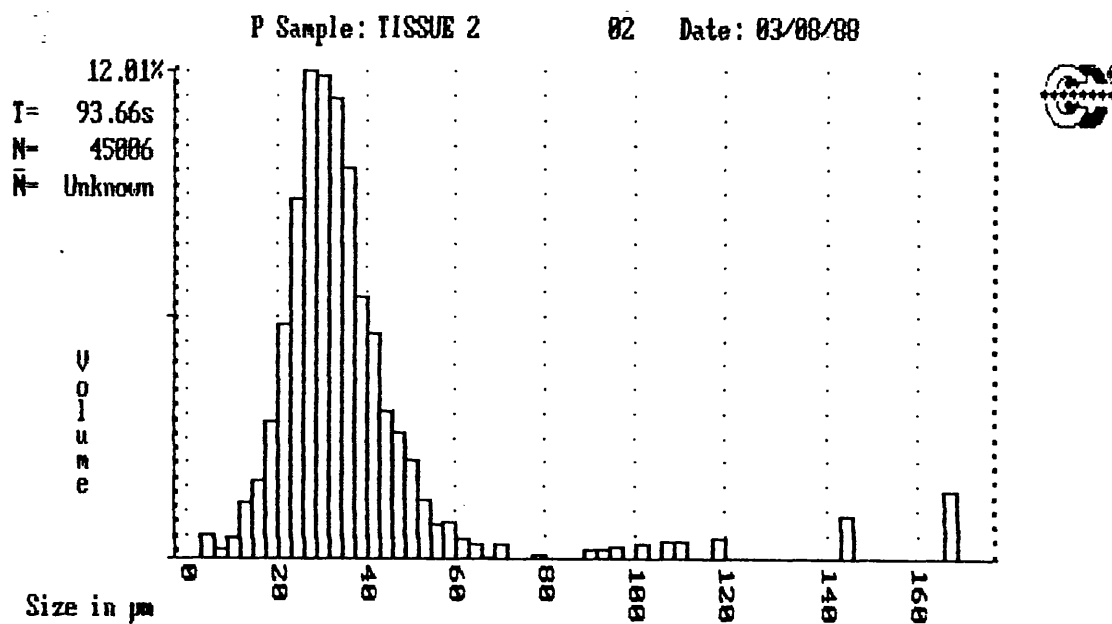


Figure 2:21. Coulter counter analysis of a prostate sample using the ELSA at 20,000 rpm.

in size were almost exclusively intact cells and particles over 500 microns were exclusively clumps of fibrous tissue.

The conceptual idea of a miniature liquidiser had been realised. It removed both soft and fibrous tissue more effectively than either the Nd:YAG laser or the CUSA. The optimum blade for penetration and tissue removal had been found. Blade speed did not alter particle distribution (over 500 micron) significantly enough to allow more efficient aspiration. Inefficient aspiration during prolonged removal of fibrous tissue remained the greatest problem at this stage. This could be overcome by reducing the diameter of the drive shaft to allow a larger aspiration channel. These proportions were apparent in the 10 mm ELSA. It was agreed by the hospital ethics committee that the 5 mm ELSA with its endoscope was safe, efficacious and could be used clinically.

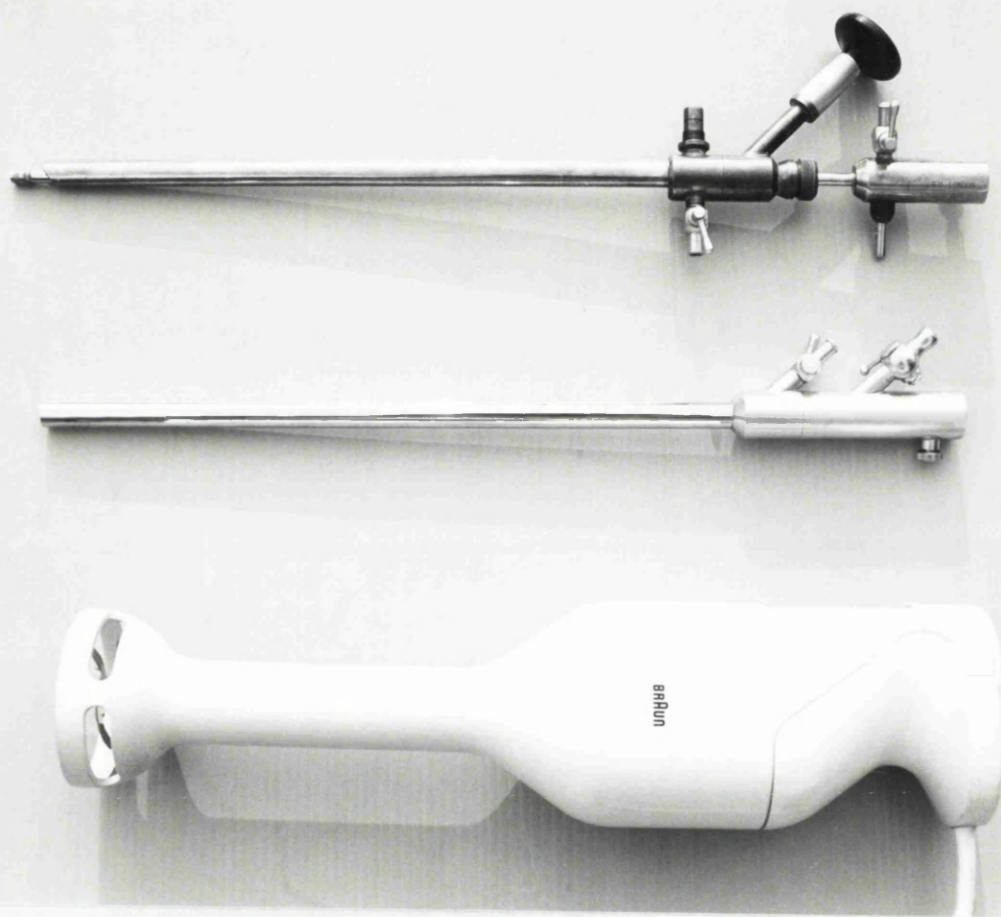


Figure 2:22. 3 liquidisers: Top, The 5 mm ELSA; middle, 10 mm ELSA; and below, the original hand held kitchen blender.

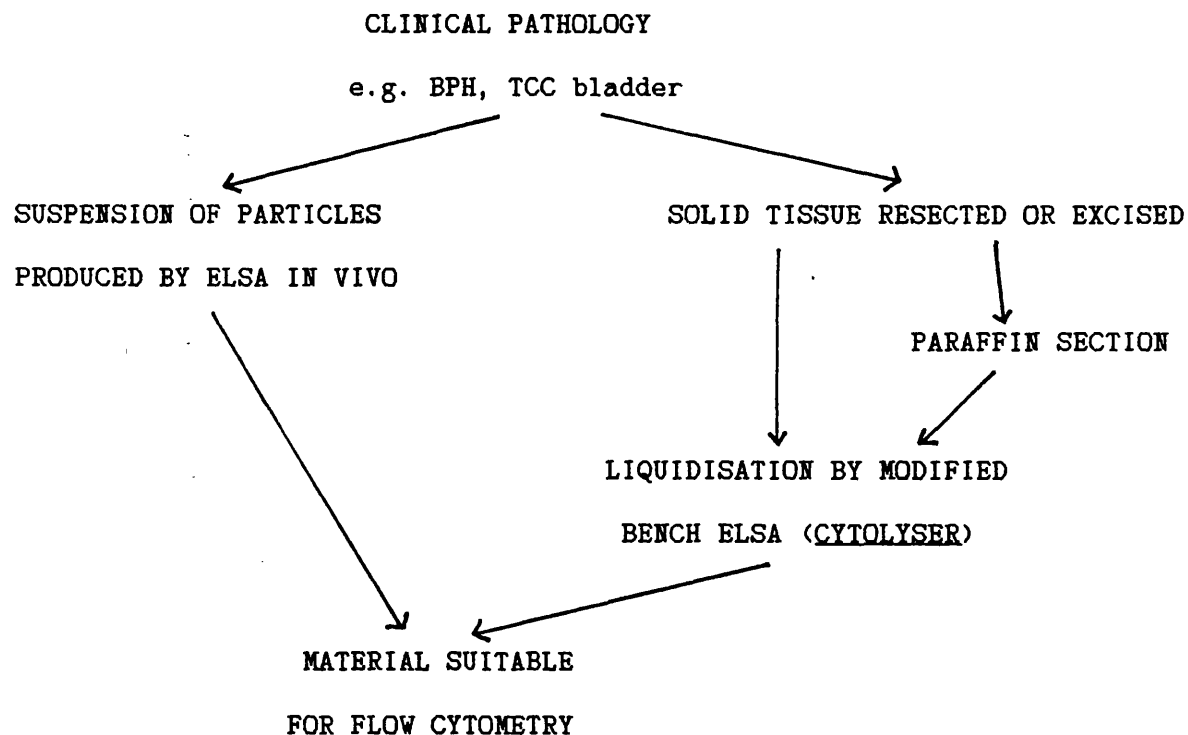
CHAPTER 3
THE INTEGRATION OF FLOW CYTOMETRY AND TISSUE
LIQUIDISATION TECHNIQUES

The ELSA produces a suspension of particles unsuitable for routine histopathological assessment. A large proportion of these particles are intact cells and nuclei (chapter 2). Cell cytology by light microscopy was slow and tedious. Flow cytometry offered a method of rapid assessment of ELSA tissue samples. Flow cytometry can provide a fingerprint of genotypic and phenotypic characteristics on a cell by cell basis, rapidly and objectively. Unfortunately the clinical relevance of these parameters is still being worked out.

The principle of a flow cytometer is to induce a stream of particles across a flow chamber by means of a pressure gradient. At a specific point along the chamber, the cells reach and cross a high intensity light beam (usually a laser with known wavelength), and stain carried by the cells is excited to emit fluorescent light. This fluorescent emission is sensed, quantified and stored by photo-electronic equipment. DNA measurements can be made and the results are expressed in a profile of sub-populations. An aneuploid profile shows a single peak or sub-population of DNA and a diploid, 2 such peaks, and so on. Early studies were on ready made suspensions such as bladder washouts. The measurement of solid tumours requires the conversion to single cell suspensions. DNA measurements made in nuclei obtained from routinely archived paraffin blocks have the advantage of a possible correlation to an already known clinical outcome.

In prostatic cancer there appears to be a step like relationship of tumour grade and stage to diploid, tetraploid and aneuploid DNA content (Frankfurt 1985). In bladder cancer, flow cytometric DNA measurements are roughly equivalent to cytology for purposes of diagnosis. Diploid tumours tend to be associated with lower grade and stage. Recurrence rates in superficial bladder tumours also appears to correlate to DNA content or ploidy (Gustafson 1982). There are conflicting reports in the literature regarding the relationship between ploidy and renal carcinoma stage and grade (Baisch 1982).

The mechanism of producing particles in the clinical ELSA setting was obviously also required in the laboratory preparation of other solid samples and paraffin sections for flow cytometry.



This chapter therefore demonstrates not only the role of flow cytometry for assessing a suspension of particles but, unexpectedly, produced a totally innovative device for the bench preparation of all solid tissue and historical paraffin section samples for flow cytometry. Its benefit was confirmed in the experiments shown below.

Two major advances which have increased our knowledge of tumour behaviour are the ability to study archival specimens in association with the clinical outcome, and the development of new monoclonal antibodies which allow fluorometric staining of intracellular components, suitable for flow cytometric analysis. Experiments based on these two advances have been used to demonstrate the value of the ELSA/Cytolyser with flow cytometry.

Methods of preparing both fresh and archival specimens for flow cytometry are well described (Hedley 1983) but there have been problems with very hard or fibrous tissues such as prostate and breast. Also, they are time consuming, and do not always yield good quality DNA histograms. In such cases, nuclei extraction requires prolonged incubation in acid saline (pH 1.7) with pepsin (0.5mg%) for up to 1.5 hours, which in turn can lead to digestion of the cellular proteins which are the object of the study.

The ELSA was modified to be a hand held instrument for use in a test tube. The new instrument was called "The Cytolyser". The cytolyser is suitable for any tissue type or tumour (even calcified), and works on fresh whole tissue, or paraffin embedded specimens alike. This has enabled us to reduce the time taken to prepare solid tissue samples, to reduce the

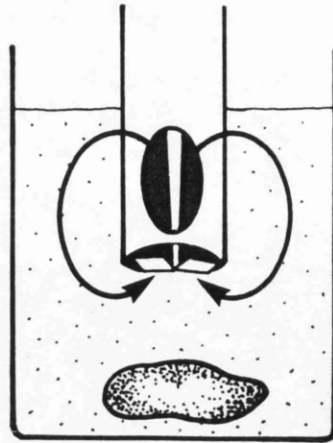


Figure 3:1. The modified housing which produced the phenomenon of CVM.

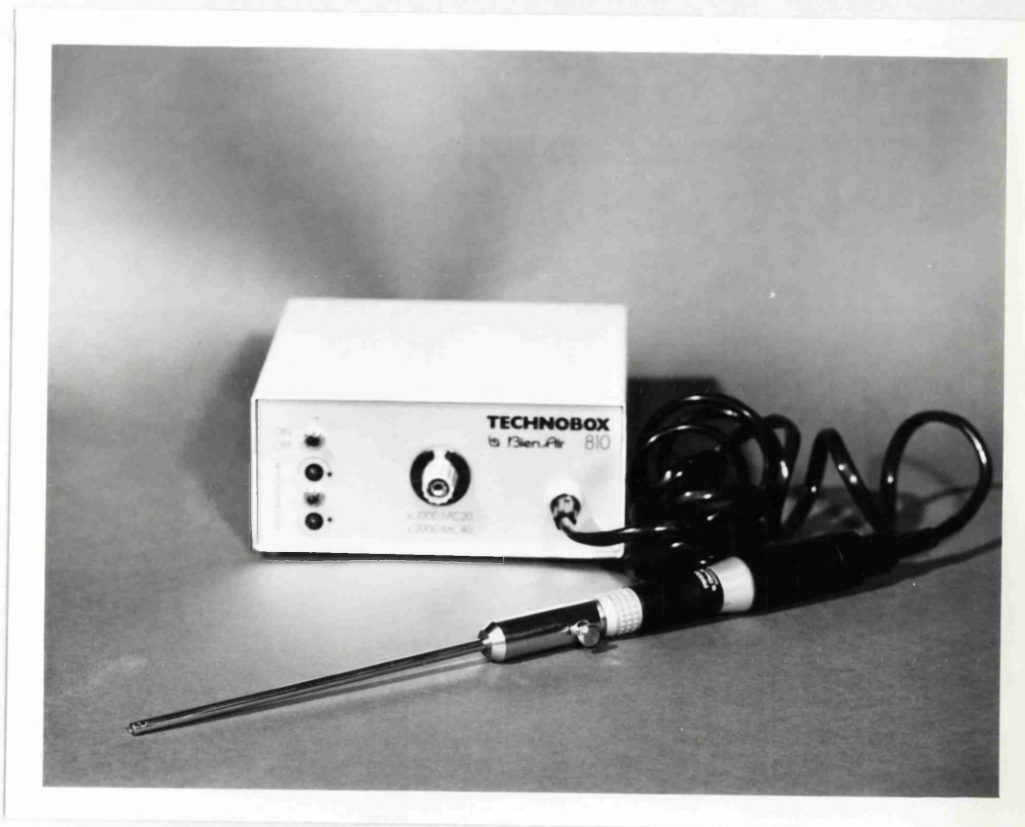


Figure 3:2. The Cytolyser.

concentration of pepsin, and in some cases, remove the pepsin stage altogether.

Construction of the Cytolyser

Because the tissue does not need to be aspirated the housing configuration could be much simpler. Also there was no need to prevent extrusion. In order to maximise the degree and speed of liquidisation the housing was constructed with side holes similar to the original "Braun Multiprac". This created the phenomenon I have called "CVM" (continuous vortex microsectioning), whereby a vortex draws the tissue accross the angled cutting blade, ensuring a consistent particulate size and distribution (fig 3:1). CVM could be dynamically demonstrated by viewing the liquidisation of liver samples that had been soaked in fluorescein for 24 hours, under ultraviolet light. Particle size could be controlled according to the rotational speed, enabling whole cells or subcellular particles to be extracted from tissue specimens as in the ELSA experiments. Apart from the end housing, the cytolyser was a replica of the 5mm ELSA (figure 3:2). The shaft was shorter (15cm) and did not require aspiration or irrigation channels. It was constructed with the assistance of the G.U. Manufacturing Company's workshop.

Particulate size and DNA histograms. Can the Cytolyser help?

The experiment was designed to determine particulate size, and assess the effect of the cytolyser on nuclei extraction (with and without pepsin), as measured by particle size and DNA histograms. Seven archival paraffin sections of benign prostate gland from 1970 were cut into 40 micron sections. The sections were halved and prepared in the manner described by Hedley, for flow cytometry. The cytolyser was applied to the paired sections for 0, 10, 20, 30, 40, 50, or 60 seconds respectively, and only one of the paired sections was incubated in 0.1% pepsin in acid saline for 30 minutes. The solutions were filtered through a 40 micron mesh filter, divided into two aliquots, and spun in an Eppendorph centrifuge for 5 minutes. One aliquot from each pair was resuspended in propidium iodide (PI) to stain for DNA, and the other aliquot was suspended in phosphate buffered saline (PBS). Fresh solid tissue samples were also assessed in the same way. The PI stained samples were analysed on the Cambridge MRC custom-built flow cytometer, and the PBS samples were analysed in a Coulter Multisizer, at the Coulter Electronics Laboratories.

Figure 3:3 shows the three best histograms of cell particle size, measured by volume as a percentage of the whole sample, after a 20 seconds application of the cytolyser. The size of the particles as measured on the Coulter multisizer shows that particles of 5 microns and below can be formed after 20 seconds with the cytolyser. There is no difference between the samples with or without pepsin, and both yield smaller cellular particles than the fresh tissue sample. Figure 3:4 shows the seven flow cytometric histograms. If the cytolyser is not used the "cleanest" peaks

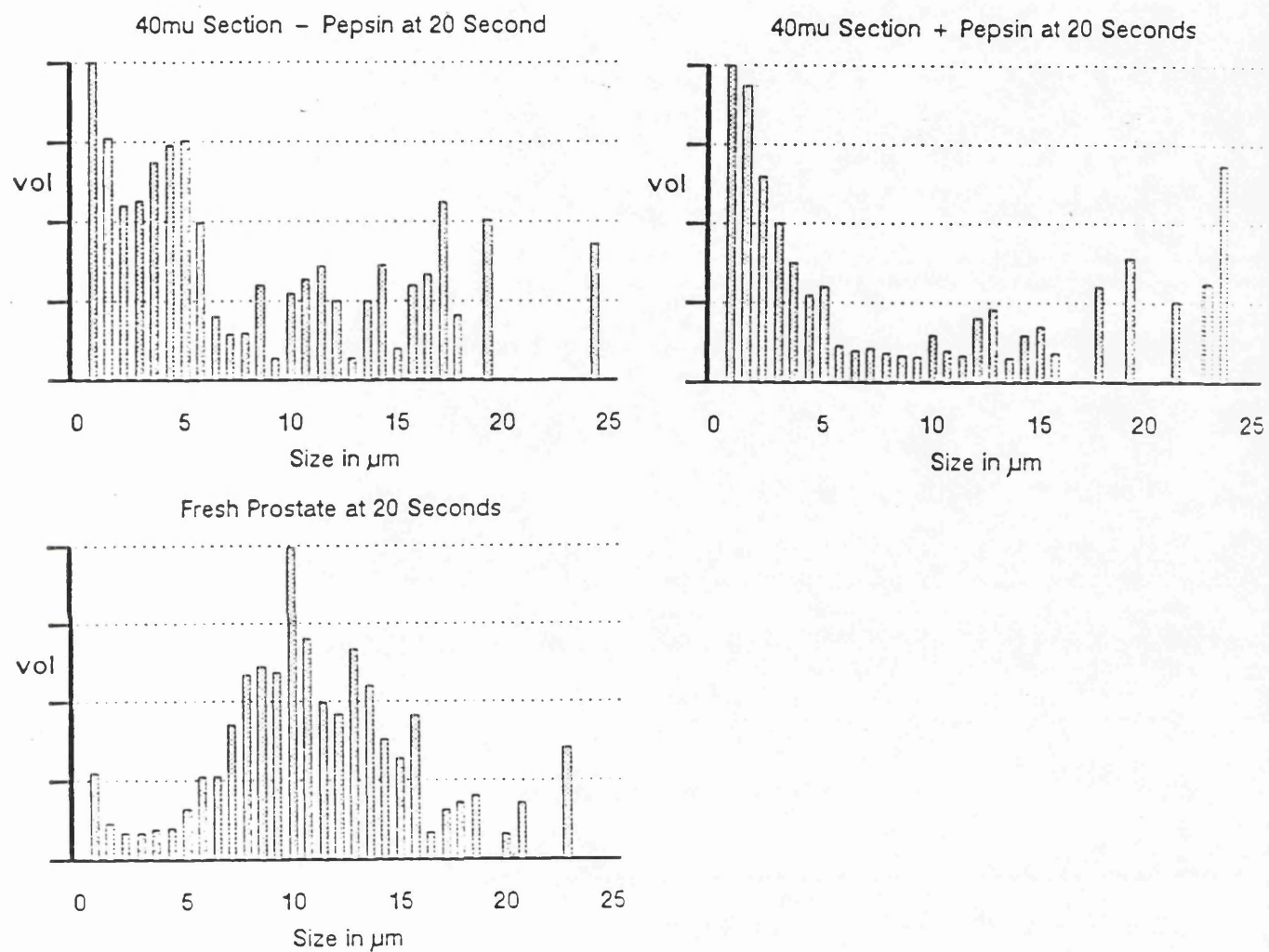


Figure 3:3. Particle size measured on the Coulter multisizer. These 3 histograms show the distribution of particles after the use of the Cytolyser for 20 seconds on a) paraffin section without pepsin digestion, b) paraffin section with pepsin, and c) fresh prostate.

DNA HISTOGRAMS

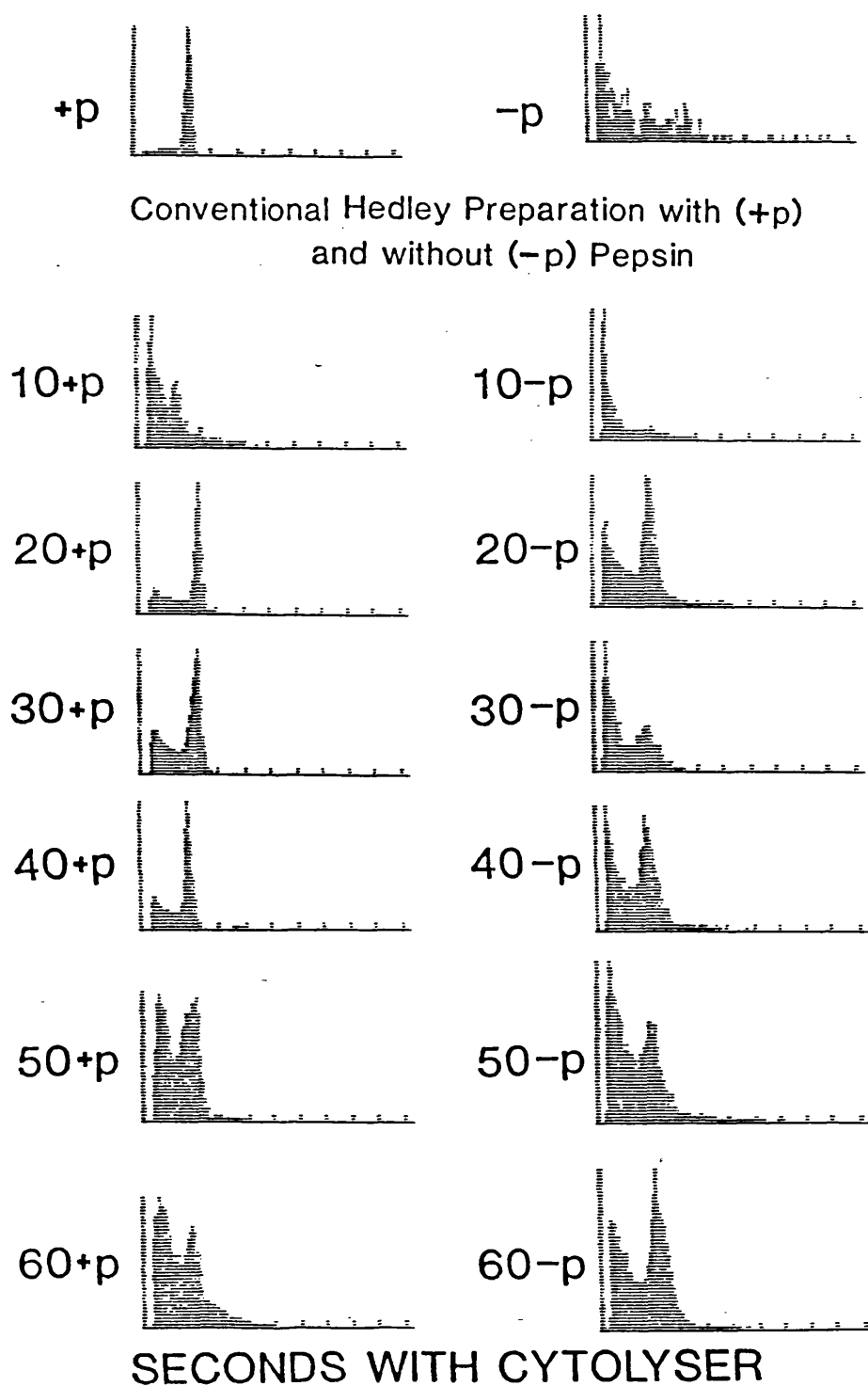


Figure 3:4. DNA histograms from a single paraffin-embedded section of benign prostrate after different application times with the Cytolyser, with and without pepsin.

are found when pepsin is used. But when the Cytolyser is used for 20 seconds or more then the clean histograms are compatible, with or without pepsin.

This experiment has shown that the cytolyser used for 20-30 seconds can greatly improve the detection of intracellular components when particulate size needs to be small enough for flow cytometric analysis. We have endeavoured to remove the stage of incubation with pepsin in acid saline, which we believe can destroy intracellular proteins. For pure DNA studies, this stage may be eliminated in some cases, for the purposes of flow cytometry. The cytolyser by itself is capable of producing a solution of cellular particles of less than 5 microns, when used for 20 seconds, at 40,000 rpm. The smaller size of particles compared to those produced by the ELSA are probably a consequence of CVM.

The value of flow cytometry for the ELSA has been reciprocated. Unfortunately flow cytometry alone cannot be used to differentiate benign prostatic tissue from well differentiated adenocarcinoma as they both produce a diploid profile (Stephenson 1986). Chapter 5 will look at the association of the ELSA with flow cytometry in a clinical study on bladder tumours.

CHAPTER 4

HAEMOSTASIS DURING PROSTATE REMOVAL.

The ELSA had been successfully evaluated in laboratory conditions, albeit still with a small question mark over the efficient aspiration of prostate tissue. However, one major clinical problem that had not been addressed was that of haemostasis during in vivo prostate removal. This chapter will describe the arterial supply to and the vascular arrangements within the human prostate. These are based on the detailed studies of Clegg (1955, 1957) who looked at normal human prostates, and my own studies on cadaveric hyperplastic prostates. This will be followed by the description of two experiments to compare the haemostatic potential of the Nd:YAG laser with diathermy.

Arterial supply of the human prostate.

A review of the literature initially suggested that there are fundamental anatomical variations (Kraas 1935, Awataguti 1939, Flocks 1937). Clegg (1955) has demonstrated that the differences in results may be explained as resulting from differences in terminology. Clegg examined 28 cadaveric pelvic specimens. In no case was pathological hypertrophy or hyperplasia present. He found that in the study of the general topography of the vascular patterns, more reliance should be placed on dissection than on locally infused radiological contrast studies. In all cases he found that the prostate was supplied by the prostatic branch of the prostatovesical artery, which was always a well

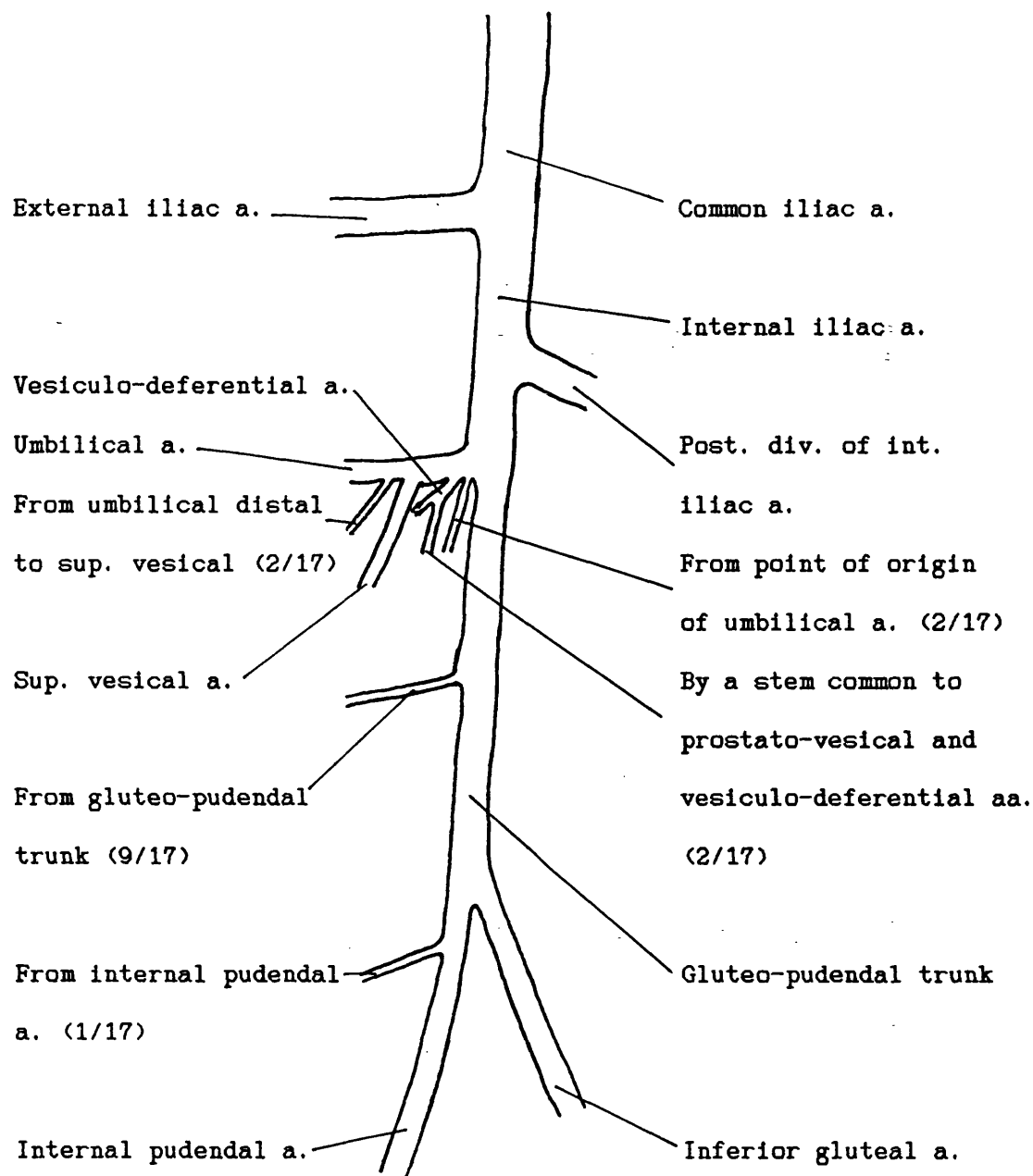


Fig 4:1. Diagrammatic representation of the origin of the prostatic-vesical artery (Clegg, 1955).

defined trunk of variable origin (table 4:1). The course of the prostato-vesical artery was fairly constant, dividing into its 2 terminal branches, the inferior vesical and prostatic arteries. This sub-division was also inconstant (table 4:2). The prostatic branch was the one constant branch of this trunk. It reaches the gland on its antero-lateral surface, and passing down the lateral border gives off fine twigs to the surface of the organ. Some of these twigs pass to the rectum and anal canal and may be classed as middle rectal arteries. Not infrequently one of these vessels may be enlarged and in such a case it may appear that the prostatic artery is a branch of the middle rectal. Clegg's radiological studies revealed very few anastomoses of arteriolar size or larger between vessels of opposite sides.

Clegg (1957) also investigated the intrinsic supply of the prostate. He used a histological staining technique which he claimed was superior to the injection of radiopaque media, setting gels or vinylite materials. Three vascular zones were observed: a capsular zone, consisting of vessels ramifying in the connective tissue surrounding the gland; an intermediate zone of vessels passing centripetally and downwards towards the urethra; and a plexus of vessels surrounding and supplying the urethra itself (fig 4:2).

The intrinsic venous channels in the prostate appear to have been little studied despite their obvious importance in clinical prostatic resections. Griffiths (1889) described numerous venous channels lying immediately deep to the mucous membrane of the anterior urethral wall. Clegg's (1957) investigations showed that the main channels of venous

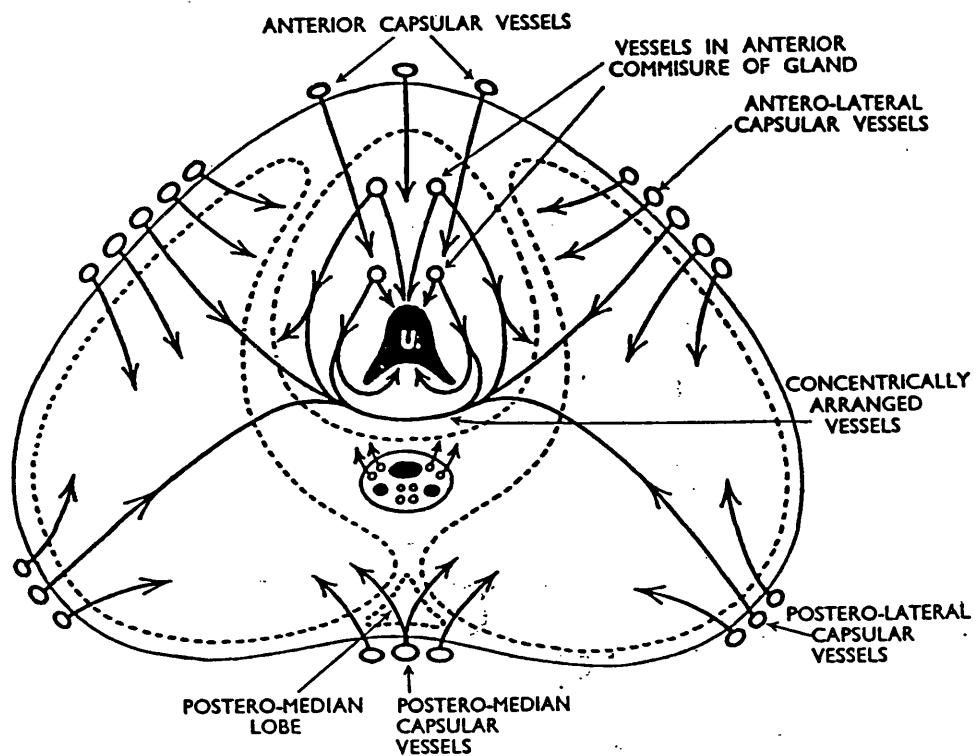


Figure 4:2. Diagrammatic cross-section of a prostate showing the distribution of the principal blood vessels.

drainage are to the lateral capsular vessels (i.e. the lateral part of the prostatic plexus), and to the irregular channels in the antero-inferior part of the gland.

Flocks (1937) suggested that the arterial supply in the hyperplastic prostate differed from the normal gland. As the prostate enlarges the internal or urethral arrangement of prostatic arteries magnify proportionately, whilst the capsular or external group remain about the same. The urethral arteries enter the base of the prostate near the bladder neck and are distributed more profusely immediately beneath the urethral mucosa than elsewhere in the gland. This arterial distribution may account for the fact that haemorrhage is more pronounced at the bladder neck and once controlled there, will make the rest of the resection much easier and possibly produce sloughing of tissue left at the apex after resection because of ischaemia.

My own work on the arterial supply of the prostate has been limited but has supported the descriptions above. Five cadaveric prostates were carefully dissected as part of my training for a radical prostatectomy. The variations in the origin and division of the prostatico-vesical artery and its distribution to the gland are recorded in tables 4:1-3. .

Table 4:1. Origin of the prostato-vesical artery. See also fig 4:1.

Origin	Frequency (n=17, after Clegg, 1955)	Frequency (n=5, after author)
Gluteopudendal trunk	9	4
Origin of umbilical artery	2	1
Umbilical artery	2	-
Common trunk with vesiculo-diferential artery	2	-
Internal pudendal artery	1	-
Obturator artery	1	-

Table 4:2. Mode of division of the prostato-vesical artery.

Division	Frequency (n=19, after Clegg, 1955)	Frequency (n=5, after author)
Prostatic and inferior vesical arteries	6	3
Large prostatic artery - small inferior vesical artery	5	-
Several inferior vesical arteries	3	-
No inferior vesical artery	5	2

Table 4:3. Distribution of the prostatic artery to the gland.

Distribution	Frequency (n=29, after Clegg, 1955)	Frequency (n=5, after author)
Branches to both surfaces	13	4
Anterior branches larger than posterior	8	1
Anterior surface only	6	-
Posterior surface only	2	-

Macrovascular casts of the prostate.

New techniques for micro- and macro-vascular casting of organs have superseded the staining techniques used by Clegg although have not been previously used for the prostate to my knowledge. Casts were made of the hyperplastic prostates removed using Batson's number 17 anatomical corrosion compound (Polysciences Inc). This technique has been described by Batson (1955) and applied to the majority of organs; the prostate being an exception. The kit consists of a partially polymerised monomer, a catalyst and a promoter to allow curing at room temperature after injection, and red and blue pigments (for separate arterial and venous injections). After the injection is cured the organ is dissolved in 40% sodium hydroxide for 6 hours, to reveal a delicate vascular cast.

Unfortunately sludging of blood in the cadaveric prostates prevented complete casts being made. However, sufficient detail could be shown to suggest that in contrast to Flocks (1937) but in support of Clegg (1957), although most vessels enter the gland between 1 and 5 o'clock and 7 and 11 o'clock (as viewed from above), vessels also enter the anterior and posterior median lines.

The blood supply to the canine prostate is similar to the human, although the feeding arteries may vary (Gordon 1960). Consistently perfect casts could be made of these prostates if the injections were carried out just prior to sacrifice of the animal. One of the many fine detail casts is shown in figure 4:3.

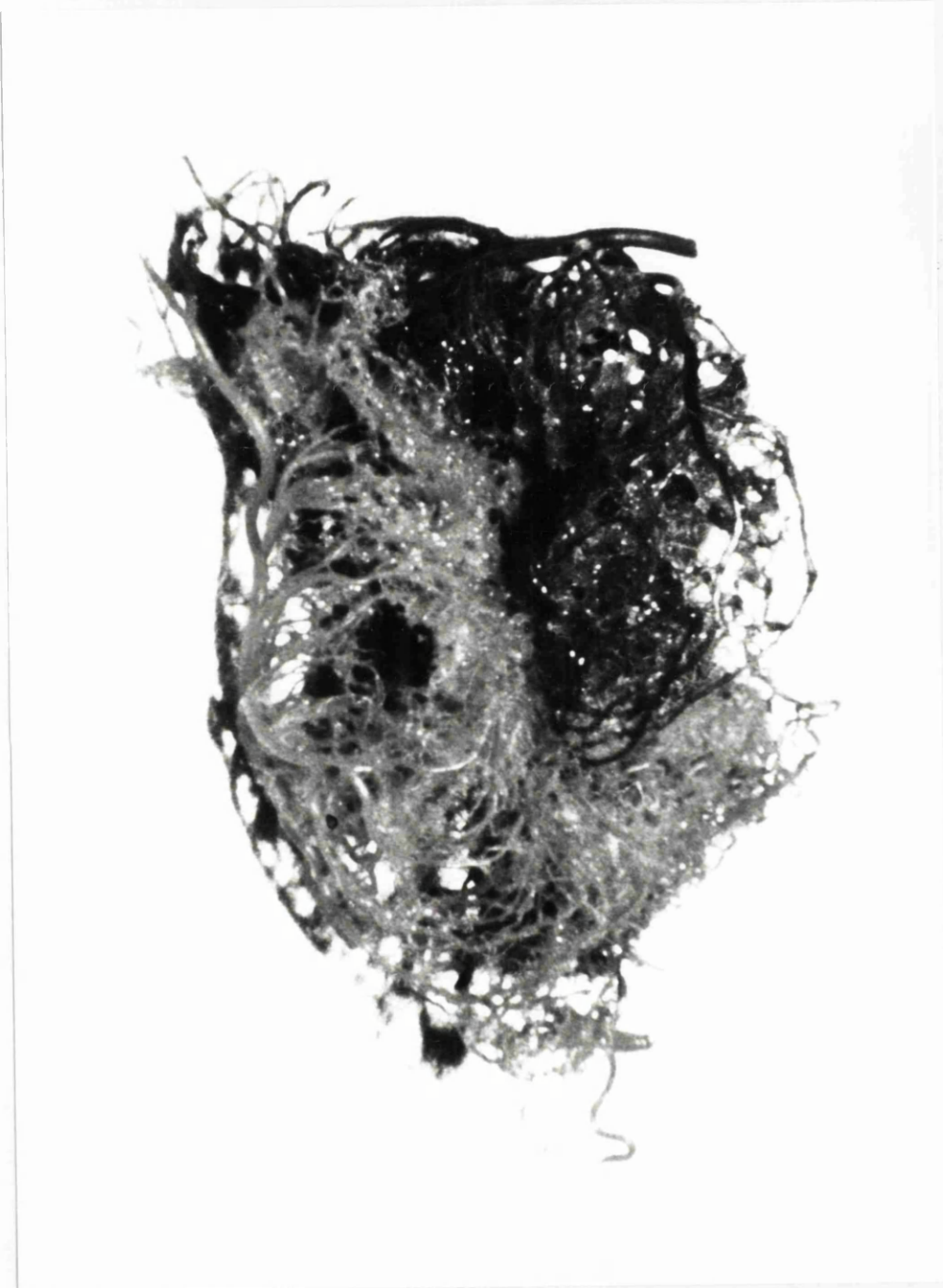


Figure 4:3. Macrovascular cast of the blood supply of the canine prostate.

Embolisation of the prostate.

Having shown that there is a great consistency in terms of the arterial supply to the prostate it would seem reasonable to consider the concept of therapeutic embolisation of the prostate. This is infrequently used as a last resort for uncontrolled post prostatic resection haemorrhage (Appleton 1988). Preoperative radiological embolisation would certainly produce a gland that could be rapidly removed by a variety of techniques (ELSA or even a mini retropubic prostatectomy). It would also carry the possible complication of impotence because of the proximity of the internal pudendal artery even using super selective embolisation techniques. Gluteal pain from inadvertent superior gluteal artery obstruction should be avoidable. This concept was later explored in detail in Chapter 6.

The ELSA and Nd:YAG laser in tandem.

Throughout the period of research for this thesis the Nd:YAG laser had been continually suggested as a viable method for transurethral prostatic tissue removal. Experiments in Chapter 2 showed that the tissue ablation rate was minimal and a gross waste of energy and money.

The Nd:YAG laser has been used in conjunction with the CUSA for canine nephrectomies (Melzer 1985). The self limiting ablation effect of the laser has been alluded to in Chapter 1. An experiment was conducted to assess the complimentary effect of the ELSA with the Nd:YAG laser. If

used in tandem then the ELSA might remove the charred tissue, allowing the laser to act further and faster. The laser would theoretically produce haemostasis in vivo and alter the material characteristics of the fibro-elastic prostate allowing efficient liquidisation and aspiration.

Two fresh open prostatectomy specimens were cut into 4 approximately 2 cm cubes. These were weighed. The non contact fibre from a Nd:YAG laser was trained under water for 2 minutes over each of 2 cubes. The remaining 2 cubes were subjected to 30 seconds of alternating laser/ELSA action for 2 minutes. All the cubes were then reweighed.

Table 4:4. Results of laser vs laser/ELSA on in vitro prostate tissue removal.

	<u>Nd:YAG</u>	<u>Nd:YAG/ELSA</u>
Mean loss of weight (g/min)	0.5	3.6

The concept of complimentation seemed to work but any application of this in vivo would be very tedious and the aim of a low-cost method would be lost. Further reassurance of the haemostatic potential of the Nd:YAG laser was required to take this any further.

The Nd:YAG laser for haemostasis.

The following experiment assesses the Nd:YAG laser for haemostasis compared with diathermy.

The prostatic arteries demonstrated in the cadaveric dissections earlier ranged between 0.5 - 3 mm. The normal prostatic arterial pressure was unknown. This was measured during a routine transurethral prostate resection. An epidural catheter was guided into a spurting artery using an Albarran lever. This was connected to a Hewlett Packard solid state transducer and multipurpose recorder, as used for intraoperative arterial pressure monitoring. Cannulation was tedious and only readings from 2 cases were obtained. The prostatic arterial pressures were 80 and 70 mm Hg (Radial B.P. 110/60 and 120/50 respectively). Whilst having no statistical significance these 2 readings did put into some perspective the results from the following haemostatic experiment.

The use of excised ox liver is the commonest example of an animal model to appraise the performance of a cautery or laser system (Auth 1986). It is more desirable to have a model with a physiological blood supply because of the convection currents caused by the blood flow and absorption of laser light by blood pigment. It was difficult to conceive how to use the prostate in this way. A compromise was to use vessels in a canine mesentery. The dogs were to be sacrificed at the conclusion of this and other experiments (Chapter 6). Roughly, two arterial sizes were used (0.5 mm and 2 mm diameter). The modalities of coagulation under comparison were:

a) Nd:YAG laser: 75 watts, 1 second, bare 600 micron fibre,
(non contact).

b) Monopolar diathermy loop: 30 Joules, just touching.

c) Monopolar diathermy loop: 30 Joules, with compression.

Each modality was used as stated on 10 x 0.5 and 10 x 2 mm arterial portions in vivo. After the specimens were resected each artery was dissected out and the bursting pressure measured. The bursting pressure was measured by gently infusing water into the open end of the vessel and measuring the pressure with the same Hewlett Packard apparatus above (figure 4:6). The bursting pressure was that pressure at which water first leaked from the previously coagulated artery.

Table 4:5. Results of mean bursting pressures (mm Hg)

<u>Coagulation Mode</u>	<u>0.5 mm artery</u>	<u>2 mm artery</u>
Nd:YAG (non contact)	130	30
Monopolar (light contact)	150	45
Monopolar (compression)	280	264

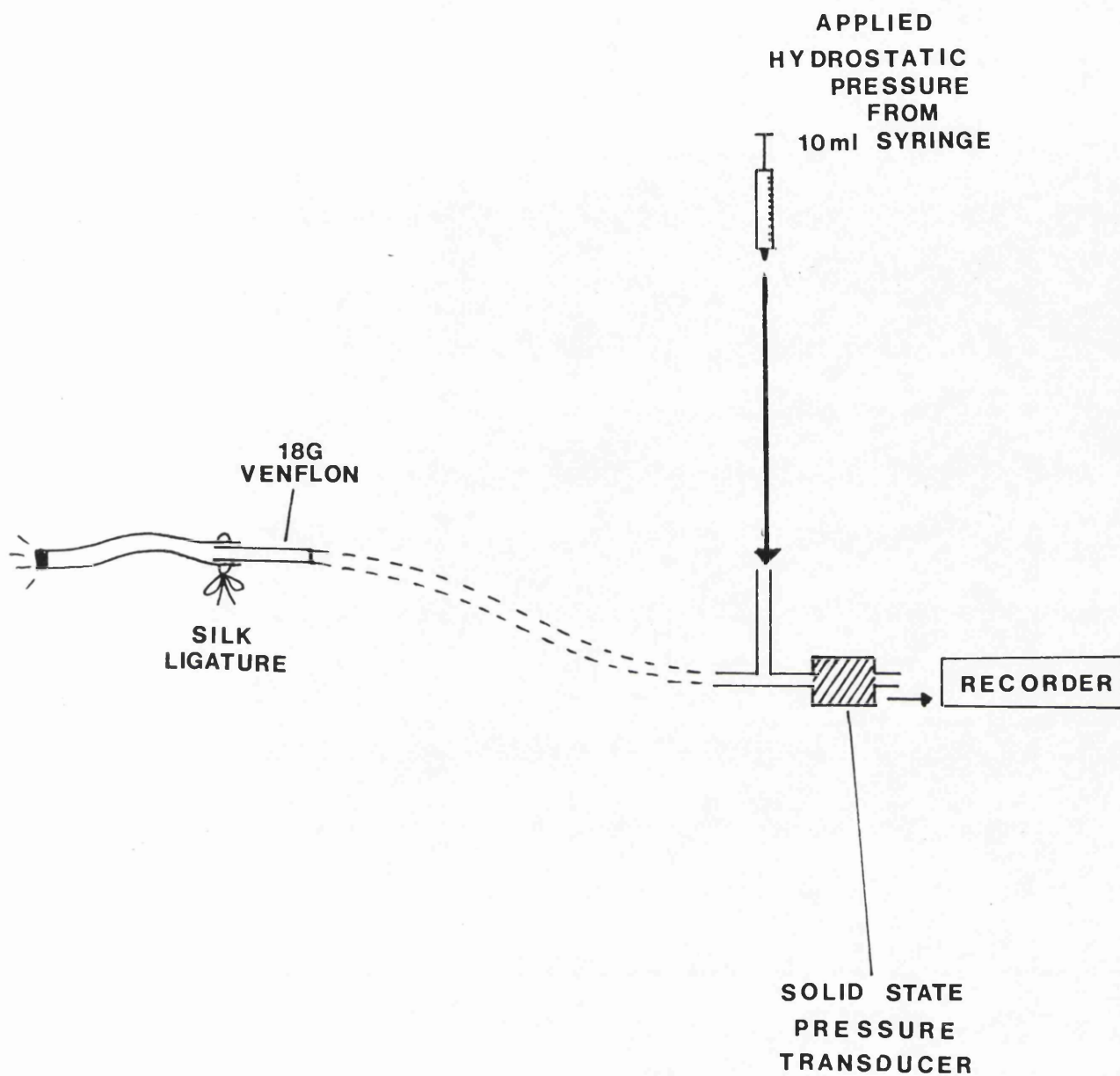


Figure 4:4. Diagram of the apparatus used to measure the bursting pressure of sealed arteries.

All modes of coagulation studied adequately sealed 0.5 mm vessels. That is, all produced bursting pressures well above the clinical model postulated of at least 100 mm Hg. The laser in its non-contact form and monopolar diathermy with only light contact were inefficient at sealing the larger 2 mm vessel. This experiment highlights the deficiencies with which endoscopic laser ablation of the prostate would be carried out. Two inferences can be made from these results. First, the Nd:YAG laser would be unsuitable for combined endoscopic laser ablation and haemostasis. Secondly, efficient haemostasis by heating from any source is magnified by coaptation of vessel walls (Sigel 1967).

Despite the advances in technology in the last 79 years the solution to the problem of haemostasis lay with diathermy. Young incorporated electrocautery into his efficient, yet bloody, punch in 1911. In the same way a diathermy plate was mounted around the housing of the 5mm ELSA (figure 4:5). This provided an excellent monopolar coagulation facility with coagulation of exposed vessels by pressing the side of the instrument's diathermy plate onto the cut surface. The feeding electrode was taken down the irrigation channel of the liquidiser. This channel was not required when used with the irrigating endoscope.

A diathermy plate was not fitted to the larger laparoscopic 10mm instrument because there already exists established methods of endo-ligation and endo-clipping (Semm 1977).

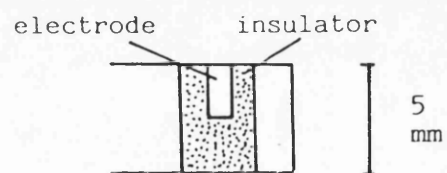
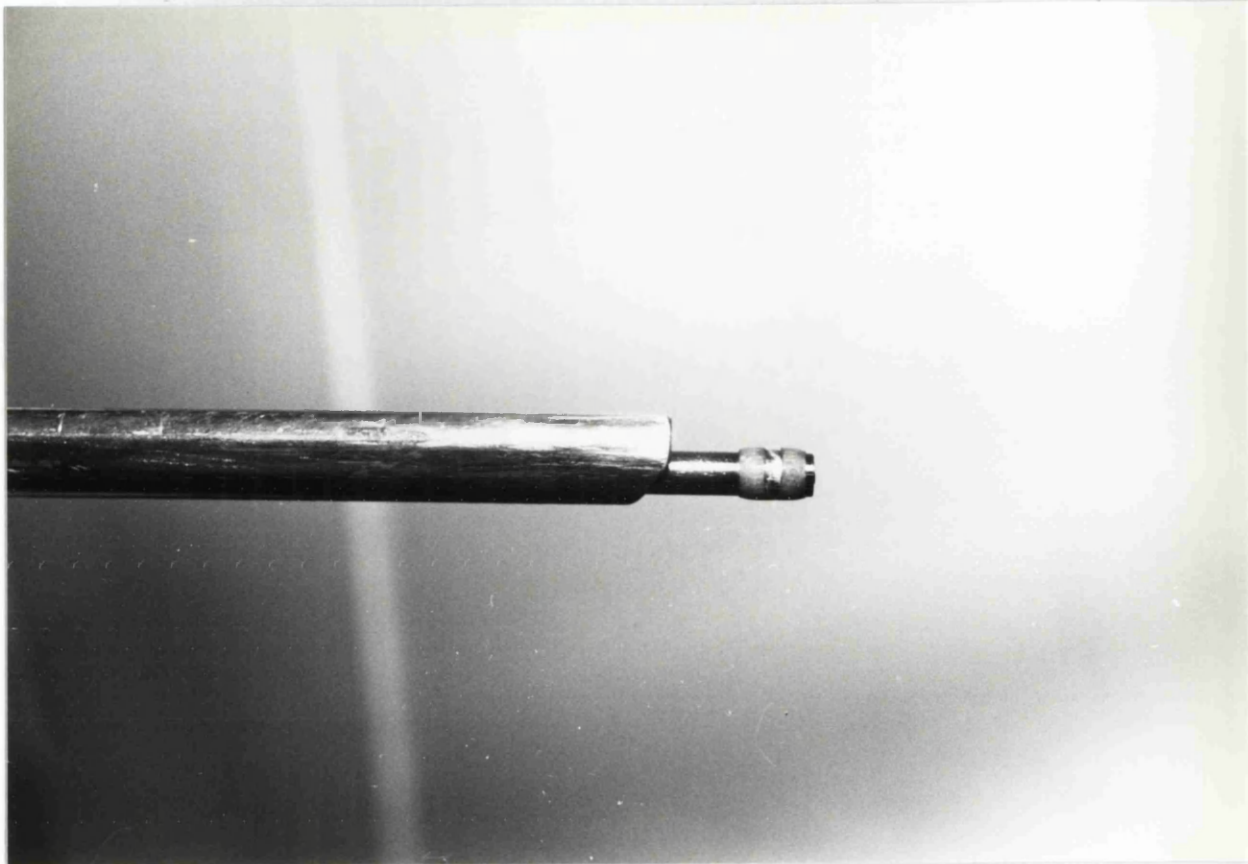


Figure 4:5. The diathermy plate on the ELSA. It lies between rings of insulation material.

CHAPTER 5

CLINICAL USE OF THE ELSA FOR PROSTATE REMOVAL

Ethical approval was granted to use the ELSA transurethrally for the removal of clinically benign prostatic hyperplasia and superficial bladder tumours. The 5 mm ELSA with its diathermy potential and integrated 27 F endoscope was used.

7 patients awaiting a routine TURP were taken from the waiting list. All gave written consent for this new procedure. The cases were chosen for their relatively small prostates palpated clinically. Their mean age was 70 years (range 63 - 79). Each patient had a pre-operative post micturition abdominal ultrasound, flow rate and culture of urine. All were in good general health with urodynamic and symptomatic evidence of bladder outflow obstruction. Transrectal ultrasound was used in only 2 patients.

All patients received a general anaesthetic and a covering dose of 120 mg gentamicin intravenously. The lithotomy position was used. Sterile drapes were as for a routine TURP. An anterior Otis urethrotomy (wound to 28 F) was carried out before insertion under vision of the 27 F ELSA endoscope. A preliminary cystoscopic inspection was made. No additional bladder pathology was seen in 6/7 patients. There was a small papillary bladder tumour present in one patient. Its subsequent removal with the ELSA is recorded in the bladder tumour section of Chapter 6.

The ELSA, with 45° raked blade, was set at 40,000 rpm and a suction pressure of 75 cm Hg. The endoscope irrigation was balanced to produce a continuous flow through the system. During removal of the prostate the endoscope tip was kept at the verumontanum, enabling the aspirator to remove tissue towards the bladder neck. The integrated monopolar diathermy plate was used for haemostasis. The aspirated tissue was all taken into the suction bottles directly in 4 cases, but in the last 3 was passed through a collection bottle with a 2 mm mesh filter (figure 5:1). A traditional diathermy resectoscope was used to tidy up any uneven surfaces and to complete haemostasis when necessary.

The results were compared with a control group of 7 patients, matched for age and approximate prostate size, who underwent a TURP by the same operator (the author).

The ELSA group: The ELSA removed the prostate tissue but every procedure was slow and punctuated by the need to unblock the aspirating channel of the liquidiser with a retrograde infusion from a syringe. The visualisation was poor once tissue removal began. The mean operating time was 85 minutes (range 50 - 120). Over such lengthy periods of use the motor/aspirator connection became loose several times requiring removal and reassembly of the instrument. A traditional resectoscope was required in each case to resect loose flaps of tissue and complete haemostasis. But on every occasion a significant bladder outflow tract had been created with the ELSA.

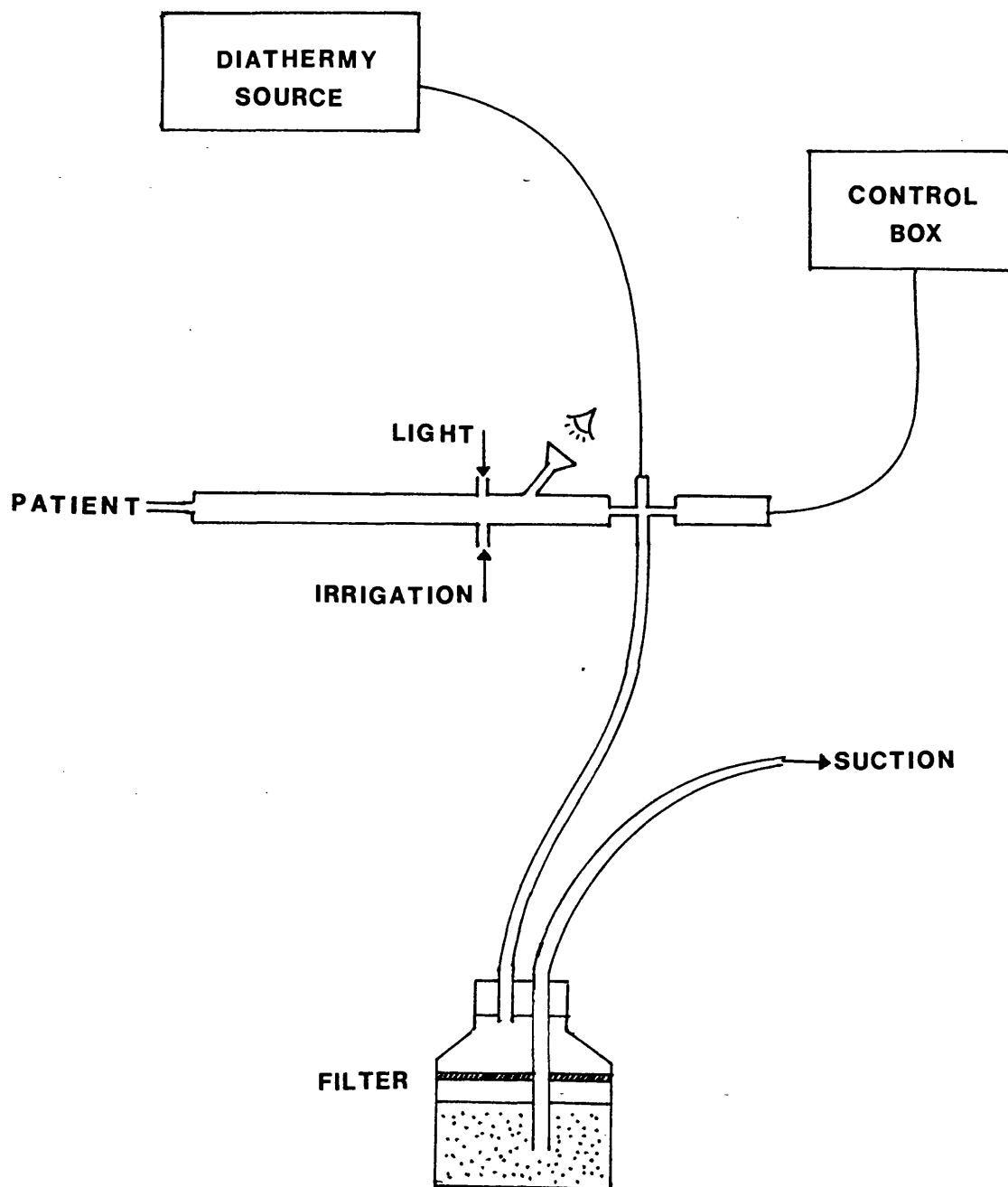


Figure 5:1.

Diagram of apparatus used for clinical ELSA prostate removal.

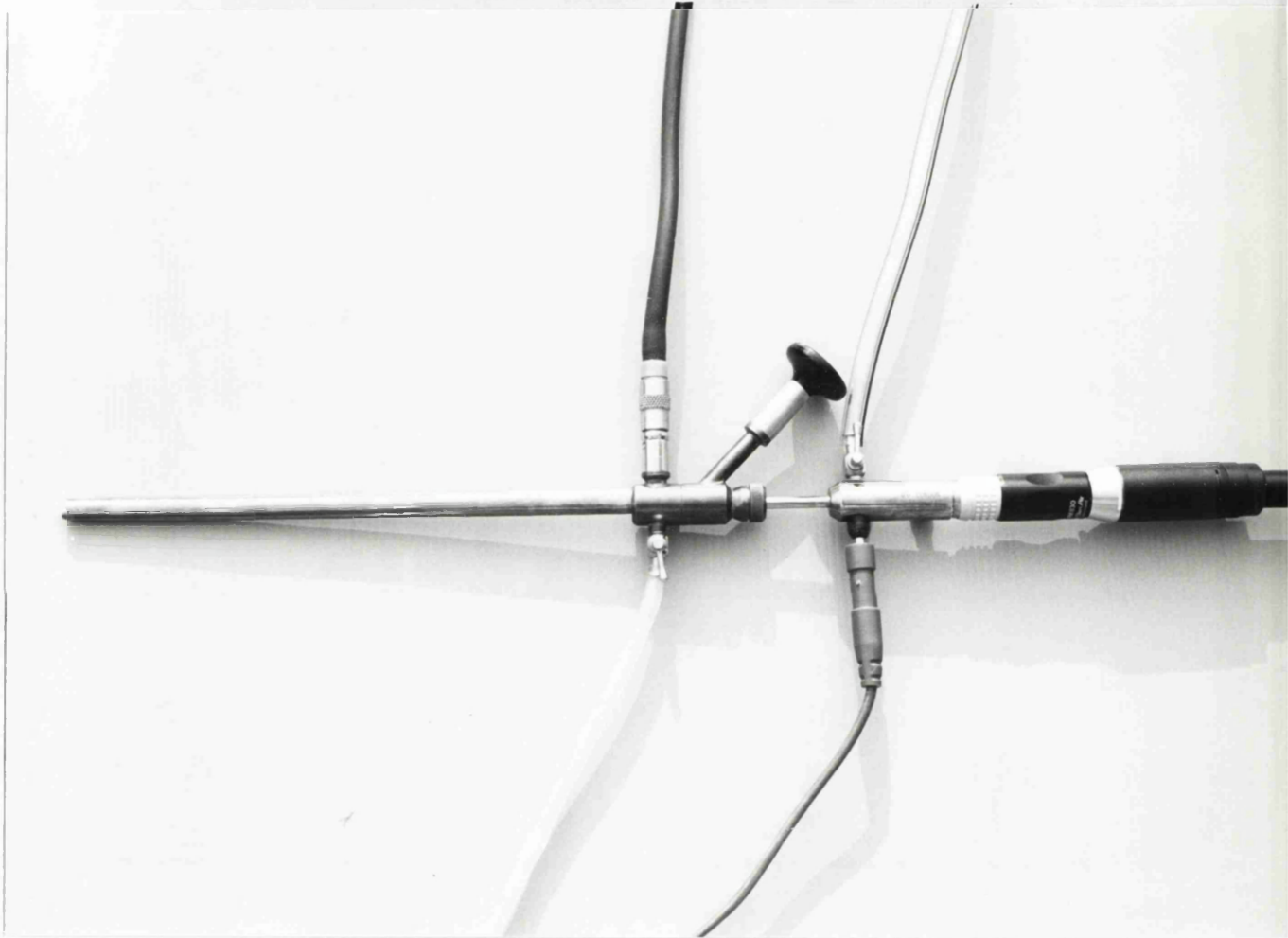


Figure 5:2. The ELSA set up for clinical use.

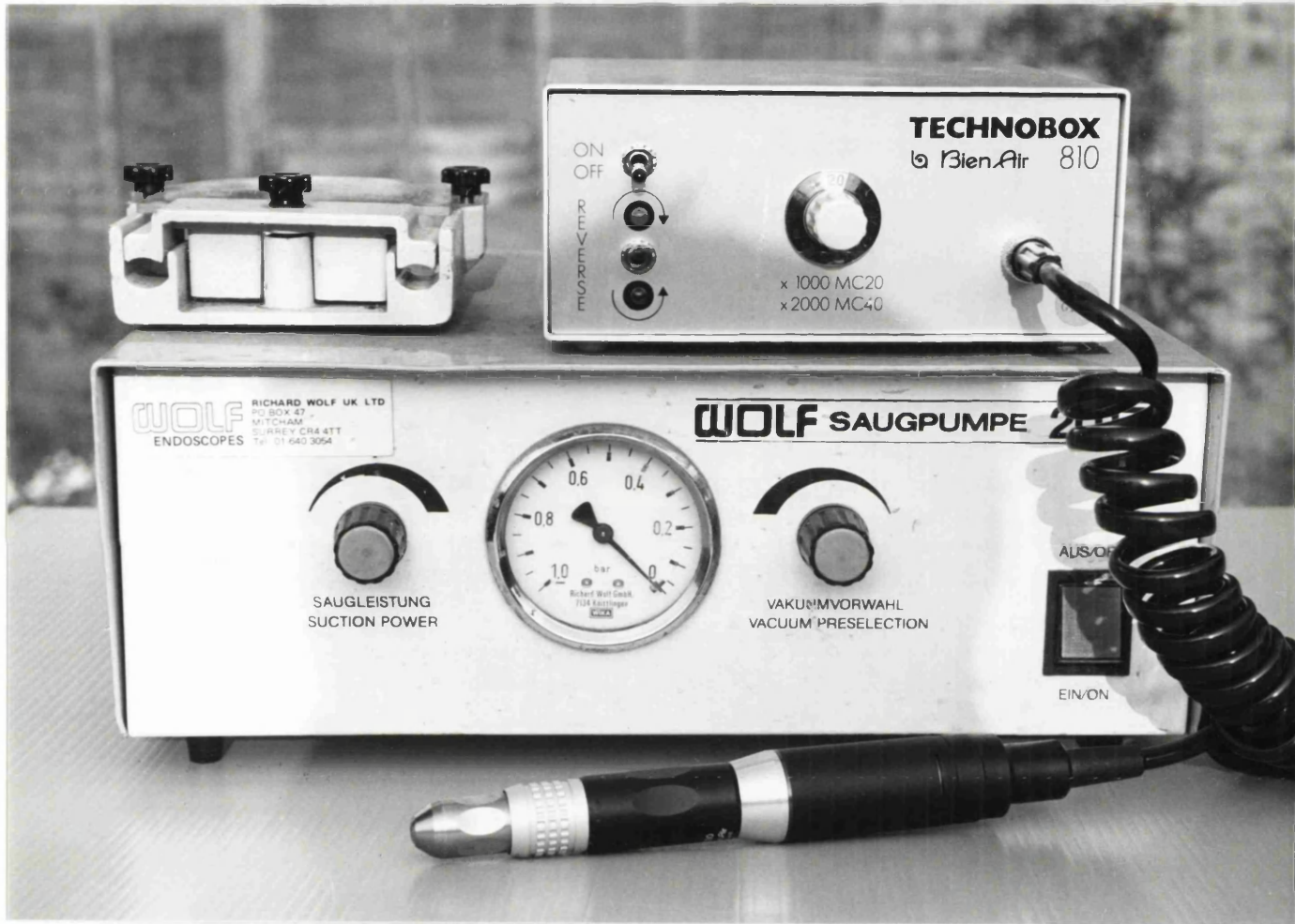


Figure 5:3. The peristaltic pump and motorised unit to drive the ELSA.

6 patients made an uneventful recovery despite prolonged operating times. Catheters were removed by the fourth postoperative day. These 6 patients regained good control of micturition with an improved flow. The mean preoperative flow rate was 11 ml/sec (range 6 - 13). Follow up studies were carried out two months after discharge in outpatients. The mean postoperative flow rate was 16 ml/sec (range 13 - 22). All postoperative postmicturition pelvic ultrasound showed a significant or complete absence of residual urine in each case.

1 patient died apporoximately 12 hours after his procedure. At the end of his procedure he had been shocked with abdominal evidence of extravasation. With adequate drainage, blood replacement and correction of hyponatraemia and metabolic acidosis he initially responded favourably. His blood pressure dropped again several hours later and he could not be resuscitated. A coroner's post mortem identified a hole in the posterior prostatic capsule with a large (2 litres) haematoma in the retroperitoneum.

Analysis of the removed tissue was made by flow cytometry on an aliquot of aspirated fluid and by traditional histology of additional resected tissue. All specimens showed benign prostatic hyperplasia.

The control group: The mean operating time was 45 minutes (range 15 - 58). There were no technical or clinical problems. Catheters were removed at the fourth postoperative day. Flow rates improved from a mean of 12 ml/sec to 20 ml/sec. All postoperative postmicturition

pelvic ultrasounds showed a significant decrease or absence of residual urine.

There was no statistical difference between the change in flow rates of the 2 groups ($t = 2.9$, $0.02 > p > 0.01$).

The liquidisation process of the ELSA was efficient but the aspiration of this material and subsequent visualisation was far from being so. The mean operating time for the ELSA was almost twice that of the control group. Long operating times using hypotonic solutions are dangerous because of absorption producing hyponatraemia and acidosis (Mebust 1989). Glycine was used in these cases to facilitate the use of the diathermy for haemostasis. The death of patient 7 undoubtedly highlights the problems of having an efficient tissue remover, the tip of which can seldom be seen, during a prolonged operation where equipment was having to be cleaned and reassembled.

Nevertheless, the potential is there for an efficient and safe instrument if the design of the irrigation and aspiration channels can be changed. In particular the aspiration channel must be widened and the right angled bend close to the exit port straightened. A more rigidly fixed motor/liquidiser connection is also required. Until these modifications are made further clinical cases are not justified in view of the death of patient 7.

It is impossible to assess how much tissue was removed by the ELSA. It cannot be weighed as can the "chips" after a traditional TURP.

Transrectal ultrasound can assess the size of the prostate . It was used pre and post operatively in 2 of these cases. It was difficult to identify any change in the volume and yet both patients had both subjective and objective improvement in their symptoms. A possible explanation of this is that only small amounts of tissue had been removed but that this was from a functionally critical portion. One might have expected a similar improvement after bladder neck incision only.

Tissue analysis will still have to depend on histological examination. Simple DNA analysis of the aspirated material showed a predominantly (80-90%) diploid DNA distribution. But whilst this pattern is usually associated with benign growth it can infrequently be found with well differentiated adenocarcinoma of the prostate.

CHAPTER 6

REMOVAL OF OTHER TISSUES USING THE ELSA

- A. Testicle (clinical).
- B. Ovary (cadaver).
- C. Bladder tumours (clinical).
- D. Kidney (cadaver, animal and clinical).

A. Testicular Tissue.

The patient was a 72 years old man with symptomatic bone metastases from prostatic carcinoma. A bilateral subcapsular orchidectomy was indicated. This was carried out with the patient under a general anaesthetic using the 5 mm ELSA hand held without its endoscope, set to 40,000 rpm, 50 cm Hg suction and 10 ml/min infusion. The skin was incised with a scalpel.

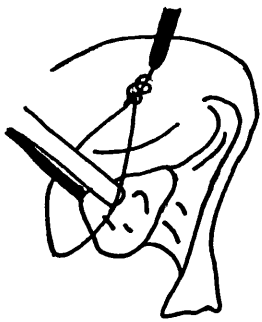
The flat blade would not penetrate the tunica, but the diamond-shaped blade did so easily. Once the soft testicular substance had been entered, the ELSA, again with the flat blade, completed the subcapsular orchidectomy with ease in 30 seconds (15 g testicular tissue was estimated to have been aspirated). When the tunica was incised further, a clear demonstration of the complete removal of the softer testicular tissue without capsular marking could be seen. This operation will never be an indication for the ELSA, but this case does serve as ^{why?} clinical confirmation of the action of the ELSA with different blades as was suggested by the experiments in Chapter 2.

B. Ovarian Tissue.

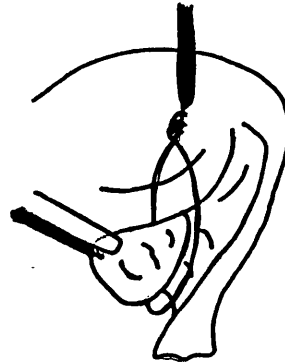
5 ovaries were removed from 3 female cadavers using the 10 mm ELSA. Semm (1977) has described a laparoscopic oophorectomy using a triple puncture technique, endoligation with special catgut loops and removal of the ovary piecemeal with a large rongeur. The same technique of access and endoligation (see figure 6:1) was used in our cadaveric operations. The 10 mm ELSA (40,000 rpm, 75 cm Hg suction and 10 ml/min infusion), used through a separate sheath to the laparoscope, was able to rapidly remove the ovaries providing the ovary was stabilised by a pair of endo-forceps. This requirement for stabilisation of the target tissue is always important. There has to be some forward pressure of the ELSA onto any tissue to produce the seal onto the housing and initiate liquification. The majority, but not all, of the liquified tissue was kept within and aspirated from the housing. The soft material of the ovary is not dissimilar to the testicle. This technique has not yet been performed clinically because one cannot guarantee that some liquified tissue which may be malignant might not be disseminated around the abdominal cavity.

C. Bladder Tumours.

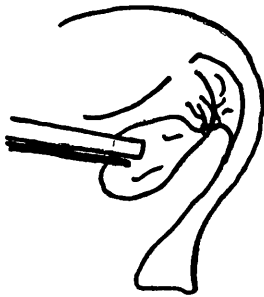
Preliminary assessment of the ELSA on a cystectomy specimen containing multiple superficial (PT1 G3) transitional tumours suggested a clinical application. Transurethral diathermy loop dissection is a successful and safe procedure in experienced hands. Its one drawback is that it



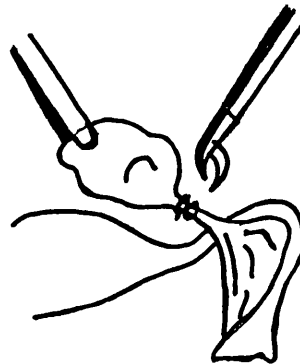
1



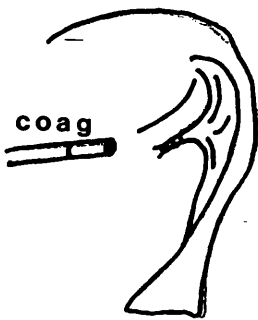
2



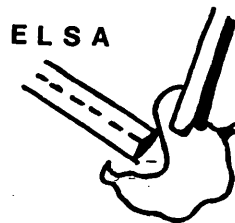
3



4



5



6

Fig.6:1. Diagram showing endoligation and aspiration of an ovary.

requires a side cutting action and tumours that are in the vault are difficult to resect. The forward action of the ELSA offered a potential for tumours in this region of the bladder. For the purpose of this clinical study, papillary tumours in all parts of the bladder were removed with the ELSA.

9 male patients were chosen because of small filling defects in the bladder outline on their intravenous urograms (mean age 70, range 57 - 81 years). All had presented with painless haematuria and were otherwise in good general health. Written consent was obtained. Preliminary cystoscopy confirmed the presence of a superficial papillary tumour in all cases. 2/9 were in the vault and 7/9 were on a lateral wall.

All the patients received a general anaesthetic and antibiotic cover (gentamicin 120 mg IV stat). The patient was prepared and draped as for a routine transurethral resection of bladder tumour (TURBT). All patients underwent a preliminary Otis urethrotomy to 28 F. An initial part resection, including muscle, was taken with the diathermy resectoscope. Subsequent tumour removal was with the 5 mm endoscopic ELSA. The set up was as for the transurethral aspiration of the prostate (figure 5:1).

Resected tissue underwent histological analysis. Samples also underwent flow cytometric analysis. An irrigating catheter was left in situ until haematuria cleared. All patients were brought back for a check cystoscopy at 3-monthly intervals for the first year.

Adequate removal and subsequent haemostasis was achieved with the ELSA in all cases. Visualisation was a lot clearer than when used for prostate removal. The 2 vault tumours were the easiest to remove. 8 of the cases made a rapid and uneventful recovery. 1 case, a vault tumour, had suprapubic fullness at the end of the procedure. Cystoscopy was unremarkable, but a cystogram showed a perforation at the vault and a small extraperitoneal collection. An urethral catheter was left for 5 days in this patient. There were no further problems.

Histological assessment showed that all the tumours were of transitional cell type and superficial (pTA/TI and G1/G2). 8/9 tumours yielded an analysable DNA profile. Only 1 of the tumours was aneuploid. Follow up is now over twelve months for all patients and therefore all have had at least 4 check cystoscopies. Only 1 patient has so far had a recurrence and this was not the patient with the perforation.

The transurethral application of the ELSA for superficial bladder tumours has been more successful than for the prostate. Subjectively it did seem easier to remove the 2 vault tumours although the perforation of 1 patient serves to remind one how indiscriminatory its action is without the purely flat blade.

Unfortunately, whilst flow cytometry is still finding its place in routine clinical urological practice, the production of a suspension of particles rather than chunks of tissue will prevent the ELSA being useful in the majority of cases.

D. Renal Tissue.

Three methods have been used to remove a kidney employing the ELSA. The first was an attempted percutaneous nephrectomy in a cadaver, the second was the removal of a kidney replaced by xanthogranulomatous pyelonephritis at an open clinical operation and the third was a percutaneous nephrectomy in a dog.

1. Percutaneous cadaveric nephrectomy: Soft renal tissue can be easily removed with the ELSA. An endoscopic nephrectomy seemed to be a possible milestone ahead. It might be possible to use Semm's endoligation techniques for the renal pedicle and coagulate any capsular vessels. However this goal has proved to be elusive because the retroperitoneal endoscopic dissection of the renal pedicle is fraught with difficulties. Access through the renal angle and also beneath the tip of the 12th rib to the kidney in 5 cadavers using carbon dioxide insufflation and standard laparoscopic equipment was relatively easy. Subsequent orientation was very difficult; in 3 cases the peritoneum was punctured and in 1 the aorta was torn during endoscopic dissection of the pedicle. An anterior approach was attempted in 2 further cadaver studies. This seemed a more logical and easier dissection but the inability to retract intraperitoneal contents prevented clear visualisation of the underlying structures.

2. Open nephrectomy with the ELSA: A 39 year old female patient had end-stage renal failure due to chronic infection and stone formation. A bilateral nephrectomy was required before being entered into the

transplant program. At operation only a left nephrectomy could be performed. The right kidney, showing evidence of severe xanthogranulomatous pyelonephritis, was deemed inoperable. Subsequent infective episodes still prevented transplantation.

In order to remove this remaining kidney safely it was embolised with Ivalon sponge via a selective transfemoral angiographic technique preoperatively. An open operation followed 6 days later. The previous scar was incised and a very adherent kidney exposed. It would have been impossible to indentify the renal pedicle.

The hand held ELSA was used to aspirate the kidney and the staghorn within it, leaving a rim of tissue adherent to surrounding structures. Neither cortex nor stones were a problem but some parts of the fibro-elastic pelvicaliceal system did wrap around the blade and require removal. No active bleeding was encountered. The patient made a rapid uneventful recovery and is now awaiting a transplant.

This would suggest that a percutaneous endoscopic nephrectomy would be feasible if the vasculature was completely blocked preoperatively by a similar radiological technique.

3. *Canine percutaneous nephrectomy*: Collateral circulation and incomplete embolisation are the main problems of organ-ablating embolisation. Recanalisation would not be a problem if there was to be a short time interval before organ removal. Rassweiler (1986) has shown that "Ethibloc" (Ethicon, Hamburg) is superior to Gelfoam powder, Ivalon

sponge and Histoacryl embolisation agents, and to central renal artery ligation in both rats and dogs. Ethibloc is the first embolisation medium especially developed for peripheral intravascular transport (Bücheler 1978). Ethibloc is an alcoholic solution (60%) of Zein (corn protein occluding agent), contrast medium, oleum papaveris (prevents file formation) and propylene glycol (disinfectant). The occlusion mechanism is a precipitation of the alcohol-soluble zein in contact with water or blood. In practice a preinjection of 40% glucose is given to slow down the precipitation process until the agent reaches the arterial capillary bed. The ratio of this glucose solution to the Ethibloc is critical in determining the extent of embolisation within the organ (Rassweiler 1986). For complete capillary embolisation of the kidney the amount of preinjected glucose should be 20-30% of the expected embolisation volume.

A series of animal experiments was carried out to determine the feasibility of a percutaneous nephrectomy. Six Beagle dogs (16 - 32kg) were used. They were all anaesthetised with an intravenous barbiturate (300mg Nembutal/Kg), and sacrificed at the conclusion of the experiment. The objectives in the first four dogs were to ascertain the ideal interval between embolisation and a safe renal ^Sdissection, and to confirm that the Ethibloc not only passed to every capillary bed but did not cross these into the systemic circulation. A complete percutaneous endoscopic nephrectomy was to be carried out in the remaining 2 dogs.

The renal arteries were catheterised in all cases via a transfemoral route with a 5 French balloon catheter (Cook). The balloon was inflated

in the renal artery. Embolisation volume ranged from 4.5 - 6.0 mls. The amount needed was estimated by pre-embolic perfusion with contrast medium. After the injections of first glucose, and then Ethibloc, a second injection of glucose was given to clear the catheter and prevent a long string of precipitated Ethibloc being left proximally as the catheter was withdrawn.

A laparotomy was performed in the first 4 dogs. The embolised kidney was exposed. The kidney was incised and then excised at progressively shorter intervals: 2 hrs, 1.5 hrs, 1 hr and 0.5 hrs. These 4 dogs were sacrificed after approximately 2 - 3 hrs and histological examination made of the embolised kidney, the heart and the lungs.

Dogs 5 and 6 underwent a nephrectomy with the ELSA. This was introduced below the 12th rib. In one dog an intrarenal technique was used via an Amplatz sheath introduced in the usual way for percutaneous intrarenal stone surgery. In the last dog an extrarenal technique was used, that is, the tissue removal began at the surface of the kidney. Carbon dioxide insufflation was used to open tissue planes and promote visualisation. Irrigation was delivered via the ELSA at 20 ml/min. The ELSA was set at 40,000 rpm, 75 cm Hg and the flat blade was inserted. At presumed completion of the nephrectomy the abdomen was inspected for inadvertant damage and haemorrhage.

The first 4 dogs showed that a minimum of 1 hour after embolisation is required to allow bloodless incision and excision of the kidney.

Histological studies showed that the Ethibloc had reached all examined

arterial capillary beds (figure 6:2) and was absent from the heart and lungs.

Both versions of the endoscopic nephrectomy were completed within 10 minutes. The contralateral kidney in each of these dogs weighed 25 and 28 g respectively. Neither nephrectomy could be achieved with adequate visualisation and yet the only iatrogenic damage was in one dog with a small laceration of the liver. Renal haemorrhage was insignificant in both cases.

It was exciting to realise this milestone that had seemed impossible until an embolisation technique was used. However, one could not explain the lack of back bleeding from the venous system in the absence of embolisation agent. Not only must this puzzle be solved but further procedures are required where the animal is not sacrificed immediately. Only then will postoperative safety from haemorrhage be more accurately assessed.

One has to accept that a percutaneous nephrectomy will not be usefully carried out under vision. But this may not be a problem. The presence of contrast medium in the Ethibloc allows continuous fluoroscopic monitoring. Another possible form of monitoring would be ultrasound. The hypothetical advantages of ultrasound would be a lack of radiation exposure to the operator's hands and the rapid ability to move the probe and so be more sensitively orientated in 3 dimensions.

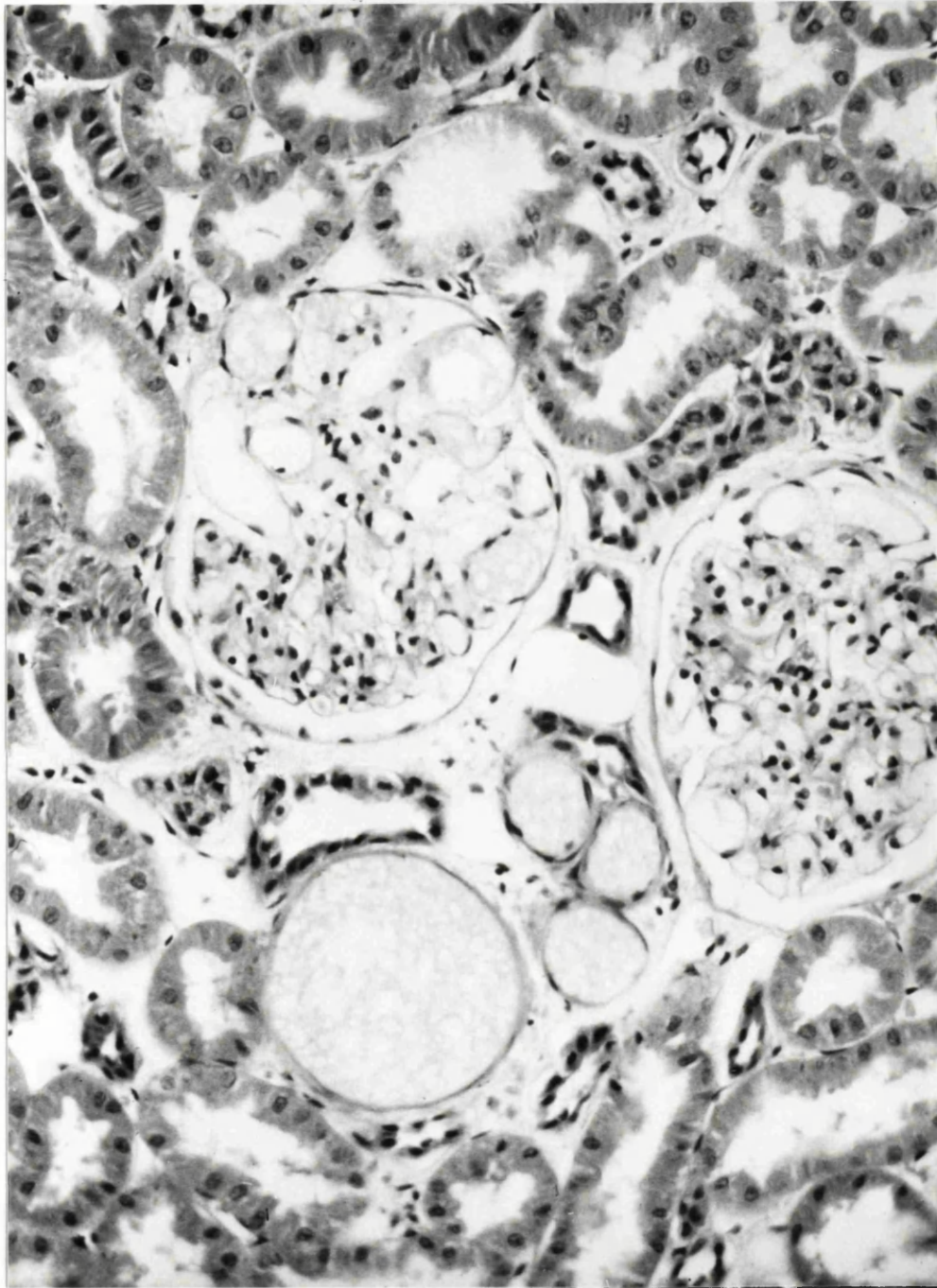


Figure 6:2. Histological section of a canine kidney 1 hour after Ethibloc embolisation. The embolisation agent has filled the glomerular arterial capillaries.

APPENDIX TO CHAPTER 6: EMBOLISATION OF THE CANINE PROSTATE.

This section has been placed as an appendix to Chapter 6 because it follows on from the successful embolisation technique employed for the kidney. It answers the rhetorical question posed on page 54.

The canine prostatic artery arises from the pudendal artery at the level of the second or third sacral vertebrae. It may sometimes arise from the umbilical artery near its origin. 3 canine prostates were embolised in vivo with Ethibloc in 3 of the male dogs used in the renal experiments, just prior to sacrifice. The prostatic arteries were intubated with 21 gauge cannulae and each artery ligated proximally. The volume of Ethibloc was again determined by a pre-injection of contrast (approximately 2.5 - 3.0 mls). 1.5 mls of Ethibloc were injected into each prostatic artery with a pre and post-injection of 40% glucose. The prostate was incised 15 minutes later. No haemorrhage occurred. The penis and prostate were excised and examined histologically. A transverse section of such an embolised prostate is shown in figure 6:3.

The same arterial access was used to obtain the macrovascular casts (figure 4:3).

The prostate could be totally embolised in the same way as the kidney. Transposing this to a clinical application begs the question whether it may be enough to leave the completely infarcted prostate in situ. This

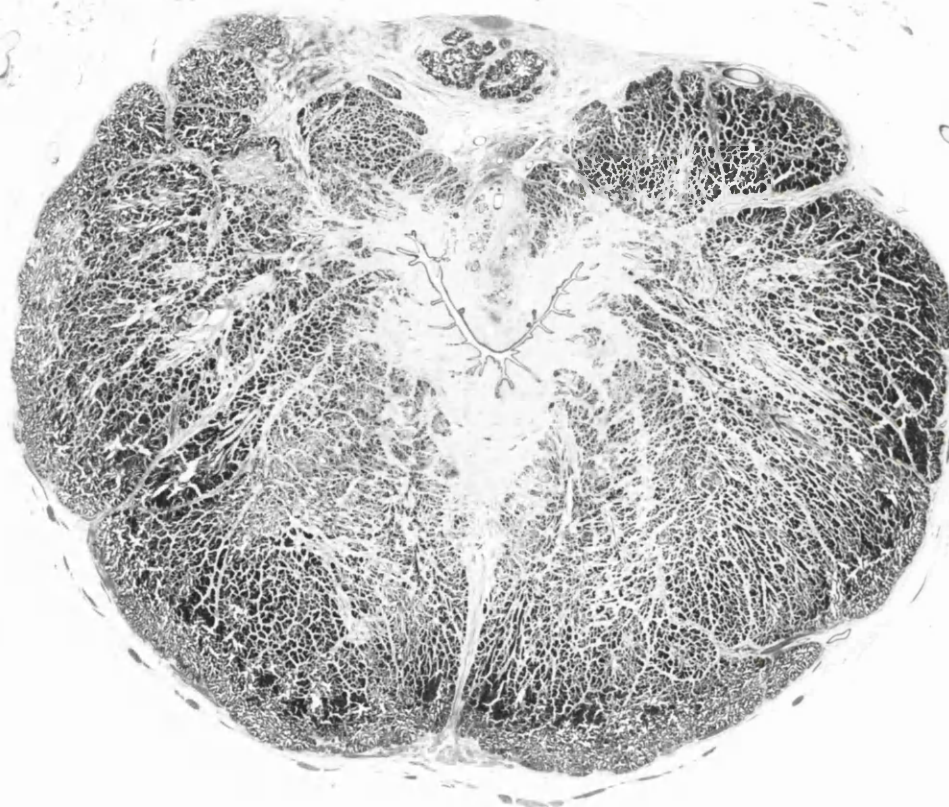


Figure 6:3 Histological section of the canine prostate after
Ethibloc embolisation.

may be applicable to cases of locally advanced carcinoma of the prostate where concomitant ischaemia of the corpora cavernosa is of minor importance.

Infarction of the corpora cavernosa without longterm recanalisation and without even partial revascularisation is a technique that those studying impotence have been seeking (Aboseif 1989). The use of Ethibloc may produce the animal ischaemic impotence model that has been so elusive. Further long term studies are required to confirm this and identify changes in the prostate before clinical applications can be investigated.

CHAPTER 7

A ROBOTIC PROSTATECTOMY: A LABORATORY ASSESSMENT

Robots entered the English vocabulary with the translation of Karel Capek's play "R.U.R." (Rossum's Universal Robots) in 1923. Capek was a Czech and in his native language the word "robot" simply meant a worker. Innovations in industrial robots have been considerable in recent years. The use of robots in medicine and surgery however has been limited to simple tasks such as patient handling devices and fetch and carry robots (Mallett 1989).

The potential contribution from a surgeon-robot is considerable. Robots are capable of positional and force control to accuracies at least equal to those of a human surgeon. Robot vision and other sensing systems can discriminate in some situations better than a human, particularly when supplemented by the visual senses of the surgeon using a camera and remote control monitor. Robots do have disadvantages. It is in the area of tactile discrimination that artificial sensors remain relatively poor compared to human capability. Also, the ability to respond appropriately in unforeseen circumstances is very limited.

One of the main reasons for the slow introduction of robots in surgery has been the consideration of safety. Legislation in industrial robot safety has meant that the operator is not allowed to be within reach of a robot when in both "teach" and "replay" modes. Of necessity, most surgical applications would require robots to be able to contact the patient even if the operator is safely out of reach, and this will require a complete

rethink of the Robotic Health and Safety codes. The ability of a robot to make a repetitive action quickly and accurately with a complex trajectory makes the endoscopic removal of prostate tissue by a robot a reasonable starting point.

The aim of this study is to demonstrate the relative simplicity and feasibility of undertaking a robotic prostatectomy in the laboratory. The success of this experiment would therefore introduce the concept of robots to surgeons and lay the groundwork for further studies on safety before applying this technique in a clinical setting.

The Robot.

The complex geometry required for a simulated prostatectomy lead to the adaptation of a 6 axis unimate "Puma" industrial robot to provide the primary motions. This robot is relatively easy to teach a repetitive yet accurate task via an associated personal computer (V.A.L. language). The robot was provided with a specially designed framework which in turn carried the Endoscopic Tissue Liquidiser and Surgical Aspirator (ELSA). The 5th (pitch) axis of the robot was used to carry the external framework which contained the endoscope. The first 5 axes allowed the endoscope to be positioned and orientated correctly. The 6th (rotation) axis was then used to carry the inner framework (figure 7:1). The latter supported the liquidiser/aspirator and also carried a motor/gearbox assembly that provided the linear motion of the instrument. An adjustable stroke length was provided using resettable micro switches. Thus the inner framework could reciprocate and rotate with reference to the outer frame in the same

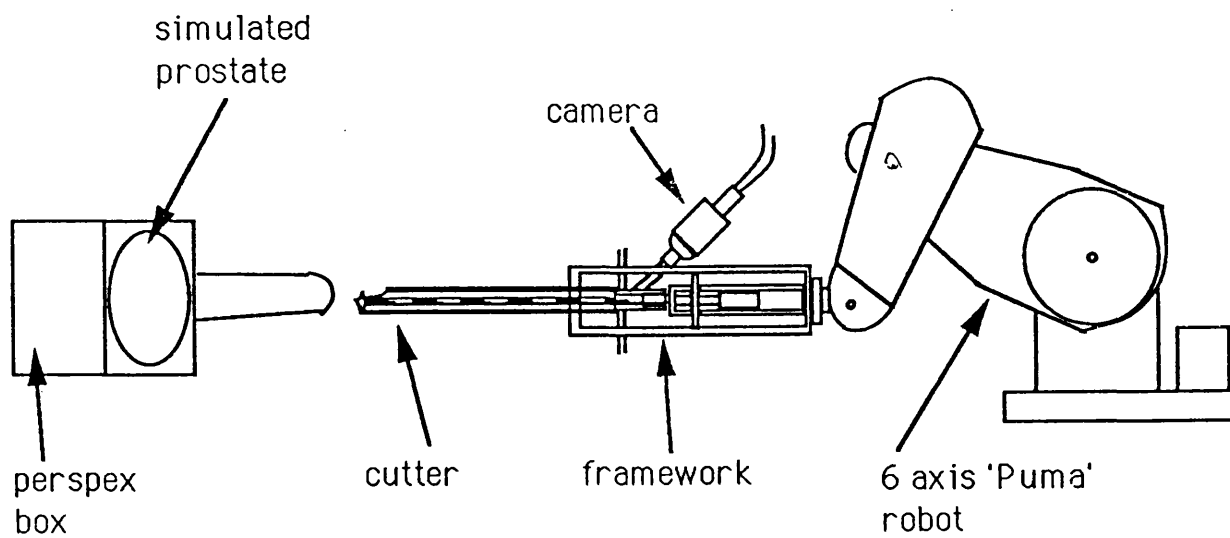


Figure 7:1 Diagram showing the ELSA fixed to a 6-axis robot.

way that a human operator could direct the liquidiser/aspirator through an endoscope. A charge coupled device (CCD) video camera was attached to the endoscope to allow continuous visualisation of the working tip of the ELSA on an external monitor.

The Prostate Model.

The target tissue was potato. Potato could be easily sculptured into the shape of the prostatic urethra and its high water content facilitated the use of monopolar diathermy both for simulated coagulation in this study and simulated diathermy loop resection when used as a mockup for routine transurethral resection of the prostate (TURP) training.

The sculptured potato was held in a perspex box at the root of an attached plastic penis. The potato was earthed to a valley lab diathermy machine. Simulated haemorrhage into the prostatic cavity was achieved in the following way. The potato was pierced in 4 quadrants with a 14 gauge medicut needle and cannula, and the cannulae retracted to the periphery of the potato. This left 4 x 2 mm diameter tunnels into the prostatic urethra which could be irrigated with red dye via lines into the cannulae. The fluid was kept at 80 mm Hg to simulate human prostatic haemorrhage (see Chapter 4). These internal openings could be sealed endoscopically by diathermy in a manner similar to that used in a TURP or with the coagulation plate around the liquidiser/aspirator of the ELSA.

Although the ideal geometric form of prostatic tissue to be removed is a curved approximation to the outlying capsule it was felt reasonable to

approximate this to an asymmetrical cone for the purpose of the robotic demonstration. This made the programming much easier. The transverse and longitudinal sections of this preprogrammed removal are shown in figure 7:2. The apex of the cone begins at the imaginary verumontanum. The dimensions described are those found to be the minimum dimensions possible within a series of cadaveric prostate glands measured. Lowsley (1912) dissected 224 cadaveric prostates and showed that in those men over 50 the average length of the gland was 3.65 cm (range 2.4 - 4.5), width 4.37 cm (range 3.3 - 5.0) and height 2.75 cm (range 2.4 - 3.4). These ranges were also seen in the dissection of cadaveric prostates in Chapter 4. The preprogrammed resection is based upon these minimum dimensions.

The variation in the angle of the ELSA when removing the defined volume was between 60° above the horizon to 30° below. Because the ELSA must pass down the penis and then pivot about the root of the penis, the robot was allowed to sweep out an inverted and amplified motion corresponding to the shape of the prostate. The amplifying effect of the ratio of length between the robot to the pivot point and pivot point to working tip was large, at around 8:1. This meant that the motion swept out by the end of the robot arm was considerable and care had to be taken to ensure that all the joints remained within the permitted range of motions during the whole operation.

The ELSA was first inserted into the penis and positioned so that it was at the centre of the prostate at its most anterior position (simulated verumontanum). The mounting frame was then moved into the correct location relative to the model and the ELSA clamped into position. In order to

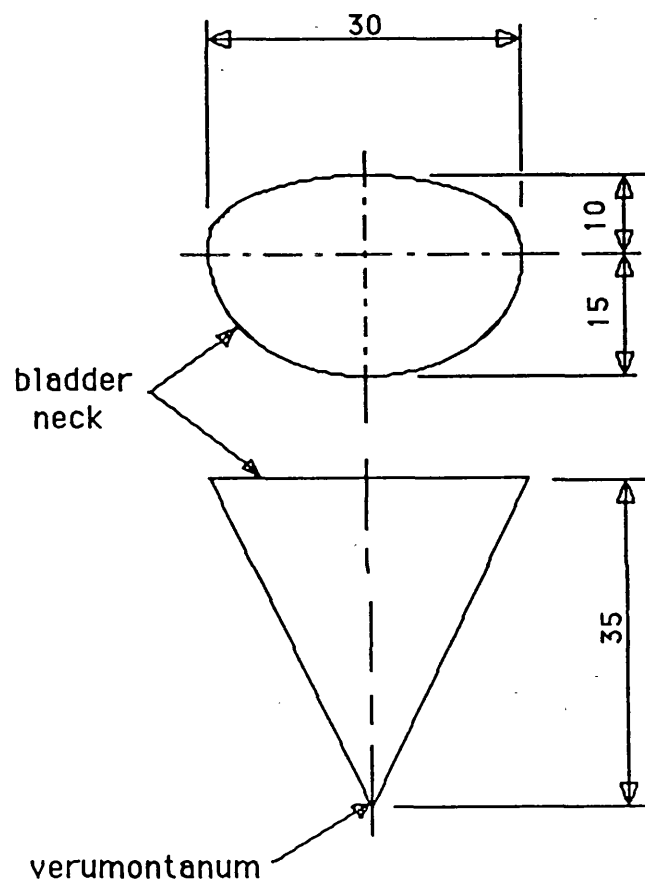


Figure 7:2. Preprogrammed dimensions of the "prostate" to be removed.

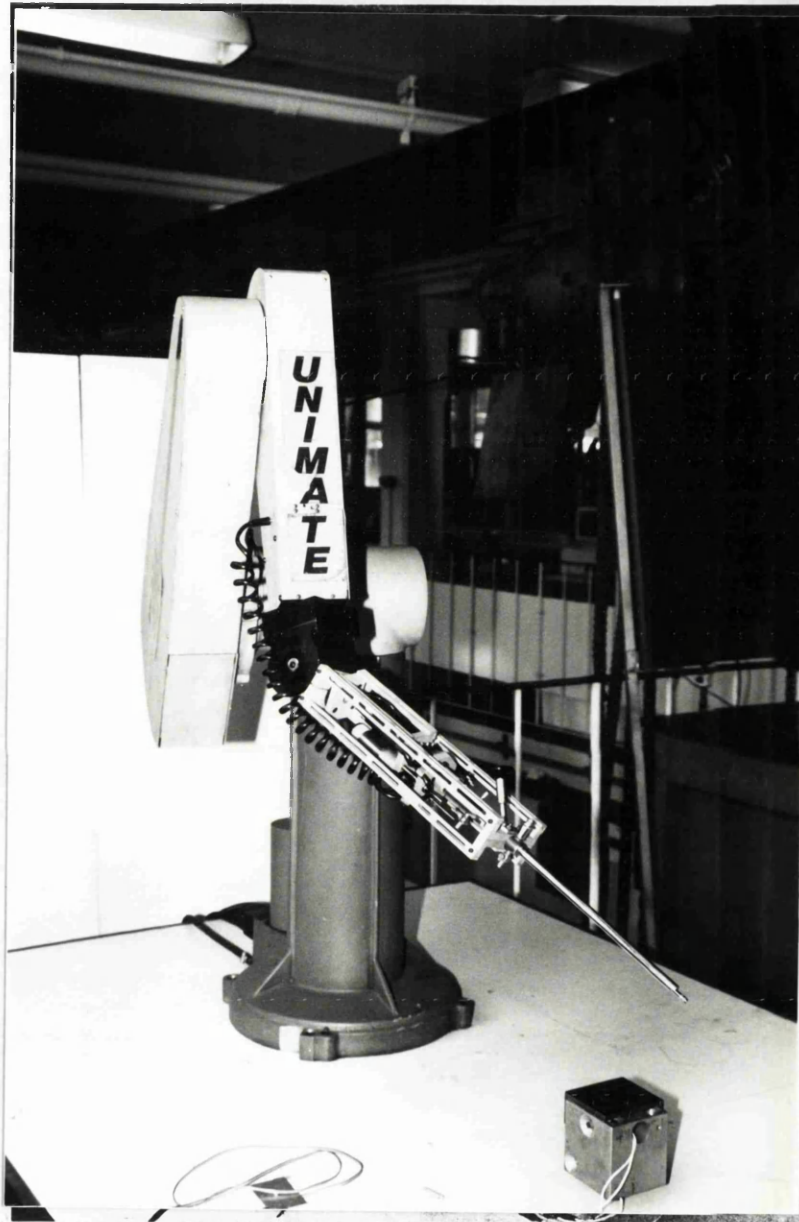


Figure 7:3. The laboratory robotic prostatectomy in progress.

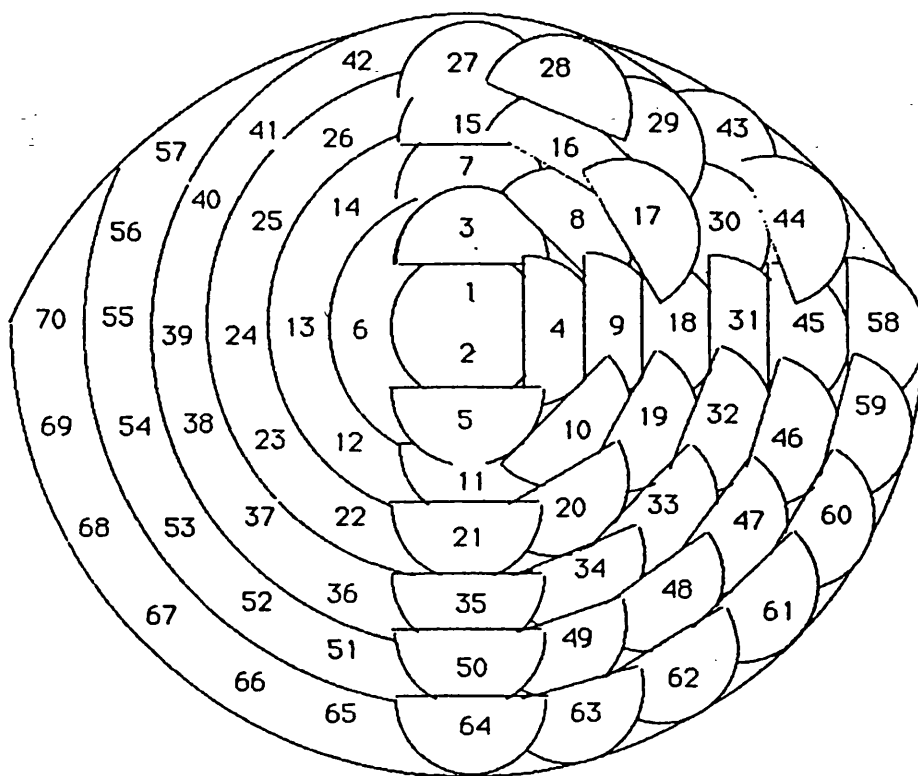


Figure 7:4. Transverse section at the bladder neck showing the sequence of cuts.

produce the required shape at the bladder neck, the area of potato/prostate to be removed was divided into a sequence of overlapping cuts (figure 7:4). Axes 1 - 5 of the robot were positioned to allow the insertion of the ELSA at the desired orientation to take the preliminary centre cut number 1. An axial cut was then taken on the forward stroke and diathermy cauterisation initiated on the return stroke. The 5th axis was readjusted to bring the endoscope to the correct position and orientation for the 2nd cut to be taken. On completion of cut number 2 the 2nd ring of cuts 3 - 6 was taken. This was achieved by again using robot axes 1 - 5 to position the endoscope in space whilst axis 6 was used to bring the working tip into contact with the tissue. When the ELSA was positioned at the 6 o'clock position (cut 5 in this row) the 4th axis was rotated back by 180° to avoid the possibility of the robot moving to such an extreme angle that a singularity point was reached when cutting in the 6 - 12 o'clock region.

At any point in the procedure the controller had the opportunity to interrupt a cut by pressing a single key on the personal computer. The robot then automatically moved back to its original neutral position. On asking the robot to resume cutting, the robot would position itself back at the interrupted cut and restart the cutting cycle for that location. The controller was asked at the end of each row of cuts if the next row was to be removed. Only when acceptance was indicated did the robot move to the next position. The asymmetrical nature of the tissue removed was achieved by the complete removal of the first 4 rows and partial removal of rows 5, 6 and 7. The whole procedure was repeated 10 times over a period of several weeks to assess the duration and reproducibility of the technique.

The experiment was repeated successfully on each 10 separate occasions. The mean time for the procedure was consistent (4.8 ± 0.05 minutes). The dimensions of tissue removed varied by less than 1 mm in all cases. There were no technical failures, and no sudden aberrations from the predetermined program of movements.

The newly described model prostate has proved itself to be eminently suitable for evaluation of a robotic prostatectomy. It has also been used by urologists in training to familiarise themselves with the action of the more traditional resectoscope (see Appendix to Chapter 7). Indeed the author has attempted to remove the same dimensions with both a resectoscope and the ELSA but hand guided. In both cases the procedure could not be achieved in the same time as the robot nor with the same evenness of cut and certainly not with the same reproducibility. Subsequent evaluation of the ELSA for removal of human prostatic tissue has been disappointing. Therefore if the robot prostatectomy is to progress further towards a clinical application then the robot arm should carry a standard diathermy resectoscope. Only minimum software changes will need to be made. Major advantages of the robot with either the ELSA or resectoscope are that both the trajectory is predictable and the robot does not get lost in space. The surgeon however, in a purely manual operation, can often lose orientation and find it necessary to go back to the start position to reestablish where he is in space. Also to ensure a good view through the endoscope it is necessary to coagulate after each cut. The robot can make a ring of cuts without losing its location and so the frequency of coagulation can be considerably reduced. Indeed since the whole cutting

sequence can be performed within 5 minutes the haemorrhage could be controlled after the final cut, reducing the operating time.

It is the accuracy and reproducibility of this robot operation that is appealing. Unfortunately there are few operations which can be distilled down to such a repetitive yet exact sequence of surgical manoeuvres. The ability of a robot to respond appropriately in unforeseen circumstances (artificial intelligence) is very limited and at present slow. It would be preferable for the present robot to respond to feedback from real time rectal ultrasound but this must await improvement in the reaction time of the intelligence system.

Although these experiments demonstrated complete control by the robot it is probable that we will see robots introduced into surgery first in a assistant's role. This would also overcome some of the safety problems mentioned above. A study by Kwok et al (1988) has used a standard robot to position a locating jig to manually drill the skull of a patient as part of a Computer Tomographically guided stereotactic neurosurgical project. Unless a robot has physical constraints so that it is inherently incapable of moving outside a specified area, and has fault tolerant software, it is unlikely that powered robot applications will be generally acceptable. One way of avoiding these difficulties is to ensure that the robot is not powered and is thus not capable of moving other than when repositioned by the surgeon. This type of approach has been taken by Soni (1987) in the use of a passive robot which acts as a positioning aid for spinal surgery.

However if a special purpose surgeon-robot was constructed it could be made intrinsically safe since it would be possible to introduce physical steps to limit the range of robot motion to "safe" areas. Also software and sensors can be triplicated to use majority voting techniques to cater for potential failure. These, together with continual monitoring by a surgeon, imply that safety criteria could be satisfied. Parallels may be drawn with the care of aircraft automatic landings in which the safety of passengers depends upon the correct operation of sensors and control systems, albeit monitored by the pilot, have gradually become accepted by the public as a routine procedure. It is my belief that a robotic prostatectomy will become a routine procedure in my lifetime.

APPENDIX TO CHAPTER 7: A TRAINING MODEL FOR TURP.

Transurethral resection of the prostate is a frequently performed procedure that requires considerable experience. Just how one acquires that experience is open to debate. There is no doubt that the first time many British surgical trainees get their hands on a diathermy resectoscope is when they do their first case. The presence of one's supervisor or even his attention to a video monitor does not automatically impart to one the tactile response learnt only after hundreds of these procedures. There is a need for a training model that will allow the trainee to coordinate the smooth lazy curve of the loop with the diathermy pedals. The potential for such a simulator was created in the laboratory assessment of the robotic prostatectomy.

It would be difficult to construct a trial to show that simulated training for a TURP produced a better operator (figure 7:5). However, having invited several diploma students from the Institute of Urology to use the model, I have witnessed dramatic improvements in technique and speed in all of them. It has sometimes taken over 2 hours of practice to teach them, but I am convinced that I would rather their mistakes were occurring on the model than in their first couple of patients.

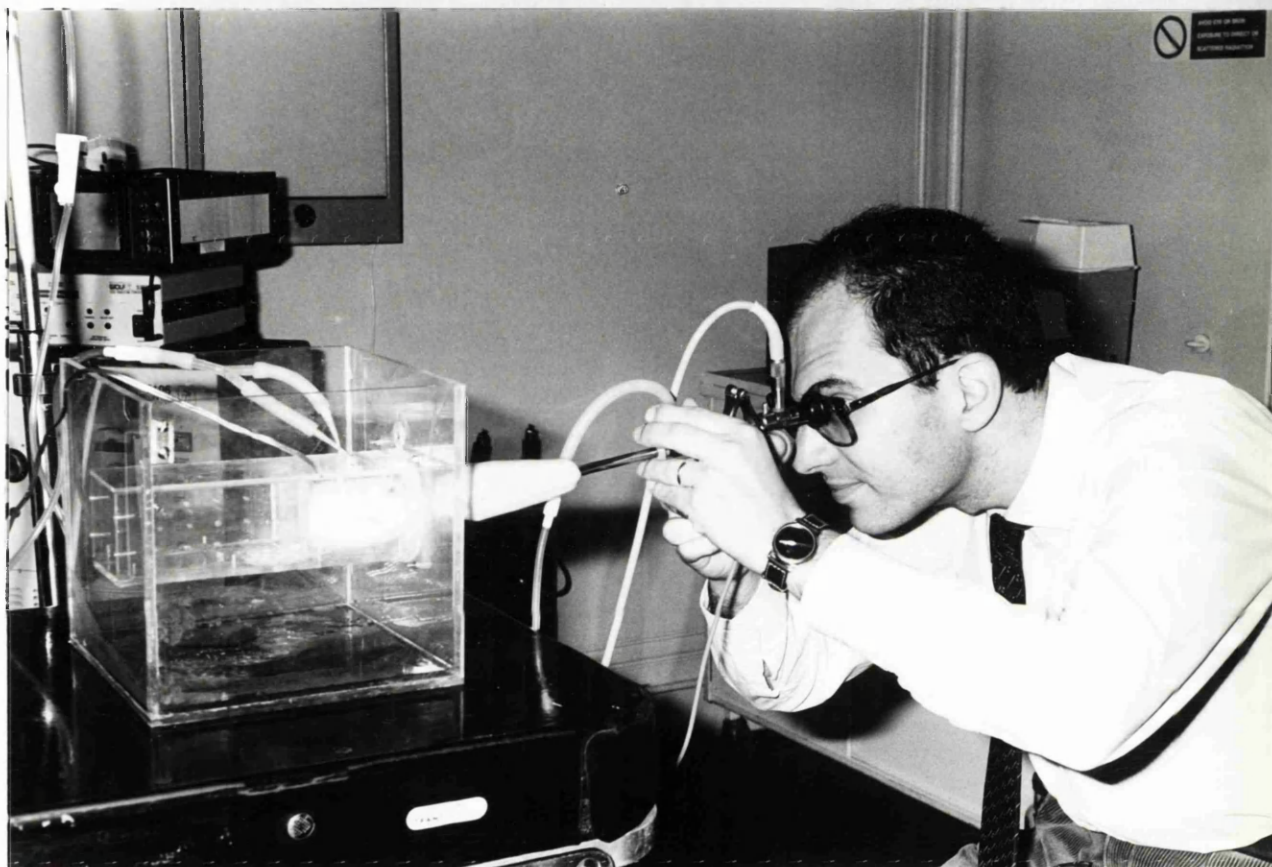


Figure 7:5. A trainee urologist using the model prostate.

CHAPTER 8

THE ELSA FOR URINARY STONE FRAGMENTATION

The endoscopic methods by which large urinary stones in the kidney and bladder can be fragmented and the resultant particles naturally or mechanically removed have transformed stone surgery. Renal stones can be approached through percutaneous tracks (Payne 1989). Bladder stones can be approached per urethra or percutaneously (McNicholas 1988). Endoscopic techniques for fragmenting these calculi include electrohydraulic and ultrasonic lithotripsy (EHL or USL). Both create shockwaves at the surface of a stone.

It is difficult to fragment hard stones such as cysteine or monohydrate oxalate calculi with either EHL or USL. Because the ELSA had the potential to drill through bone it was also evaluated for stone fragmentation. This chapter describes the current concepts of stone fragmentation and the role of EHL and USL. A laboratory comparison of the ELSA with EHL and USL is followed by a clinical study using the ELSA on bladder and renal stones.

Mechanism of stone fragmentation.

When a stone is struck by a shockwave, a series of stress waves radiate from the point of impact and move off into the body of the stone. They reach the further boundaries of the stone and are then reflected back as

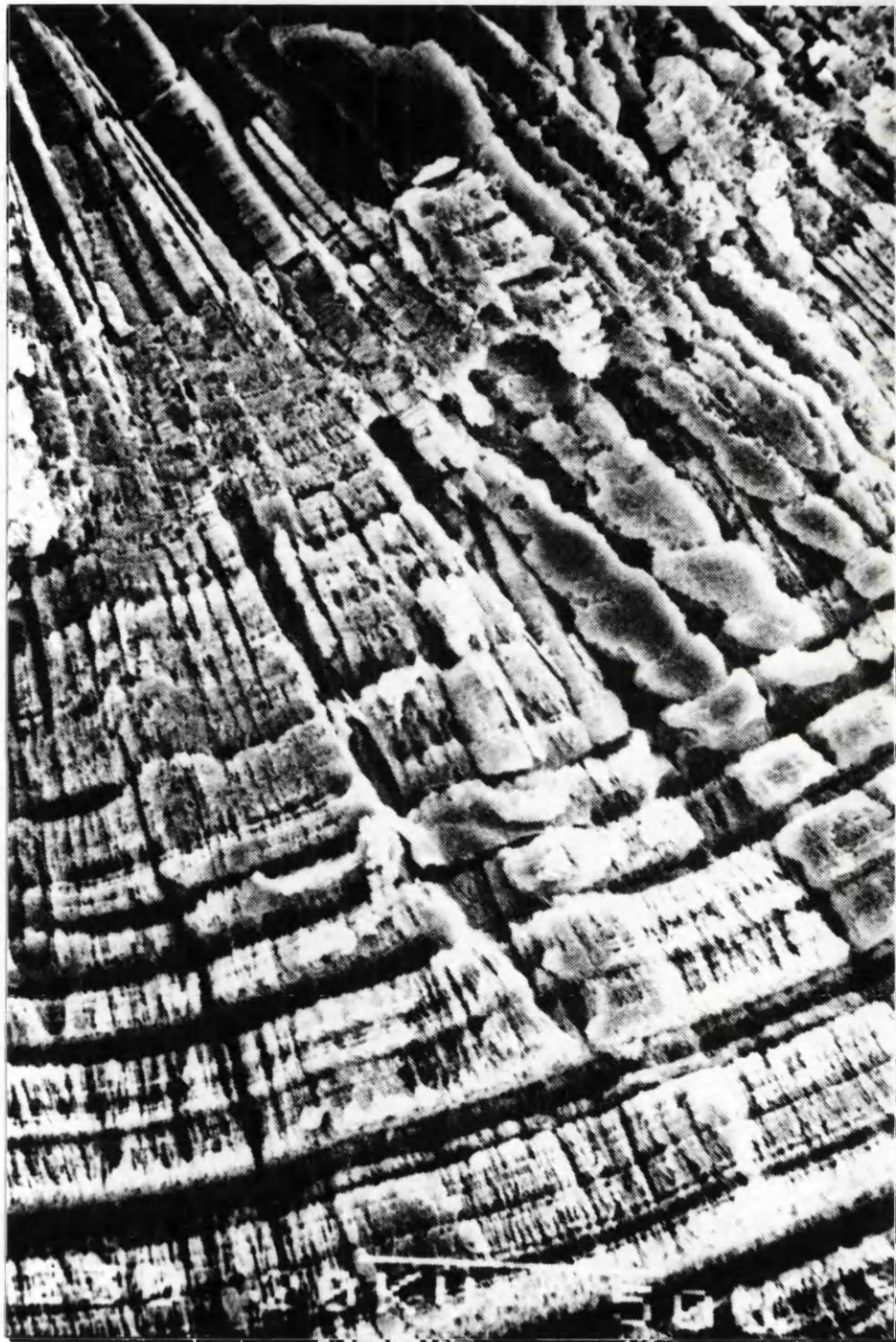


Figure 8:1. Electron microscopy of a cut oxalate stone.



Figure 8:2. Sequential photographs during crushing of an urinary stone.

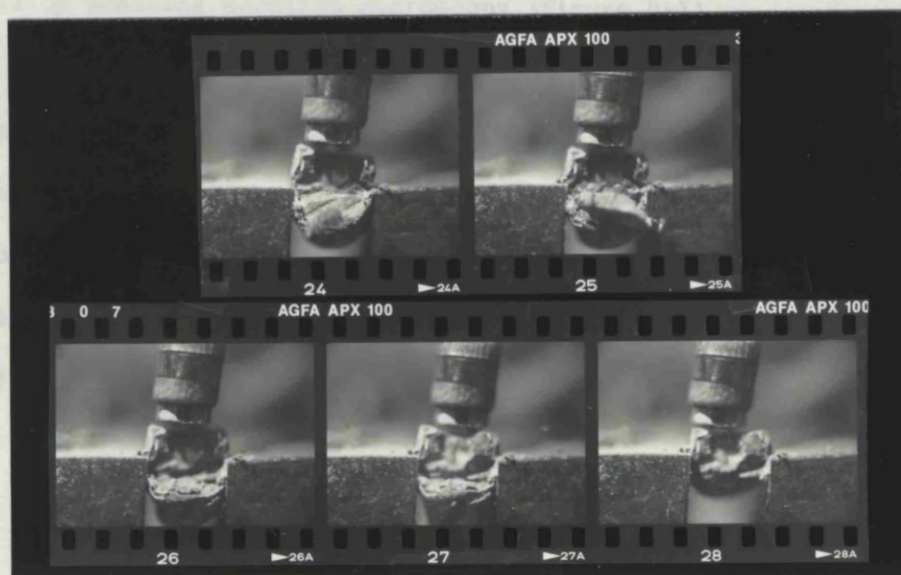
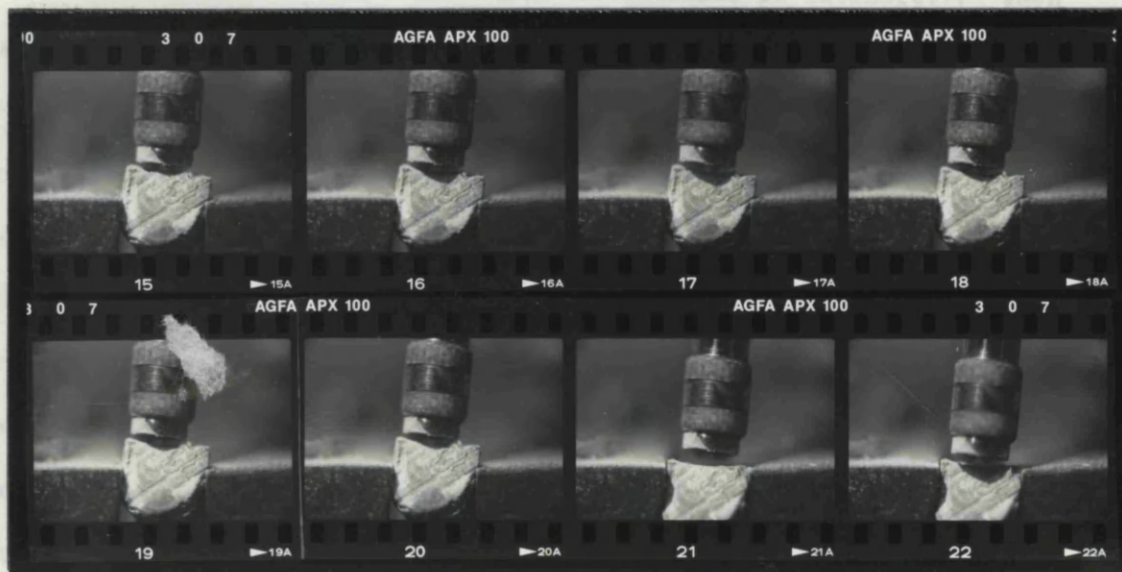


Figure 8:3.

Sequential photographs showing the primary abasive and secondary fragmentation action of the ELSA on an urinary stone.

a kind of echo with little attenuation (or decrease in intensity). When the reflected shockwave meets the outgoing one there is a concentration of stress. This may be sufficient to create a crack, especially at a point of weakness (e.g. crystal boundary) which may be sited well away from the original point of impact (Coptcoat 1990). A similar situation occurs when a loosely supported square ceramic tile, which one presumes is uniform, is struck a measured blow in the centre of one flat face; in many cases the tile breaks at the corners and not where it was struck. The stress waves are reflected and crowded into the corners. These concepts, though largely hypothetical, would account for the variability of stone fragmentation with composition. The fragility of a stone is due to the irregularity of its macrostructure as well as its composition. Defects in a chemically uniform oxalate stone are highlighted by scanning electron microscopy (figure 8:1).

These phenomenon can be demonstrated by fast frame photography of a stone being slowly compressed. A series of 35 mm photographs taken using a motor drive at 3/second is shown in figure 8:2. When a device such as the EHL, USL or the ELSA is used on a stone there is both a surface effect specific to that modality and a secondary effect within the stone. This can be seen in the sequence of photographs in figure 8:3.

Experiments on stone strength.

Before any laboratory comparison could be made between the various fragmentation devices a reference for stone hardness was required. Young's modulus is a mathematical expression of strength.

$$\text{Young's Modulus (E)} = \frac{\text{Stress (MN/m)}}{\text{Strain}}$$

Strain

The compression tests on various renal calculi, gallstones, chalk and a sugar cube were carried out on an INSTRON 112 testing machine at the University of Sussex. The parameters studied were similar to that obtained on the rig described in Chapter 2. Unfortunately that rig could not produce forces great enough to crush a stone or sensitive enough to record its consequent strain.

The Instron uses a moving crosshead, driven at constant strain by 2 motor driven screws, to exert a load on a sample mounted on a load cell. To measure the load applied by the crosshead the machine employs a universal load weighing system. This comprises a metal bar, mounted within a load cell, with a series of strain gauges attached along its length. As the load increases the bar begins to bend so distorting the balance of the strain gauges. The signal from the gauges is amplified to give a linear pen response on a simultaneously driven chart recorder, previously callibrated and set to zero.

The stones were measured using a metric micrometer screw gauge with an accuracy of +/- 0.001 cm and a top pan balance with an accuracy of +/- 0.01 g. Due to the irregularity of the biological samples a sphere model was employed to aid calculation of stress and strain values. The measurements and dimensions of the stones were averaged to give an

overall diameter of a sphere. The value of stress for such a regularly shaped sample is:

$$\text{Stress} = \frac{\text{Force}}{\text{cross-sectional area}}$$

The crosshead was set to descend at a speed of 0.05 mm/min. The chart recorder was started while zero load was being applied shortly before the crosshead came into contact with the test specimen under investigation and was stopped after the first fracture was indicated by a sharp drop in the applied load. A typical compression test graph is shown in figure 8:4. The fracture point is clearly seen as a rapid decrease in applied load. Using the values of chart speed in mm/min and crosshead speed in mm/min, a value for the distance moved by the crosshead to cause the first fracture could be determined.

$$\text{Strain} = \frac{\text{change in length (l)}}{\text{original length}}$$

The peak value of load could be directly read from the graph and converted to a force, in Newtons, by multiplying by g, the acceleration due to gravity (9.81 m/s²).

This value for force was divided by the cross-sectional area of each sample to produce a measurement of stress. With values of stress and strain Young's Modulus could be calculated for each "stone". The results are shown in Table 8:1.

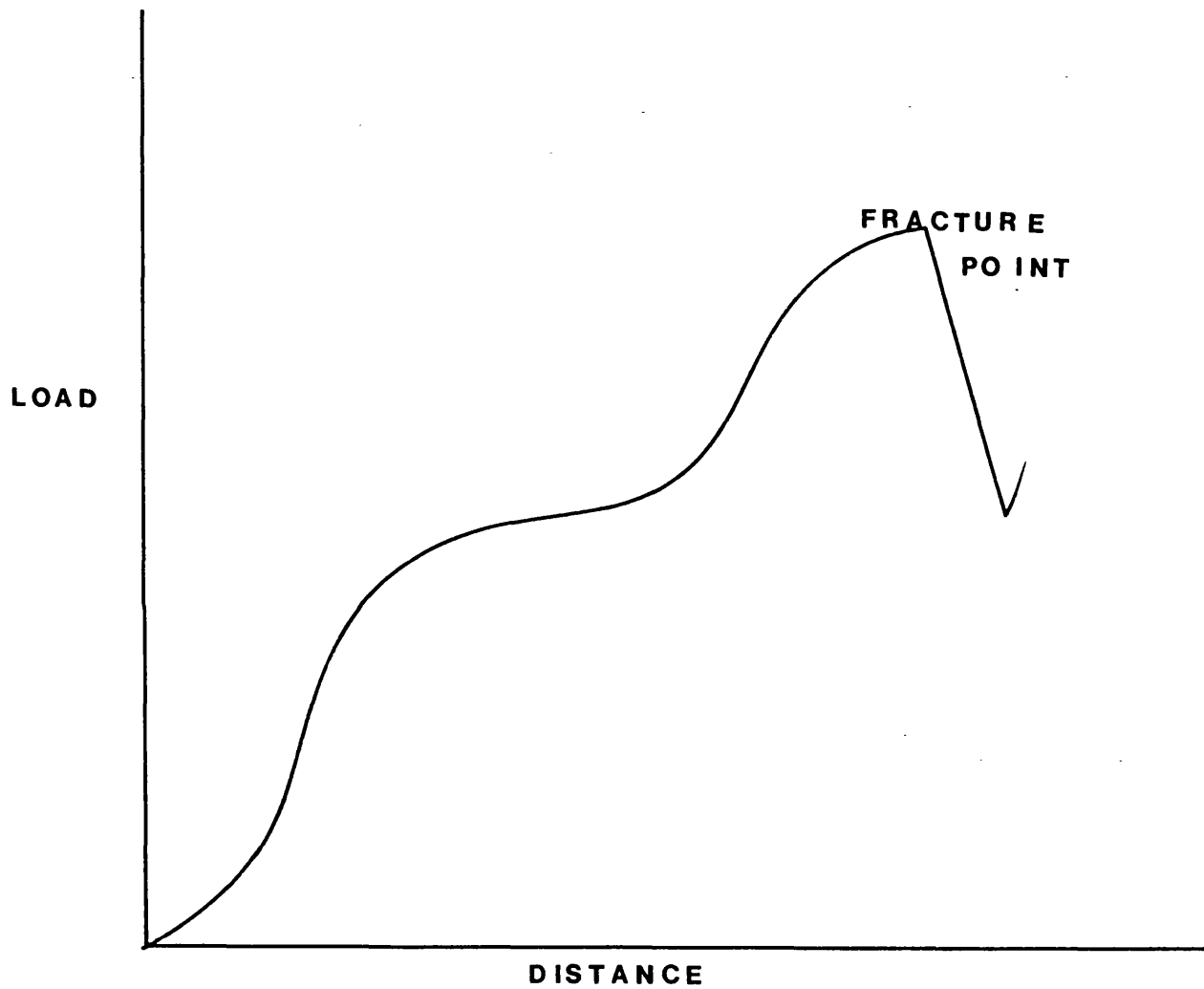


Figure 8:4. Typical compression test graph for a hard material such as an urinary stone.

As one would expect from a clinical experience of Extracorporeal Shockwave Lithotripsy (ESWL), phosphate and dihydrate oxalate stones have the lowest Young's Modulus. These always require less acoustic energy for fragmentation. The dihydrate oxalate and cysteine stones had higher values. These are the stones that are clinically hardest to fragment with either ESWL or endoscopic techniques such as EHL or USL. But on a scale of hardness that includes such materials as a sugar cube and limestone then they too are quite fragile. Their relative fragility

Table 8:1. Results for Young's modulus

<u>Stone type</u>	<u>Mean E (MN/m)</u>	<u>S.D.</u>
Phosphate (n=10)	44.43	15.09
Dihydrate oxalate (n=10)	50.60	2.10
Monohydrate oxalate (n=10)	61.82	29.71
Cysteine (n=4)	118.82	12.19
Pigment gallstone (n=5)	38.25	2.31
Chalk (n=5)	30.23	1.2
Sugar cube (n=1)	168.25	
Limestone (n=1)	381.64	
Plaster of Paris (a) (n=5)	30.52	3.78
Plaster of Paris (b) (n=5)	160.40	9.23

is probably due to the multiple crystalloid boundaries within each stone. These are the sites of weakness (vide supra). A uniform simple sugar cube is three times as strong as an irregular dihydrate oxalate stone.

A laboratory comparison between EHL, USL and the ELSA for stone fragmentation.

1. *Electrohydraulic lithotripsy (EHL).* This is a device that creates a high tension discharge between 2 electrodes at the tip of a flexible probe. The electrodes are manufactured according to 2 patterns; coaxial and parallel. If 2 electrodes are placed in a fluid medium and a high tension voltage passed between them for a very short time, the fluid will be vaporized and a bubble will be generated that will spread out at the speed of sound (Coptcoat 1990). As one might expect, the resultant shockwave can damage anything in close proximity, be it stone or urothelium. When used for urinary stone fragmentation the resultant particles must be removed, or left to pass naturally if small enough. The probe can be used with a flexible or rigid endoscope.

2. *Ultrasonic lithotripsy.* This method of endoscopic stone fragmentation differs from EHL in that the mechanism is one of drilling. Ultrasonic drilling of calculi involves the piezo-electric excitation of a quartz crystal creating expansion and contraction, and thus producing vibration energy. Increasing the frequency of an applied alternating potential causes the crystal to vibrate at high speed with the production of a sine-wave displacement. Transmission of this vibration

to a metal probe or cylinder will cause the probe to vibrate in sympathy. Probe tip movement will be maximal if the maximum amplitude of the sine-wave is coincident with the tip of the probe. As the hollow probe enters a stone, small fragments can be aspirated through its centre. This is its great advantage over EHL. At the same time shockwaves pass out from the tip causing fractures at distant sites in the stone. This rigid probe requires a rigid endoscope with an offset eye piece.

3. *The ELSA.* The action of the ELSA on hard materials is similar to the drilling/aspiration effect of the ultrasound probe with secondary fragmentation occurring distant from the point of action. However, with the clinical experience of the timidity of action of the USL on hard stones (Miller 1985), one would expect the ELSA to be of benefit since it had been found to pass through bone and limestone (Chapter 2).

Experimentation with blade design for the ELSA to fragment stones required standardisation of the target material. Estimation of Young's Moduli for various stones (vide supra) had shown that simple chalk was not dissimilar in its hardness. One solution was to create a standard stone from Plaster of Paris (PofP). The water content could be varied to produce a harder or softer stone. Empirical experimentation led us to establish 2 standard stone models: one with a Young's Modulus similar to a phosphate stone (mixture a; 15 g P of P + 15 ml water, $E = 30$) and one with a Young' Modulus similar to a cysteine stone (mixture b; 15 g P of P + 5 ml water, $E = 160$). These were tested with the Instron machine as described above to verify the values. Their values of E were more

consistant than those of chemically identical urinary stones and so provided the ideal model.

The same blades which were assessed for "soft" tissue removal were now reassessed on the 2 model stones.

- (See fig. 2:11)
1. Diamond shaped blade.
 2. Propellor blade with 45° rake.
 3. Flat bar.

A prototype 5 mm ELSA without a diathermy plate was run at 40,000 rpm, 75 cm Hg suction and 10 ml/min infusion (required for cooling). Each blade was used for each of the 2 stone models five times over a 2 minute run. The majority of the fragmented plaster was aspirated but some did spill out from the housing.

The best removal rate (see Table 8:2) on the "phosphate" model was achieved by the propellor blade. The best removal rate on the "cysteine" model was the diamond (cf: drill) blade.

There is no clinical problem in fragmenting softer stones such as phosphate or dihydrate oxalate and so a laboratory comaparison between the 3 fragmentation modalities (EHL, USL, and ELSA) was made on the hard "cysteine" model.

Each modality was used on such a model for 2 minutes and repeated 5 times. The stone models were weighed before and after fragmentation.

The difference in weight is described as the fragmentation rate. The comparative fragmentation rates are shown in Table 8:3.

Table 8:2. Results of "stone" removal rate (g/min +/- 1SD) with different ELSA blades.

<u>BLADE</u>	<u>"PHOSPHATE" MODEL</u>	<u>"CYSTEINE" MODEL</u>
Diamond	2.3 +/- 1.0	2.1 +/- 0.8
Propellor	5.6 +/- 1.2	0.6 +/- 0.3
Flat bar	1.0 +/- 0.4	0.2 +/- 0.04

Table 8:3. Results of fragmentation rates on a hard stone model using EHL, USL, and the ELSA (diamond blade).

<u>MODALITY</u>	<u>FRAGMENTATION RATE (g/min +/- 1SD)</u>
EHL	3.6 +/- 1.9
USL	2.0 +/- 0.6
ELSA	2.3 +/- 1.0

EHL is the most efficient at fragmentation as reflected in the difference in weight of the stone model before and after treatment. This must be balanced by the production of multiple fragments up to 4mm in diameter which although not part of the parent stone would require separate removal in a clinical setting. Both the USL and ELSA aspirate the much smaller particles that they create producing much less in the way of large secondary fragments. In this respect the USL is superior to the ELSA.

Clinical comparison between EHL, USL, and ELSA for renal and bladder stone removal.

11 patients with either renal (5 cases) or bladder stones were assessed in this study. There were 8 males and 3 females (mean age 47 years, range 28 - 72).

8 renal stones - phosphate x 3

- mixed oxalate x 1
- phosphate/oxalate mix x 2
- cysteine x 2.

3 bladder stones - phosphate x 3.

All patients gave their written consent and were treated at the Institute of Urology, London.

1. *Renal stones.* A routine percutaneous puncture and track dilatation was made into the pelvicaliceal system. All the stones required endoscopic fragmentation. Crudely, 2 parameters were being measured. First, the ease of fragmentation by each modality, and second, the rate of removal by USL and ELSA when used alternatively for 5 minutes. The former was assessed visually and the latter by weighing the aspirated stone particles after filtering.

2. *Bladder stones.* Stones over 5 - 6cm had previously been a relative contraindication for endoscopic fragmentation. With the routine introduction of a suprapubic approach, using the same principles as percutaneous renal access (McNicholas 1988), larger stones could potentially be fragmented and withdrawn. The 3 bladder stones were all over 5 cm in diameter. The fragmentation modalities were compared in the same way as for the renal stones.

The results are set out in Tables 8:4 and 8:5. All the procedures went smoothly and no unwanted sequelae occurred. Any fragments too large to be aspirated were removed with forceps. Each patient was cleared completely of stone after 1 procedure.

Table 8:4. Results of clinical renal stone fragmentation and removal.

<u>Stone Type</u>	<u>Ease of fragmentation</u>			<u>Aspiration rate (g/min)</u>	
	<u>EHL</u>	<u>USL</u>	<u>ELSA</u>	<u>USL</u>	<u>ELSA</u>
Phosphate	Easy	Easy	Easy	3.2	2.0
Phosphate	Easy	Easy	Easy	4.8	1.2
Phosphate	Easy	Easy	Easy	2.5	0.8
Oxalate	Easy	Easy	Easy	3.0	1.3
Phosphate/Oxalate	Easy	Hard	Easy	-	-
Phosphate/Oxalate	Easy	Mod.	Easy	-	-
Cysteine	Hard	Hard	Easy	0.2	1.3
Cysteine	Hard	Hard	Easy	0.3	0.9

Table 8:5. Results of clinical bladder stone fragmentation and removal.

<u>Stone type</u>	<u>Ease of fragmentation</u>			<u>Aspiration rate (g/min)</u>	
	<u>EHL</u>	<u>USL</u>	<u>ELSA</u>	<u>USL</u>	<u>ELSA</u>
Phosphate	Easy	Easy	Easy	3.3	2.8
Phosphate	Easy	Easy	Easy	2.9	2.5
Phosphate	Easy	Easy	Easy	4.0	3.0

It is already established that EHL is more efficient than USL at fragmenting hard stones (Miller 1985). The advantage of USL is that there is a controlled aspiration of the stone particles and a tedious grovel around distant calices is not usually necessary. The ELSA has shown both in laboratory and clinical situations it can fragment almost anything, and certainly any stone. However the aspiration of stone particles by the ELSA was always inferior to the USL.

The role of the ELSA for urinary stone fragmentation should be as a back up when very hard stones such as largely monohydrate oxalate and cysteine are encountered. At present it requires its own endoscope because the 5 mm ELSA is slightly too large for the working channel of most nephroscopes. The operations in this study were all carried out safely but the potential for soft tissue injury with the ELSA must be considered if it is not used carefully.

CONCLUSION

A summary of the results of this work can be found in the abstract to this thesis. This conclusion will concentrate on the fulfillment of the ELSA for the criteria of the ideal endoscopic tissue remover that was put forward in the introduction.

- a) All types of tissue can be reduced to a liquid state. Even hard substances such as bone and urinary stones can be reduced to small particles.
- b) Large volumes of tissue can only be removed rapidly if the aspiration channel of the 5 mm instrument remains unobstructed. The 10 mm instrument was disproportionately more efficient because of its larger aspiration channel. Modifications to the design of the smaller instrument should rectify this.
- c) A good endoscopic view was possible in both transurethral and laparoscopic procedures but the former was very sensitive to the efficient aspiration of material. A percutaneous nephrectomy may be safely monitored by ultrasound and not rely on endoscopy.
- d) No dead tissue is left at the margin of the removal unless diathermy was used excessively.
- e) It can be operated in both a liquid or gaseous medium.

f) A haemostatic effect could only be seen if diathermy was added.

Alternatively there is great potential for superselective embolisation techniques of various organs prior to removal using Ethibloc.

g) It is easy to control the ELSA but both the raked and diamond blades can cause significant tissue damage.

h) The use of the ELSA produced complications in 2 patients, during prostate and bladder tumour removal. The numbers are too small to be statistically relevant but suggest that at least as much respect and hence training must be given to the ELSA as is to the diathermy resectoscope.

i) The ELSA is easy and inexpensive to construct and is a complete contrast to the plethora of high technology innovations for tissue destruction.

LEGENDS

- Figure 1:1. Young's original cold punch.
- Figure 1:2. CUSA handpiece.
- Figure 1:3. Chang's motorised aspirator.
- Figure 2:1. The first experimental bench liquidisor/aspirator.
- Figure 2:2a. Diagram of the first experimental bench liquidisor/aspirator.
- Figure 2:2b. Diagram of housing parameters in bench model.
- Figure 2:3. End on view of blades made for the bench model in figure 2:1.
- Figure 2:4. Bien Air MC 40 GT DC motor connected to the 5 mm clinical liquidiser.
- Figure 2:5. Design of the 5 mm liquidiser/aspirator of the ELSA.
- Figure 2:6. Removal rate of liver plotted against blade speed for 3 different suction pressures, using the 5 mm clinical ELSA. Each coordinate is a mean of 10 measurements.
- Figure 2:7. Removal rate of liver and prostate tissue plotted against time with the 5 mm clinical ELSA at 40,000 rpm and 75 cm Hg suction. Each coordinate is a mean of 10 measurements.
- Figure 2:8. Blades made for the clinical ELSA.
- Figure 2:9. Apparatus assembled for measuring load/stain characteristics of different soft tissues.
- Figure 2:10. Diagram and key to apparatus shown in figure 2:9.
- Figure 2:11. Load/strain curves for kidney, prostate and muscle samples.
- Figure 2:12. Load/strain (displacement) curves in renal cortical tissue showing the effect of the working ELSA with flat and diamond blades.
- Figure 2:13. Load/strain (displacement) curves in muscle tissue showing the effect of the working ELSA with different blades at varying speeds.

- Figure 2:14. Load/strain (displacement) curves in benign prostatic tissue showing the effect of the working ELSA with different blades.
- Figure 2:15. The complete 5 mm ELSA showing the liquidiser/aspirator within the modified nephroscope.
- Figure 2:16. Microscopic appearance of renal tissue liquidised by the 5 mm clinical ELSA for 30 seconds at 40,000 rpm.
- Figure 2:17. Microscopic appearance of prostatic tissue liquidised by the 5 mm clinical ELSA for 30 seconds at 40,000 rpm.
- Figure 2:18. Graph showing particle distribution from a liver sample at 2 blade speeds, assessed by light microscopy.
- Figure 2:19. Graph showing particle distribution from a prostate sample at 2 blade speeds, assessed by light microscopy.
- Figure 2:20. Coulter counter analysis (by volume) of a liver sample using the ELSA at 3 speeds (top: 10,000, middle: 20,000, below: 40,000 rpm). Sample size has been gated at 200 microns.
- Figure 2:21. Coulter counter analysis of a prostate sample using the ELSA at 20,000 rpm.
- Figure 2:22. 3 liquidisers: Top, The 5 mm ELSA; middle, 10 mm ELSA; and below, the original hand held kitchen blender.
- Figure 3:1. The modified housing which produced the phenomenon of CVM.
- Figure 3:2. The Cytolyser.
- Figure 3:3. Particle size measured on the Coulter multisizer. These 3 histograms show the distribution of particles after the use of the Cytolyser for 20 seconds on a) paraffin section without pepsin digestion, b) paraffin section with pepsin, and c) fresh prostate.
- Figure 3:4. DNA histograms from a single paraffin-embedded section of benign prostate after different application times with the Cytolyser, with and without pepsin.
- Figure 4:1. Diagrammatic representation of the origin of the human prostatic artery (Clegg 1955).
- Figure 4:2. Diagrammatic cross-section of a prostate showing the distribution of the principal blood vessels.
- Figure 4:3. Macrovascular cast of the blood supply of the canine prostate.

- Figure 4:4. Diagram of the apparatus used to measure the bursting pressure of sealed arteries.
- Figure 4:5. The diathermy plate on the ELSA. It lies between rings of insulation material.
- Figure 5:1. Diagram of apparatus used for clinical ELSA prostate removal.
- Figure 5:2. The ELSA set up for clinical use.
- Figure 5:3. The peristaltic pump and motorised unit to drive the ELSA.
- Figure 6:1. Diagram showing endoligation and aspiration of an ovary.
- Figure 6:2. Histological section of a canine kidney 1 hour after Ethibloc embolisation. The embolisation agent has filled the glomerular arterial capillaries.
- Figure 6:3. Histological section of the canine prostate after Ethibloc embolisation.
- Figure 7:1. Diagram showing the ELSA fixed to a 6-axis robot.
- Figure 7:2. Preprogrammed dimensions of the "prostate" to be removed.
- Figure 7:3. The laboratory robotic prostatectomy in progress.
- Figure 7:4. Transverse section at the bladder neck showing the sequence of cuts.
- Figure 7:5. A trainee urologist using the model prostate.
- Figure 8:1. Electron microscopy of a cut oxalate stone.
- Figure 8:2. Sequential photographs during crushing of an urinary stone.
- Figure 8:3. Sequential photographs showing the primary abasive and secondary fragmentation action of the ELSA on an urinary stone.
- Figure 8:4. Typical compression test graph for a hard material such as an urinary stone.

REFERENCES

- Aboseif S.R., Breza J., Orvis B.R., Lue T. and Tanagho E.A. (1989). Erectile response to acute and chronic occlusion of the internal and pudendal arteries. J. Urol. 141: 398-402.
- Addonizio J.C., Choudhury M.S., Sayegh N. and Chopp R.T. (1984). Cavitron Ultrasonic Surgical Aspirator. Urology. 25:417.
- Appleton D.S., Sibley G.N.A., and Doyle P.T. (1988). Internal iliac artery embolisation for the control of severe bladder and prostate haemorrhage. Br. J. Urol 61. 45-47.
- Asimov I. (1953). 1 Robot. Panther Books, London.
- Auth D.C. (1986) Animal testing of endoscopic haemostasis with lasers and other devices. Endoscopy 18:36-39 (supplement 2).
- Awataguti S. (1939). Beitrag zur Kenntnis der Arterienverteilung im mannlichen Becken sonderer Berucksichtigung der Blutversorgung der Prostata. Mitt. allg. Path. Sendai, 10, 58.
- Bailey and Love (1981). Short practice of surgery. Page 1253. H.K. Lewis & Co Ltd, London.
- Baisch H., Otto U., Konig K. et al. (1982). DNA content of human kidney carcinoma cells in relation to histological grading. Br. J. of Cancer 48. 878-885.
- Batson O.V. (1955). Mtg. Amer. Assoc. Anatomists (68th session), Phila, PA.
- Blandy J.P. (1977). Surgery of the benign prostate. The first Sir Peter Freyer Memorial Lecture. J. Irish Med. Ass. 70, 517.
- Blandy J.P. (1978). Transurethral Resection. 2nd Edition. Pitman, London.
- Bleeham N.M. (1982). Hyperthermia in the treatment of cancer. Br. J. Cancer 45, Suppl V, 96-100.
- Bottini E. (1877). Radicale behandlung der auf hypertrophic der prostata beruhenden ischurie. Arch. Klin. Chir. 21:1.
- Bown S.G., Salmon P.R., Storey D.W. et al. (1980). Nd:YAG laser photo-coagulation in the dog stomach. Gut 21:818-25.
- Braasch W.F. (1918). Median bar excisor. J.A.M.A. 70:758.

Bücheler E., Hupe W., Klosterhalfen H. et al. (1978). Neue substanz zur therapeutischen embolisation von nierentumoren. Fortschr. Geb. Röntgstrahl. NuklMed. 128: 599-603.

Bumpus H.C. jr and Antopol W. (1934). Distribution of blood to the prostatic urethra. J.Urol. 32:354-358.

Caulk J.R. (1920). Infiltration anaesthesia for the internal vesical orifice for the removal of minor obstruction: presentation of a cautery punch. J.Urol. 4:399.

Chan K.K., Watmough D.J., Hope D.T., and Moir K. (1986). A new motor-driven surgical probe and its in vitro comparison with the CUSA Ultrasound. Med. Biol. 12. 4:279-283.

Chisholm G.D. (1989). Benign prostatic hyperplasia: the best treatment. Br. Med. J. 299:215-216.

Chopp R.T., Sarah B.B., and Addonizio J.C. (1983). Use of ultrasonic surgical aspirator in renal surgery. Urology 22:157.

Clegg E.J. (1955). The arterial supply of the human prostate and seminal vesicles. J. Anat., Lond., 89, 209-216.

Clegg E.J. (1958). The vascular arrangements within the human prostate gland. Br. J. Urol. 112:428-435.

Coptcoat M.J., Ison K.T., Timoney A., and Wickham J.E.A. (1989). The ELSA: the development and clinical use of a new endoscopic tissue remover. W. J. Urol. 7:138-141.

Coptcoat M.J., Ison K.T., and Wickham J.E.A. (1990). Principles of stone fragmentation. From Scientific Foundations of Urology, 679. Edited by Chisholm and Fair.

D'Arsonval A. (1983). Production des courants de haute frequence et de grande intensite leurs effets physiologiques. C. R. Soc. Biol. (Paris) 45.

Desnos M.E. (1914). Histoire de l'Urologie. Encyclopedie Francaise d'Urologie. Paris, Doin.

Devonee M., Dargzynkiewicz Z., Kostyrka-Claps M.L. et al. (1982). Flow cytometry of low stage bladder tumours. Cancer 48:109-118.

Epstein F.J. (1983). The cavitron ultrasonic aspirator in tumour surgery. Clin. Neurosurg. 31:497-505.

Fenwick E. Hurry (1895). Urinary Surgery, 2nd Ed. John Wright, Bristol.

Flocks R.H. (1937). Arterial distribution within the prostate gland: Its role in transurethral resection. J.Urol. 37:524-548.

Fourman J., and Moffat D.B. (1971). The blood vessels of the kidney. Blackwell, Oxford.

Frankfurt O.S., Chin J.L., and Enlander L.S. (1985). Relationship between DNA ploidy, glandular differentiation and tumour spread in human prostate cancer. *Cancer Res.* 45:1418-1423.

Freudenberg A. (1897). Eine modificirter bottinischer incisor. *Zentbl Chir.* 24:788.

Geraghty J.T. (1922). Sphincterotomy per urethram, a simple and safe procedure for the cure of contracture of the vesical orifice. *J. Urol.* 7:367.

Gordon J.E. (1968). The new science of strong materials. Penguin Books, London.

Gordon N. (1960). Surgical anatomy of the bladder, prostate and urethra in the male dog. *J. Am. Vet. Med. Assoc.* 136:215-221.

Griffiths J. (1889). Observations on the anatomy of the prostate. *J. Anat. Physiol.*, 23, 374.

Gustafson H., Tribukait B. and Esposti P.L. (1982). DNA pattern, histological grade and multiplicity related to recurrence rate in superficial bladder tumours. *Urol. Res.* 10:13-18.

Gutierrez R. (1933). History of Urology. Ed. Bransford, Lewis, 2, 137. Williams & Wilkins, Baltimore.

Guthrie G.J. (1836). On the anatomy and diseases of the urinary and sexual organs. Churchill, London.

Hedley D.W., Friedlander M.L., Taylor I.W., Rugg C.A., and Musgrove E.A. (1983). Method for analysis of cellular DNA content of paraffin-embedded pathological material using flow cytometry. *Journal of Histochemistry and Cytochemistry*, 31:1333-1335.

Hodgson W.J.B and Aufses A. (1979). Surgical ultrasonic dissection of the liver. *Surg. Rounds* 68.

Inglesias J.J and Stams V.K. (1975). How to prevent the TUR syndrome. *Urol.* 14, 287.

Kadir S., Marshall F., White jnr R., Kaufman S., and Barth K. (1983). Therapeutic embolisation of the kidney with detachable silicone balloons. *J. Urol.* 129:11-13.

Kelman C.D. (1973). Phaco emulsification and aspiration: A report of 500 consecutive cases. *Am. J. Ophthalmol.* 75:764-768.

Koontz W.W. and Smith M.J. (1985). Application of the cavitron ultra-sonic surgical aspirator for low-grade transitional cell carcinoma of the renal pelvis. *J. Urol.* 133:165A.

Kraas E. (1935). Die arterielle Gefassversorgung von Blasenhalss und Prostata. *Arch. Klin.* 183, 595-606.

- Krawitt D.R. and Addonizio J.C. (1987). Ultrasonic aspiration of prostate, bladder tumours and stones. *Urology*: 30. 6:579-580.
- Kreutzmann H.A.R. (1925). An improved knife for Young's prostatic punch. *Ibid.* 14:311.
- Kwoh Y.S., Hou J., Jonckheere E.A., and Hayati S. A Robot with Improved Absolute Positioning Accuracy for CT Guided Stereotactic Brain Surgery. *IEEE Trans. Biomedical Eng.*, Vol 35, No 2.
- Lowsley O.S. and Kirwin T.J. (1940). *Clinical Urology*. Williams & Wilkins Co. Baltimore.
- Mallett R. (1989). Machines march into a brave new world of medicine. *Hsp. Doc.* May 18:22.
- McCarthy J.F. (1931). A new apparatus for endoscopic plastic surgery of the prostate, diathermia and excision of vesical growths. *J. Urol.* 26:695-696.
- McNicholas T.A., Ramsey J.W.A., Carter S.St., and Miller R.A. (1988). Suprapubic endoscopy: a percutaneous approach. *Br J. Urol.* 61.3:221-223.
- Mebust W.K., Holtgrewe H.L., Cocket A.T.K., Peters P.C. and writing committee (1989). Transurethral prostatectomy: Immediate and postoperative complications. A cooperative study of 13 participating institutions evaluating 3,885 patients. *J. Urol.* 141:243-247.
- Melzer R.B., Wood T.W., Landau S.W. and Smith J.A. (1985). Combination of CUSA and neodymium:YAG laser for canine nephrectomy. *J. Urol.* 134: 620-622.
- Merklin R.J. and Michels N.A. (1958). The Significance of the renal capsular arteries. *Br J. Radiol* 40. 949-956.
- Mieta J.T., Barclay A.E., Daniel P.M., Franklin K.J., and Prichard M.M.L. (1947). *Studies in the renal circulation*. Blackwell, Oxford.
- Miller R.A. (1985). Endoscopic application of shockwave technology for the destruction of renal calculi. *W. J. Urol.* 7:138-141.
- Morotti E. (1891). Bottini's galvanocaustic treatment of enlarged prostate. *Brit. Med. J.* 1,1121.
- Nation E. (1976). Evolution of knife-punch resectoscope. *Urology*, 7,417.
- Paré Ambroise (1840). *Oeuvres Completes avec Figures*. Ed. J.F. Malgaigne. Paris, Bailliere.
- Payne S.R. and Webb D.R. (1989). *Percutaneous renal surgery*. Churchill Livingstone, London.
- Ramsay J.W.A. (1986). Advances in endoscopic diathermy. *Brit. Med. Bul.* 42:3:314-317.

- Rassweiler J., Kauffmann G.W., Richter G., Fuchs G. and Miller K. (1986). Experimental basis of angioinfarction for the treatment of renal hypertension. *Urol. Int.* 41:42-56.
- Richmond I.L. and Hawksley C.A. (1983). Evaluation of the histology of brain tumour tissue obtained by ultrasonic aspiration. *Neurosurgery.* 13:415-419.
- Semm K. (1977). Atlas of gynaecological laparoscopy and hysteroscopy. Saunders, Philadelphia.
- Shanberg A.M., Tansey L.A. and Baghdassarian R. (1985). (1987). The Nd:YAG laser in prostatotomy. *J. Urol. suppl.* 133:331A.
- Student (1908). *Biometrika.* 6,1.
- Sigel B. and Hatke F. (1967). Physical factors in electrocoaptation of blood vessels. *Arch Surg;* 95:54-58.
- Soni A.H., Gudavelli M.R., and Herndon W.A. (1987). Application of a Passive Robot in Spine Surgery. *IEEE Robotic and Automation International Conf.* Raleigh NC, USA.
- Stephenson R.A. and Herr H.W. (1986). Flow cytometry in urologic oncology. *Urologic clinics of N. America,* 13,3:525-530.
- Stern M. (1926). Resection of obstructions at the vesical orifice. *J.A.M.A.* 87:1726-1729.
- Svaasand L.O., Doiron D.R., and Profio A.E. (1981). Light distribution in tissues during photoradiation therapy. Medical imaging Science Group Report 900-01. University of California, Los Angeles.
- Thompson G.J. (1934). Transurethral prostatic surgery. *Mayo Clin. Proc.* 26:349.
- Tolson H.L. (1925). An electrode for use with Young's punch. Diathermy as a supplement to the prostatic punch operation. *Ibid.* 14:63.
- Walker K.M. (1925). Periurethral operations for prostatic obstruction. *Br. Med. J.* 1:201.
- Wallace D.M. (1973). New Lamps for old. *Proc. Roy. Soc. Med.* 66,455.
- Watson J.V., Sikora K., and Evan G.I. (1985). A simultaneous flow cytometric assay for c-myc oncoprotein and DNA in nuclei from paraffin-embedded material. *Journal of Immunological Methods.* 83:179-192.
- Wright B.M. (1976). Cryosurgery for prostate obstruction using liquid nitrous oxide. *Br J. Urol* 48:203-206.
- Yamada H. (1970). Strength tests of Biological materials. Edited by Groves. Published by Witley and Chapman, London.

Young H.H. (1913). A new procedure (punch operation) for small prostatic
bars and contracture of prostatic orifice. J. Amer. Med. Ass. 60,253.

Young H.H. (1932). Discussion after symposium on resection.
J. Urol. 28:585

University of London

in association with St. Peter's Hospitals

172 Shaftesbury Avenue, London, WC2H 8JE.

Telephone: 01-240 9115

21st October 1987

Mr. M.J. Coptcoat,
Research Fellow,
Urological Academic Unit.

Dear Malcolm,

Endoscopic liquidisation and aspiration of benign prostatic tissue
and superficial bladder tumours, and the development of a robotic
prostate aspiration system

I am pleased to let you know that at the Joint Research Committee held on the 5th October, and the Ethics Committee on the 19th October 1987, the above project submitted by you was considered and approved.

Yours sincerely

J.M. Wolfenden (Mrs)
Secretary